IMC Krems University of Applied Sciences

Medical and Pharmaceutical Biotechnology

Adaptive Laboratory Evolution of *E. coli* 498 to Toxic Paint and Resin Residues in Industrial Reaction Water (RW)

Bachelor Thesis

submitted in partial fulfilment of the requirements for the degree of

Bachelor of Science in Engineering

Elijá Samuel Friedrich-Ulrich

Supervisor: Prof.(FH) DI Dominik Schild

Krems, May 2026

STATUTORY DECLARATION

I declare on my word of honour that I have written this paper on my own and that I have not used any sources or resources other than stated and that I have marked those passages and/or ideas that were either verbally or textually extracted from sources. This also applies to drawings, sketches, graphic representations as well as to sources from the internet. The paper has not been submitted in this or similar form for assessment at any other domestic or foreign post-secondary educational institution and has not been published elsewhere. The present paper complies with the version submitted electronically.

Krems, May 2026

Elija S. Friedrich-Ulrich

Signature

DECLARATION OF AI-ASSISTED TOOLS

In accordance with the academic integrity guidelines of IMC Krems University of Applied Sciences, the use of artificial intelligence (AI) tools during the preparation of this thesis is disclosed below.

- **Claude Opus 4.6 (Anthropic):** language editing and proofreading of English text; assistance with Python script development for data visualization.

All AI-generated or AI-assisted content was critically reviewed, verified against the original data and sources, and revised by the author before inclusion. The experimental design, data collection, scientific analysis, interpretation of results, and conclusions presented in this work are entirely the author's own. The author assumes full responsibility for the accuracy and integrity of the final text.

ACKNOWLEDGEMENTS

This thesis was conducted within the framework of the EcoCoat project at IMC Krems University of Applied Sciences.

I wish to thank my supervisor, Prof.(FH) DI Dominik Schild, for his guidance, patience, and consistent support throughout the research process and the writing of this thesis. His feedback influenced both the experimental design and how the results are presented here.

I also thank David Klingholz, BCs for collaboration on the experimental work, for many productive discussions at the bench, and for troubleshooting the Replifactory hardware on more occasions than either of us would like to count.

I thank Luis Hilpert for his collaboration and support as a colleague on the REELACS project, which ran alongside this thesis work.

I am grateful to Catalin Rusnac for designing and developing the Replifactory morbidostat platform, for making the devices available, and for his technical assistance throughout the experimental series. Without the Replifactory hardware, this work would not have been possible.

Reaction water samples were provided by Kansai Helios Slovenija d.o.o. (Količevo plant, Slovenia), whose cooperation made this research possible. I acknowledge Kansai Helios Austria GmbH for supporting the industrial partnership behind this project.

I thank the faculty and staff of the Medical and Pharmaceutical Biotechnology programme at IMC Krems for providing the academic and laboratory infrastructure necessary for this work.

Finally, I thank my family, especially my mother, my partner Johanna and friends for their encouragement and patience throughout the duration of this thesis.

CONTENTS

LIST OF FIGURES

LIST OF TABLES

ABSTRACT

Industrial reaction water (RW) from polyester resin synthesis via polycondensation is a complex, acutely toxic effluent containing neopentyl glycol (NPG), ethylene glycol (EG), phenolic oligomers, organic solvents, and residual catalysts. Current disposal by high-temperature incineration is cost-intensive and carries a high carbon footprint. Biological treatment has not been established because standard microbial cultures cannot survive the acute toxicity of untreated RW.

This study investigated whether *Escherichia coli* strain 498, a K-12 derivative, could be evolved via adaptive laboratory evolution (ALE) in a Replifactory morbidostat to tolerate and catabolise the organic constituents of an industrial RW batch (RW#2, native pH 1.88) as a proof-of-concept for biological RW remediation. Twenty morbidostat experiments (REP_001–REP_020) were performed across three phases: Phase I (LB-based adaptation to RW#2, REP_001–REP_007), Phase II (defined minimal medium with and without glucose, REP_008–REP_015), and Phase III (cross-tolerance validation with a second batch RW#3, native pH 5.56, REP_016–REP_020). RW#2 was pH-neutralised to 7.0 ± 0.2 with 5 M NaOH prior to use; RW#3 was used without neutralisation. Growth was monitored continuously by OD_{600} via the Replifactory's built-in photodiode sensor.

What this thesis demonstrates. Wild-type *E. coli* 498 cannot grow in pH-neutralised RW#2 without prior adaptation (REP_001). Under morbidostat selection, adapted strains tolerated $>$21 % (v/v) RW#2 within 12 days (REP_002) and reached up to 72 % (v/v) RW#2 in individual vials within 10 days under LB conditions (REP_005). In the absence of glucose (M9 $-$ glucose + RW#2), adapted strains sustained measurable growth over 12 and 25 days (REP_011, REP_014), while wild-type controls did not, providing direct evidence that one or more RW constituents were assimilated as a carbon and energy source. Adaptation acquired against RW#2 transferred to RW#3 without re-adaptation: a pre-adapted lineage reached 91 % (v/v) RW#3 with confirmed cell proliferation (REP_018, V3), the high-

est tolerance recorded across the series; concurrent wild-type controls reached individual final concentrations of 53–61 % (v/v) RW#3 (mean $\approx$57.6 %, $n = 3$) only after a longer lag phase. RW tolerance was substantially reduced when LB was replaced with defined minimal medium plus glucose, with the ceiling dropping to approximately 4 % (v/v) RW#2 (REP_008), showing that the nutritional background contributes materially to apparent tolerance. Biofilm formation on vial walls and tubing was identified as a recurring, OD-inflating confounder of growth monitoring, and the dark colour of RW at concentrations above $\sim$50 % (v/v) was shown to drive a positive feedback loop in the morbidostat's photodiode-based dose-escalation algorithm (REP_018, V1/V2), an inherent limitation of optical density monitoring in coloured industrial feedstocks.

What remains open. The specific RW constituents being catabolised, the kinetics and stoichiometry of their consumption, and the fraction of the total organic load actually removed were not quantified in this study. Pollutant removal endpoints such as chemical oxygen demand (COD) reduction, residual glucose and glycol concentrations, and acute ecotoxicity (*Aliivibrio fischeri* EC_{50}, Microtox) were outside the experimental scope and are not reported. Whether the observed glucose-free growth reflects genuine mineralisation of RW carbon or reactor-level detoxification accompanied by limited carbon assimilation cannot be distinguished from the data presented and is identified as the central question for follow-up work.

Escherichia coli 498 can be evolved by morbidostat-based ALE to tolerate near-undiluted industrial reaction water from polyester resin production and to grow without an external carbon source in its presence. Quantification of pollutant removal, identification of degradation pathways, and ecotoxicity assessment of treated effluent are required before biological treatment can be evaluated as a process alternative to incineration.

CHAPTER 1

AIMS OF THE THESIS

The central aim of this thesis is to investigate whether *Escherichia coli* strain 498 can be evolved, through adaptive laboratory evolution (ALE) in a morbidostat system, to tolerate and grow in industrial reaction water (RW) from polyester resin production, and whether the adapted strains can be shown to actively catabolise the organic pollutant load of the RW rather than merely surviving in its presence.

The RW used in this study originates from polyester polycondensation at the Količevo plant of Kansai Helios Slovenija d.o.o. and contains neopentyl glycol, ethylene glycol, unreacted polymer fragments, residual catalysts, and trace organic solvents (Pirman, 2025; "RD Project Order — Reduction of Waste-Water and Waste-Solvent from Resin Production", 2025). Current disposal relies on incineration at considerable economic and environmental cost ("Q-A Samples of Reaction Water", 2025). A biological treatment process capable of reducing the organic content of the RW would provide a sustainable alternative (Nair K et al., 2021; Tripathy et al., 2025; Viktoryová et al., 2022), but requires organisms that can tolerate the acute toxicity of the waste stream at industrially relevant concentrations. Morbidostat-based ALE is a suitable tool for evolving such tolerance, as previously demonstrated for antibiotics (Toprak et al., 2012, 2013) and for organic-solvent stress (Dragosits & Mattanovich, 2013; Hirasawa & Maeda, 2022).

1.1 Research Questions

Research Question 1: Adaptation Potential

To what extent can *E. coli* 498 be evolved to tolerate and grow in increasing concentrations of pH-neutralised industrial RW in a continuous Replifactory morbidostat culture (Rusnac, 2024)?

Research Question 2: Metabolic Strategy

Does the adapted strain actively metabolise the toxic organic constituents of the RW, and does adaptation proceed more effectively under catabolic conditions (RW as the sole carbon and energy source) or co-metabolic conditions (RW supplemented with glucose)?

Research Question 3: Biofilm Influence

How does biofilm formation within the morbidostat system affect the stability and reproducibility of the ALE process? Is biofilm a disruptive artefact that compromises OD-based growth monitoring, or does it confer a survival advantage against toxic shocks?

1.2 Success Criteria

To render the central aim experimentally testable, the following success criteria are defined *a priori*. Each research question is judged against quantitative or operationally explicit endpoints derived from the morbidostat data and the experimental design.

RQ1 — Adaptation Potential. Adaptation is considered demonstrated when (i) at least one adapted lineage sustains growth ($OD_{600} > 0.1$ with positive growth rate over $\geq$24 h) at an RW concentration at least 10 percentage points higher than the maximum tolerated by concurrent wild-type controls under identical conditions, and (ii) this elevated tolerance is reproduced in at least one independent experiment using cryopreserved cells of the same lineage. Adaptation *strength* is reported as the maximum sustained RW concentration (% v/v) reached by an adapted lineage and as the time-to-reach-50 % RW for adapted versus wild-type controls. Adaptation *breadth* is judged by whether the phenotype transfers between RW batches (RW#2 $\rightarrow$ RW#3, Phase III).

RQ2 — Metabolic Strategy. The metabolic question is operationalised by a three-condition contrast (Boronat et al., 1983):

- LB + RW: tolerance with the full nutritional background available.
- M9 + glucose + RW: co-metabolic regime; glucose is the defined primary carbon source while RW components may be partially transformed.

- M9 − glucose + RW: catabolic regime; RW constituents are the only available carbon and energy source.

Catabolic utilisation is considered demonstrated when adapted strains show sustained OD_{600} increase and positive growth rate in M9 − glucose + RW over a duration that exceeds plausible carry-over of intracellular reserves from the inoculum (operationally $\geq$5 days), while concurrent wild-type controls in the same medium do not grow. The directly measured endpoint in this study is the comparative OD_{600} trajectory across the three conditions.

Endpoints not measured in this thesis but explicitly relevant for assessing biological treatment. Quantitative pollutant removal — chemical oxygen demand (COD) reduction, residual glucose and glycol concentrations, identification of degradation products — requires chemical analytics (HPLC, GC-MS) that were outside the present experimental scope. These endpoints are addressed in the parallel master thesis by David Klingholz on the same RW batches and are listed here as the criteria by which the practical value of biological RW treatment will ultimately be judged (Tripathy et al., 2025; Viktoryová et al., 2022). Acute ecotoxicity reduction (*Aliivibrio fischeri* EC_{50}, Microtox bioassay) is the corresponding biological endpoint (Abbas et al., 2018; Soupilas et al., 2008) and is similarly deferred to follow-up work.

RQ3 — Biofilm Influence. Biofilm interference is considered confirmed when documented qualitatively (visual inspection of vial walls and stirring bars) and shown to coincide with quantitative artefacts in the OD_{600} signal, such as inflated baseline readings, inappropriate dilution events triggered by surface-attached biomass, or recovery of planktonic populations after washout consistent with re-seeding from a surface reservoir.

1.3 Experimental Scope

These three research questions are addressed through a series of 20 morbidostat experiments (REP_001 through REP_020): 15 experiments using RW#2 as the feedstock (Phases I and II) and 5 experiments using RW#3 (Phase III) to assess transferability of the adapted phenotype across RW batches. The experimental design progresses from complex medium (LB) through defined minimal medium

(M9 with glucose) to carbon-source-free conditions (M9 without glucose), so that co-metabolic tolerance and catabolic degradation can be distinguished against the success criteria defined above.

CHAPTER 2

INTRODUCTION

Industrial manufacturing generates large volumes of process wastewater that contains complex mixtures of organic pollutants, heavy metals, and residual solvents (Phulpoto et al., 2016; Ravikumar et al., 2012; Tripathy et al., 2025). In the coatings and resins industry, polyester resin synthesis via polycondensation produces a by-product stream known as reaction water (RW), which contains unreacted monomers such as neopentyl glycol (NPG) and ethylene glycol (EG), oligomeric resin fragments, residual catalysts, and volatile organic solvents including butyl acetate, methyl ethyl ketone (MEK), methyl isobutyl ketone (MiBK), butyl glycol, and xylene (Pirman, 2025; "RD Project Order — Reduction of Waste-Water and Waste-Solvent from Resin Production", 2025). The Količevo plant of Kansai Helios Slovenija d.o.o. generates approximately 3,000 tonnes of this RW annually. The waste stream comprises two distinct fractions: the initial 75%, collected during the pre-vacuum phase of the polycondensation process, contains lower pollutant concentrations, while the final 25%, from the vacuum phase, is heavily concentrated with unreacted monomers, catalysts, and organic solvents ("Q-A Samples of Reaction Water", 2025). Current disposal relies on incineration, which imposes significant economic costs and releases carbon dioxide, contributing to the environmental burden of the production process.

Conventional physicochemical treatment technologies for organic-laden industrial effluents include activated carbon adsorption, advanced oxidation processes (Fenton, ozone, UV/H_2O_2), and membrane filtration (Nair K et al., 2021; Tripathy et al., 2025; Viktoryová et al., 2022). While effective at reducing pollutant loads, these methods are energy-intensive, generate secondary waste streams (spent adsorbents, chemical sludge), and do not convert the organic pollutants into biomass or harmless end products. Biological treatment takes a different approach: microorganisms can mineralize organic pollutants to CO_2 and water, incorporate carbon into

biomass, and operate at ambient temperature and pressure with minimal chemical input. Biological systems have been applied successfully to a range of industrial effluents, including textile dyes, phenolic wastewaters, and petroleum hydrocarbons (Asgher et al., 2008; Liu et al., 2020; Shindhal et al., 2021; Singh et al., 2024; Thanavel et al., 2020). The feasibility of biological treatment depends, however, on whether suitable organisms can be identified or developed that tolerate the specific toxicity profile of the waste stream.

2.1 Adaptive Laboratory Evolution

Adaptive laboratory evolution (ALE) is an experimental strategy in which microbial populations are subjected to defined selective pressures over extended periods, allowing natural selection to drive the accumulation of beneficial mutations that improve fitness under the imposed conditions. ALE has been applied extensively to improve microbial tolerance to industrially relevant stresses, including organic solvents, heavy metals, extreme pH, and inhibitory substrate concentrations (Dragosits & Mattanovich, 2013; Hirasawa & Maeda, 2022). Unlike rational metabolic engineering, which requires prior knowledge of the genetic targets, ALE operates without assumptions about the molecular basis of adaptation and can therefore discover novel tolerance mechanisms.

The duration required for ALE depends on the complexity of the target phenotype and the population size maintained during selection. Typical ALE experiments run for tens to hundreds of generations, with bacterial populations of 10^8 to 10^{10} cells providing sufficient genetic diversity for selection to act upon (Tenaillon et al., 2012, 2016). Serial transfer in batch culture is the simplest ALE format: populations are grown to saturation under stress, diluted into fresh medium containing the selective agent, and the cycle is repeated. While accessible, serial transfer imposes fluctuating selective pressure because the stress concentration decreases as cells grow and dilute the medium, and increases abruptly at each transfer. This fluctuation can select for tolerance to stress transitions rather than sustained growth at high stress concentrations.

2.2 The Morbidostat Principle

The morbidostat, introduced by Toprak et al. (2012), addresses this limitation by maintaining a constant level of growth inhibition through dynamic feedback control. In a morbidostat, optical density (OD) measurements are used to estimate growth rate in real time, and the concentration of the inhibitory agent is adjusted automatically: when growth rate exceeds a threshold, the inhibitor concentration is increased; when growth rate drops below a threshold, the inhibitor is diluted. This feedback loop keeps the population near its maximum tolerated concentration of the stressor, selecting for progressively more tolerant variants while preventing population collapse (Toprak et al., 2013).

The morbidostat was originally developed for studying the evolution of antibiotic resistance. Toprak et al. (2012) demonstrated that *Escherichia coli* populations evolved increasing resistance to chloramphenicol, trimethoprim, and doxycycline over approximately 25 days in morbidostat culture, accumulating multiple resistance mutations in a stepwise manner that could not be observed in fixed-concentration experiments. Subsequent work adapted the morbidostat concept for studying resistance to biocides (triclosan), quaternary ammonium compounds, and other antimicrobial agents. Gopalakrishnan et al. (2022) developed EVE, a low-cost open-source morbidostat for educational settings, showing that the platform is accessible and inexpensive enough for teaching laboratories.

Applying morbidostat-based ALE to industrial pollutant tolerance, rather than antibiotic resistance, is a comparatively new idea that has received little attention in the literature. In conventional antibiotic resistance studies, the selective agent is a defined chemical with a known mechanism of action. Industrial RW, by contrast, is a complex mixture of multiple toxic compounds at varying concentrations, each with potentially distinct mechanisms of toxicity. Adapting bacteria to tolerate such a mixture likely requires the concurrent evolution of several tolerance mechanisms, and the morbidostat's feedback control maintains the sustained selective pressure needed to drive this kind of multi-target adaptation.

2.3 The Replifactory System

The experimental work in this thesis was performed using the Replifactory, an open-source, 3D-printed, multiplexed morbidostat platform developed by Rusnac (2024). The Replifactory extends the morbidostat concept with several features suited to parallel evolution experiments: seven independent culture vials per unit, each with integrated magnetic stirring and OD_{600} measurement via a built-in photodiode sensor; three peristaltic pumps for drug-free medium, drug-containing medium, and waste removal; and a Raspberry Pi controller with a web-based interface for real-time monitoring and parameter adjustment. Multiple Replifactory units (designated IMC1, IMC2, and IMC3 in this study) could be operated simultaneously, enabling biological replicates and control conditions within a single experimental run. A total of 20 morbidostat experiments (REP_001 through REP_020) were conducted: 15 targeting adaptation to RW#2 (Phases I and II) and 5 targeting cross-tolerance validation with RW#3 (Phase III).

The Replifactory operates in morbidostat mode by default but can also function as a turbidostat (OD-triggered dilution at a fixed threshold) or chemostat (time-triggered dilution at fixed intervals). In morbidostat mode, the system adjusts the ratio of drug-free to drug-containing medium in each dilution event based on the estimated growth rate, implementing the feedback logic described in Section 2.2. Pump calibration, OD calibration against external spectrophotometer standards, and configurable parameters for stress escalation and relief thresholds enable precise control of the selective environment.

2.4 *Escherichia coli* as a Model Organism for ALE

Escherichia coli is the most extensively studied prokaryotic organism and the standard model for ALE experiments. Its short generation time (approximately 20 minutes under optimal conditions), well-characterized genome, extensive genetic toolbox, and non-pathogenic status (K-12 derivatives, Risk Group 1, BSL-1) make it the organism of choice for laboratory evolution studies (Jee et al., 2016; Tenaillon et al., 2016). *E. coli* K-12 strains have been subjected to ALE for a wide range

of phenotypes, including tolerance to organic solvents such as ethanol and butanol (Hirasawa & Maeda, 2022; Tian et al., 2023), thermal stress, osmotic stress, and nutrient limitation.

The strain used in this thesis, *E. coli* 498, is a K-12 sub-strain obtained from the internal culture collection at IMC Krems. While *E. coli* is not traditionally associated with the degradation of complex industrial pollutants (a role more commonly attributed to *Pseudomonas*, *Rhodococcus*, or white-rot fungi), its genetic tractability and rapid growth make it an effective platform for proof-of-concept ALE studies. If *E. coli* can be evolved to tolerate and metabolize RW constituents, the adaptation mechanisms identified could inform the engineering of more robust industrial strains.

2.5 Biodegradation of Industrial Effluents

Biological degradation of organic pollutants in industrial wastewater has been studied across a range of waste streams and organism classes. Phenolic compounds, which are structurally related to the resin monomers and oligomers present in paint and coatings RW, are among the most thoroughly investigated substrates for biodegradation. *Pseudomonas* species degrade phenolics via catechol dioxygenase pathways (Majumder et al., 2014; Sivapuratharasan et al., 2022; Wynands et al., 2023); *Rhodococcus* species employ peroxidases for aromatic oligomer breakdown (Larkin et al., 2005); and white-rot fungi such as *Bjerkandera adusta* and *Phanerochaete chrysosporium* produce lignin peroxidase (LiP) and manganese peroxidase (MnP) systems capable of mineralizing recalcitrant phenolic polymers (Arregui et al., 2019; Asgher et al., 2008; Biko et al., 2020; Falade et al., 2017; Konan et al., 2024; S., 2001).

The distinction between tolerance and degradation is critical. A microorganism may tolerate a toxic compound (surviving in its presence without metabolizing it) or actively degrade it (using it as a carbon and energy source, or co-metabolizing it in the presence of an alternative substrate). For industrial wastewater treatment, only active degradation reduces the chemical oxygen demand (COD) of the effluent. ALE in a morbidostat selects primarily for tolerance, because the feedback algorithm rewards growth rate regardless of whether the organism is degrading or merely surviv-

ing in the stressor. Distinguishing between these two outcomes requires additional experimental evidence, such as growth in the absence of alternative carbon sources (catabolism), or direct measurement of pollutant removal.

2.6 Catabolism vs. Co-metabolism

Two metabolic strategies are relevant to the biological treatment of RW:

Co-metabolism occurs when an organism grows on a primary carbon source (e.g., glucose) while enzymatically transforming a co-occurring pollutant. The pollutant is not required for growth and may be only partially oxidized. Co-metabolic processes can reduce pollutant concentrations but do not necessarily mineralize the organic load to CO_2 and water.

Catabolism occurs when the organism uses the pollutant itself as the sole carbon and energy source. Catabolic degradation directly removes organic carbon from the waste stream and is therefore the mechanism most relevant to industrial wastewater remediation.

The experimental design of this thesis enables distinction between these strategies by testing adapted *E. coli* 498 under three conditions: (1) complex medium (LB) with RW, where multiple carbon sources are available; (2) minimal medium (M9) with glucose and RW, where glucose is the defined primary carbon source; and (3) minimal medium without glucose and RW, where RW constituents are the only available carbon source. Growth under condition (3) provides direct evidence for catabolic utilization of RW components.

2.7 Ecotoxicity Assessment

Beyond chemical analysis, ecotoxicity bioassays provide a biological measure of the hazard potential of industrial effluents before and after treatment. The Microtox assay quantifies the inhibition of bioluminescence in *Aliivibrio fischeri* as a half-maximal effective concentration (EC_{50}) and is widely used for rapid ecotoxicity screening of industrial wastewaters (Abbas et al., 2018; Soupilas et al., 2008). A reduction in EC_{50} following biological treatment would provide direct evidence that bioremediation reduces the acute toxicity of the effluent, not merely its organic load.

While ecotoxicity testing was not performed in the present study, it represents an important validation step for assessing the practical applicability of biological RW treatment.

2.8 Biofilm Formation in Continuous Culture Systems

Biofilm formation is a bacterial survival strategy in which cells adhere to surfaces and produce an extracellular polymeric substance (EPS) matrix. In continuous culture systems such as the morbidostat, biofilm formation on vial walls, stirring bars, and tubing is a recurring operational challenge. Biofilm accumulation interferes with OD-based growth monitoring by inflating optical density readings with surface-attached biomass, and acts as a reservoir of adapted cells that can re-seed the planktonic population after washout events.

In the context of toxic waste exposure, biofilm formation has both beneficial and detrimental aspects. Biofilm-associated cells exhibit increased tolerance to toxic compounds due to diffusion limitation through the EPS matrix and phenotypic heterogeneity within the biofilm community. Biofilm formation also complicates the interpretation of morbidostat data because the planktonic growth rate, which drives the feedback algorithm, may not reflect the total biomass or the true adaptive state of the population. Characterising the role of biofilm in the ALE process is therefore relevant both for interpreting the experimental data and for assessing the feasibility of scale-up.

2.9 Research Gap

Despite the extensive literature on ALE for antibiotic resistance and solvent tolerance, the application of morbidostat-based ALE to complex, multi-component industrial waste streams has not been explored. No published study has reported the evolution of *E. coli*, or of any single organism, to tolerate and catabolise the mixed organic pollutants present in reaction water from polyester resin production. This thesis addresses the gap by systematically evolving *E. coli* 498 in a Replifactory morbidostat under progressively increasing RW concentrations, distinguishing co-metabolic tolerance from catabolic degradation, and evaluating the transferability of

the adapted phenotype across different RW batches.

CHAPTER 3

MATERIALS AND METHODS

3.1 Bacterial Strain and Culture Conditions

3.1.1 Organism and Cryopreservation

Escherichia coli strain 498, a K-12 sub-strain, served as the sole test organism across all adaptation experiments. The strain was obtained from the internal culture collection at IMC Krems University of Applied Sciences. K-12 derivatives are well-characterized, non-pathogenic (Risk Group 1, BSL-1), and represent the standard model organism for adaptive laboratory evolution (ALE) studies due to their genetic tractability and extensive physiological documentation (Jee et al., 2016; Tenaillon et al., 2016).

Wild-type (WT) cultures were maintained as glycerol stocks (25% v/v glycerol in LB broth) at -80 °C. For experimental use, frozen stocks were revived by streaking on LB agar plates and incubating overnight at 37 °C. A single colony was then inoculated into liquid LB broth and grown overnight (16–18 h) at 37 °C with orbital shaking at 180 rpm. The resulting culture was diluted to a target OD_{600} of approximately 0.25 in fresh medium before transfer into the morbidostat.

Pre-adapted strains originated from the best-performing vials of prior morbidostat runs. At the conclusion of each successful experiment, the adapted culture was harvested by centrifugation ($4{,}000 \times g$, 10 min), resuspended in 25% (v/v) glycerol in LB, and stored at -80 °C. These cryopreserved stocks served as inocula for subsequent experiments, so that adaptation could accumulate over successive experiments. The propagation lineage within the RW#2 adaptation series was: REP_002 (V2, V3, V5) $\rightarrow$ REP_004/005 $\rightarrow$ REP_007 (V1, V3). Strains from this lineage were subsequently tested against RW#3 in a cross-tolerance validation experiment (Section 3.4.1).

3.1.2 Culture Media

Three media formulations were employed across the experimental series:

Complex Medium: Luria–Bertani (LB) Broth

Table 3.1: Composition of LB broth.

Component	Concentration
Tryptone	10 g/L
Yeast extract	5 g/L
NaCl	10 g/L

LB was used as the standard complex medium in experiments REP_001–REP_007. It served both as the drug-free medium reservoir (Pump 1) and as the diluent base for RW stock solutions (Pump 2).

Minimal Medium: M9 with Glucose

Table 3.2: Composition of M9 minimal medium with glucose.

Component	Concentration
$Na_2HPO_4 \cdot 7\,H_2O$	12.8 g/L
KH_2PO_4	3 g/L
NaCl	0.5 g/L
NH_4Cl	1 g/L
$MgSO_4$	2 mM
$CaCl_2$	0.1 mM
Glucose	16.5 g/L

M9 + glucose was introduced from REP_008 onward as the defined medium to test whether adapted strains could utilize RW constituents as a supplementary carbon source under nutrient limitation.

Minimal Medium: M9 without Glucose

Identical to the above but without glucose supplementation. Used in REP_011 and REP_014 to test whether adapted *E. coli* 498 could sustain growth on RW as the sole carbon and energy source (catabolic conditions).

All media were sterilized by autoclaving at 121 ℃ for 20 min. Glucose and $CaCl_2$ solutions were autoclaved separately and added aseptically after cooling.

3.2 Feedstock Characterization and Pre-treatment

3.2.1 Origin of Reaction Water

Industrial reaction water (RW) was provided by Kansai Helios Slovenija d.o.o. (Količevo plant, Slovenia) as part of a research collaboration with IMC Krems University of Applied Sciences. The RW originates as a by-product of polyester resin synthesis via polycondensation and contains neopentyl glycol (NPG), ethylene glycol (EG), unreacted polymer fragments, residual catalysts, and trace organic solvents including butyl acetate, methyl ethyl ketone (MEK), methyl isobutyl ketone (MiBK), butyl glycol, and xylene (Pirman, 2025; "RD Project Order — Reduction of Waste-Water and Waste-Solvent from Resin Production", 2025). The Količevo plant generates approximately 3,000 tonnes of this effluent annually.

The RW stream consists of two distinct fractions: the initial 75% collected during the pre-vacuum phase, which contains lower pollutant concentrations, and the final 25% from the vacuum phase, which is heavily concentrated with unreacted monomers, catalysts, and organic solvents ("RD Project Order — Reduction of Waste-Water and Waste-Solvent from Resin Production", 2025).

RW#2 (native pH 1.88) was used as the sole feedstock for all adaptation experiments (REP_001 through REP_015). RW#2 is raw, unprocessed reaction water sampled prior to the implementation of any on-site cleaning process by Kansai Helios Slovenija. It represents the full, untreated pollutant load and constitutes the worst-case feedstock for adaptation.

A second batch, **RW#3** (native pH 5.56), from the same production process was used in a single cross-tolerance validation experiment to confirm that strains adapted to RW#2 retained their tolerance when exposed to a different RW batch (Section 3.4.1).

3.2.2 pH Neutralization and Sterilization

For experiments requiring pH-neutralized RW, the pH was adjusted to 7.0 ± 0.2 using 5 M NaOH with continuous stirring, monitored by a benchtop pH meter. Sterilization of RW-containing media was achieved by autoclaving at 121 °C for 20 min. It was also differentiated between autoclaved and non-autoclaved RW, as heating to high

temperatures may change the acute toxicity of the constituents present.

3.3 The Morbidostat System (Replifactory)

3.3.1 Hardware Setup

Adaptive laboratory evolution was performed using the Replifactory, an open-source, 3D-printed morbidostat platform designed for multiplexed continuous evolution experiments (Rusnac, 2024). Three physical Replifactory units (designated IMC1, IMC2, and IMC3) were used across the experimental series.

Each Replifactory unit consists of seven glass culture vials (12 mL working volume) with integrated magnetic stirring and optical density measurement. The system is controlled by a Raspberry Pi single-board computer running a web-based interface for parameter configuration, data logging, and real-time monitoring.

Three peristaltic pumps manage liquid handling:

- **Pump 1 (Media):** Delivers drug-free medium (LB or M9 $\pm$ glucose) to the culture vials.
- **Pump 2 (Drug/RW):** Delivers the RW-containing stock solution at a defined concentration.
- **Pump 3 (Waste):** Removes excess culture volume to the waste reservoir.

Pump calibration was performed prior to each experimental run by measuring the dispensed volume per rotation at multiple speeds (1, 5, 10, and 50 rotations), yielding a mL/rotation coefficient for accurate dispensing of volumes as small as approximately 0.05 mL (Rusnac, 2024).

The built-in OD sensor employs a photodiode-based transmission measurement at 600 nm (OD_{600}). OD calibration was conducted using translucent paper probes of known OD values, cross-referenced against an external spectrophotometer. At high RW concentrations, the intrinsic colour of the RW can interfere with OD_{600} readings. External spectrophotometer measurements were taken periodically to validate the in-line readings in such cases.

3.3.2 Control Logic and Feedback Loop

In morbidostat mode, the system dynamically adjusts the RW concentration in the culture based on real-time growth rate estimation. The operating logic follows these principles:

1. **Dilution trigger:** When the culture OD_{600} exceeds a defined threshold (`od_dilution_thre` or when a maximum time delay between dilutions (`delay_dilution_max_hours`) is reached, a dilution event is initiated.

2. **Stress escalation:** If the estimated growth rate exceeds a minimum threshold (`threshold_growth_rate_increase_stress`) and the culture OD_{600} exceeds a minimum value (`threshold_od_min_increase_stress`), the RW concentration in the subsequent dilution is increased by a defined factor and/or additive amount (`dose_increase_factor`, `dose_increase_amount`).

3. **Stress reduction:** If the growth rate drops below a critical threshold (`threshold_growth_r` a dilution with drug-free medium only (Pump 1) is triggered, thereby reducing the RW concentration.

4. **Dilution volume:** Governed by the `dilution_factor` parameter, which defines the fraction of the culture volume replaced per dilution event. For the standard dilution factor of 1.6 and a working volume of 12 mL, each event removed and replaced approximately 7.2 mL (60% of the culture volume). The ratio of drug-free medium (Pump 1) to RW-containing medium (Pump 2) within this volume was adjusted according to the stress escalation logic described above.

This feedback mechanism ensures that the bacterial population is continuously maintained near its maximum tolerated RW concentration, driving selection for adapted variants while preventing population collapse.

3.3.3 Biofilm Formation in the Morbidostat

Biofilm formation on vial walls, stirring bars, and tubing was observed as a recurring phenomenon across the experimental series, particularly in prolonged runs

($>$7 days) and at elevated RW concentrations. Biofilm accumulation interfered with the morbidostat's feedback control in two ways: (1) OD_{600} readings were inflated by the optical contribution of surface-attached biomass, leading the system to overestimate planktonic cell density and trigger inappropriate dilution events; and (2) biofilm acted as a reservoir of adapted cells that could re-seed the planktonic population after washout events, complicating the interpretation of growth rate dynamics.

Biofilm was managed operationally by periodic manual removal (scraping of vial walls, replacement of stirring bars) and by shortening run durations in later experiments. The extent of biofilm formation was documented qualitatively in the lab journal for each experiment.

3.4 Adaptive Laboratory Evolution (ALE) Protocol

3.4.1 Experimental Timeline and Phases

A total of 20 morbidostat experiments were conducted between September 2025 and February 2026: 15 targeting adaptation to RW#2 (REP_001 through REP_015, September 2025 – January 2026) and 5 targeting cross-tolerance to RW#3 (REP_016 through REP_020, January – February 2026). The experimental series followed an iterative optimization logic, with each experiment building on the findings and failures of prior runs. Two distinct phases can be identified:

Phase I: Establishment and Complex Medium (REP_001–REP_007)

All experiments used LB broth with RW#2 (pH-neutralized to 7.0). This phase established the feasibility of RW adaptation, identified key operational parameters, and produced the first confirmed adapted strains. REP_002 demonstrated adaptation to $>$21% RW before termination by contamination. REP_005 reached 72% RW in individual vials. REP_007 provided the first evidence of RW utilization as a carbon source.

Phase II: Minimal Medium and Carbon Source Testing (REP_008–REP_015)

M9 minimal medium replaced LB to decouple carbon metabolism from the complex nutrient background. REP_008 revealed significantly reduced RW tolerance under defined medium conditions. REP_011 and REP_014 (M9 without glucose) confirmed that adapted *E. coli* 498 could sustain growth using RW constituents as

the sole carbon and energy source.

Phase III: Cross-Tolerance to RW#3 (REP_016–REP_020)

Five experiments tested whether strains adapted to RW#2 retained their tolerance when exposed to RW#3 (native pH 5.56, no pH neutralisation). All Phase III experiments used LB medium. RW#3 was used at up to 100% (v/v, undiluted) as the drug stock. Pre-adapted strains from the REP_007 lineage and its descendants (REP_017_V3, REP_018_V3) were compared against wild-type controls. These results are reported in Chapter 4 (Results, Section 4.3).

The standard vial assignment across experiments was:

- **Vials 1–3:** Pre-adapted strains (from glycerol stocks of the best-performing vials of prior experiments)
- **Vial 4:** Negative control (sterile medium $\pm$ RW, no inoculation)
- **Vials 5–7:** Wild-type *E. coli* 498 (freshly revived from frozen stock)

Table 3.3: Overview of morbidostat experiments REP_001 through REP_015.

Exp.	Date	RW	Medium	Unit	Key Outcome
REP_001	2025-09-01 – 09-03	RW#2 pH 7	LB	IMC1	No growth; initial RW too high
REP_002	2025-09-03 – 09-15	RW#2 pH 7	LB	IMC1	Adaptation observed; $>$21% RW. Contamination
REP_003	2025-09-15 – 09-23	RW#2 pH 7	LB	IMC1	Contamination; filter blockage
REP_004	2025-09-24 – 10-03	RW#2 pH 7	LB	IMC1	Contamination day 4; OD threshold adjusted
REP_005	2025-09-30 – 10-10	RW#2 pH 7	LB	IMC2	72% RW in some vials; contamination day 3
REP_006	2025-10-09 – 10-24	RW#2 pH 7	LB	IMC1	Data quality insufficient

Exp.	Date	RW	Medium	Unit	Key Outcome
REP_007	2025-10-17 – 11-05	RW#2 pH 7	LB	IMC1	Evidence of RW as carbon source
REP_008	2025-10-24 – 11-03	RW#2 pH 7	M9+Glc	IMC1	First M9 run; reduced tolerance vs. LB
REP_009	2025-11-06 – 11-13	RW#2 pH 7	M9+Glc	IMC1	Data loss; high OD deviation
REP_010	2025-11-06 – 12-01	RW#2 pH 7	M9+Glc	IMC2	Low inoculum; biofilm interference
REP_011	2025-11-18 – 11-30	RW#2 pH 7	M9−Glc	IMC1	Growth without glucose confirmed
REP_012	2025-12-04 – 12-09	RW#2 pH 7	M9+Glc	IMC3	Complete data loss (software bug)
REP_013	2025-12-04 – 12-11	RW#2 pH 7	M9+Glc	IMC1	Pump 2 air leak; aborted
REP_014	2025-12-11 – 01-05	RW#2 pH 7	M9−Glc	IMC2	Growth without glucose confirmed (extended)
REP_015	2025-12-11 – 01-05	RW#2 pH 7	M9+Glc	IMC1	High variability between replicates
Phase III: Cross-tolerance to RW#3 (no pH neutralisation, native pH 5.56)					
REP_016	2026-01-13 – 01-14	RW#3	LB	IMC1	Drug pump failure; data unusable
REP_017	2026-01-12 – 01-19	RW#3	LB	IMC3	Cross-tolerance confirmed; WT $\sim$50%
REP_018	2026-01-21 – 01-26	RW#3	LB	IMC3	V3 reached 91%; OD feedback loop discovered
REP_019	2026-01-28 – 02-05	RW#3	LB	IMC3	Contamination; aborted

Exp.	Date	RW	Medium	Unit	Key Outcome
REP_020	2026-02-12 – 02-19	RW#3	LB	IMC3	Growth stagnation; max. concentration attempts

3.4.2 Stress Ramps and Adaptation Thresholds

The morbidostat's feedback control imposes a dynamic stress ramp that is not pre-programmed but emerges from the interplay between bacterial growth rate and the system's dilution logic (Section 3.3.2). The effective stress trajectory depends on the following configurable parameters:

- **Starting drug concentration** (`dose_init`): The RW concentration (% v/v) at experiment start. Set between 1% and 10% across the series, depending on the strain's prior adaptation history.
- **Dose increase factor/amount** (`dose_increase_factor`, `dose_increase_amount`): The multiplicative and/or additive increment applied when growth rate exceeds the escalation threshold. Typical values: factor 1.1–1.3, amount 0.5–2.0 percentage points.
- **Growth rate thresholds**: `threshold_growth_rate_increase_stress` (above which stress escalates) and `threshold_growth_rate_decrease_stress` (below which stress is relieved). These thresholds define the adaptive corridor.

Adaptation was operationally defined as sustained growth ($OD_{600} > 0.1$ with positive growth rate) at RW concentrations exceeding those tolerated by the WT control vials under the same conditions. A strain was considered "adapted" for propagation to the next experiment when it maintained stable growth at $\geq$10 percentage points higher RW concentration than the concurrent WT controls for $\geq$24 h.

3.4.3 Metabolic Strategies: Catabolism vs. Co-metabolism

The experimental design enabled distinction between two fundamentally different metabolic strategies for RW tolerance:

Co-metabolism (M9 + glucose + RW): The bacterium grows on glucose as the primary carbon and energy source while tolerating the presence of RW constituents. RW components may be partially transformed or detoxified but are not required for growth. This was the dominant metabolic regime in LB-based experiments (REP_001–REP_007) and in M9 + glucose experiments (REP_008–REP_010, REP_012–REP_013, REP_015).

Catabolism (M9 $-$ glucose + RW): The bacterium must utilize RW constituents (primarily NPG and EG) as the sole carbon and energy source for growth. No alternative carbon source is available. This was tested in REP_011 and REP_014, both of which confirmed that adapted *E. coli* 498 could sustain measurable growth under these conditions, providing direct evidence for enzymatic degradation of RW components, not merely passive tolerance.

The distinction between co-metabolism and catabolism is central to the thesis question of whether biological treatment can reduce the chemical oxygen demand of the RW, as only catabolic degradation removes organic carbon from the waste stream. Co-metabolic tolerance, while valuable for process robustness, does not by itself achieve remediation.

3.5 Growth Monitoring (OD_{600})

Culture density was monitored continuously via the Replifactory's built-in photodiode sensor (Section 3.3.1) and validated periodically by offline measurement using an external spectrophotometer at 600 nm. Samples were diluted in the corresponding sterile medium when OD_{600} exceeded the linear range of the instrument (typically $>$1.0).

Growth rates were estimated from OD_{600} time-series data between dilution events using the relationship:

$$r = \frac{\ln(2)}{t_d} \tag{3.1}$$

where r is the specific growth rate (h^{-1}) and t_d is the doubling time (h) estimated by the Replifactory software from the OD_{600} increase between consecutive dilution events (Rusnac, 2024).

A systematic bias in the built-in OD sensor was identified at high RW concen-

trations ($>$50% v/v), where the intrinsic absorbance of the coloured RW contributed to the OD_{600} reading independently of cell density. This artefact led to false-positive growth signals, triggering inappropriate stress escalation. External OD_{600} measurements were used to verify actual cell density in these cases.

3.6 Data Recording and Visualization

All experimental metadata (experiment ID, date range, organism, RW batch, medium, vial assignments, run parameters, and outcomes) were recorded in a structured Notion database (EcoCoat_DB_Experiments). Daily observations, deviations, and sampling events were documented in a digital lab journal (EcoCoat_DB_Lab Journal).

The Replifactory software logged OD_{600} readings, dilution events, pump volumes, and calculated drug (RW) concentrations at regular intervals throughout each run. Data were exported as CSV files for downstream analysis.

Data visualization was performed using a custom Python 3.14.2 script developed for this study, employing the pandas 3.0.1, NumPy 2.4.2, and Matplotlib 3.10.8 libraries. The script processed CSV files exported from the Replifactory software, each containing a datetime `Time` column together with pre-calculated growth rate μ (h^{-1}), OD_{600}, and RW concentration (% v/v) for each vial. Prior to plotting, growth rate values outside the range of -2.0 to $+2.0$ h^{-1} were masked as NaN to exclude artifacts introduced by dilution events. For each experiment–vial combination, a two-panel figure was generated with a shared time axis: the upper panel displayed OD_{600} as a black scatter plot with RW concentration (% v/v) overlaid as a green line on the right y-axis; the lower panel displayed the filtered growth rate as a blue scatter plot with the same concentration line repeated on the right y-axis. Figures were exported as PNG files at 300 DPI (10×8 inch format) following the naming convention `REP_XXX_vialY_plot.png`.

3.7 Ethical and Safety Considerations

E. coli 498 is classified as Risk Group 1 (BSL-1) and was handled according to standard microbiological safety practices. Reaction water was handled in a fume

hood due to the presence of volatile organic solvents (xylene, MEK, MiBK). Waste containing RW and bacterial cultures was autoclaved at 121 °C for 30 min before disposal. Ethanol (96%) was added to the waste collection vessels during morbidostat runs as an additional decontamination measure.

CHAPTER 4

RESULTS

This chapter presents the results of 20 morbidostat experiments (REP_001 through REP_020) targeting the adaptive laboratory evolution of *E. coli* 498 to industrial reaction water. Results are organised chronologically within three experimental phases: Phase I (REP_001–REP_007) established adaptation to RW#2 in complex medium (LB); Phase II (REP_008–REP_015) tested RW#2 tolerance under defined minimal medium (M9) conditions, distinguishing co-metabolic from catabolic growth; and Phase III (REP_016–REP_020) evaluated cross-tolerance to a second RW batch (RW#3) and explored upper concentration limits.

4.1 Phase I: Adaptation in Complex Medium (REP_001–REP_007)

4.1.1 REP_001: Initial Exposure and Failure

The first experiment (1–3 September 2025) exposed wild-type *E. coli* 498 directly to RW#2 in LB broth. No sustained growth was observed in any vial except one, which showed transient OD increases that could not be reproduced. The initial RW concentration in the drug stock was set too high, exceeding the tolerance threshold of the unadapted wild-type strain. The experiment was terminated after two days. The outcome established that *E. coli* 498 cannot tolerate high concentrations of pH-neutralized RW#2 without prior adaptation, and that subsequent experiments required a lower starting concentration with gradual escalation via the morbidostat feedback loop.

4.1.2 REP_002: First Evidence of Adaptation

REP_002 (3–15 September 2025) was initiated with a lower starting RW concentration and used both pre-adapted inocula (vials 1–3, from REP_001) and wild-type controls (vials 5–7). Adaptation was observed over the 12-day run: adapted strains grew faster at equivalent RW concentrations and tolerated progressively higher lev-

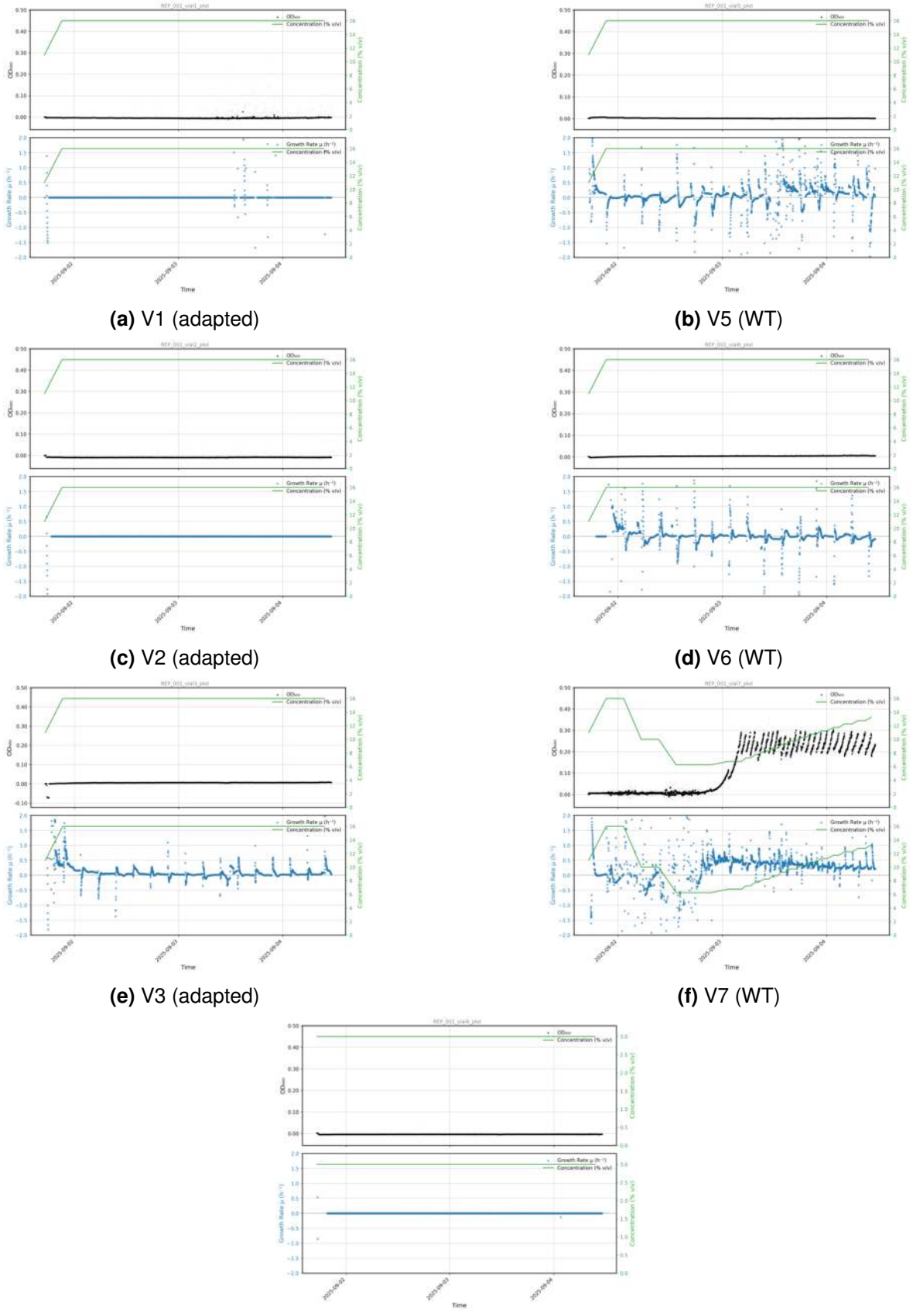

(a) V1 (adapted)

(b) V5 (WT)

(c) V2 (adapted)

(d) V6 (WT)

(e) V3 (adapted)

(f) V7 (WT)

(g) V4 (NC)

Figure 4.1: OD_{600}, RW concentration (% v/v), and growth rate μ (h^{-1}) for all seven vials of REP_001 (1–3 September 2025). V1–V3: *E. coli* 498 adaptation group; V4: sterile negative control; V5–V7: wild-type. No sustained growth was observed except in V7 (see Appendix A).

els. The best-performing vials (V2, V3, V5) reached RW concentrations exceeding 21% (v/v) before the experiment was terminated due to contamination from day 12 onward. The lag phase following inoculation lasted approximately 10 hours.

Despite the contamination-forced termination, REP_002 provided the first clear evidence that *E. coli* 498 could adapt to RW#2 under morbidostat selection. Cultures from V2, V3, and V5 were harvested by centrifugation, resuspended in 25% (v/v) glycerol in LB, and cryopreserved at -80 °C for use in subsequent experiments. This established the propagation lineage that carried through the remainder of the experimental series.

4.1.3 REP_003: Contamination and Filter Issues

REP_003 (15–23 September 2025) aimed to continue adaptation using the cryopreserved strains from REP_002. The drug stock concentration was increased to 50% (v/v) to enable higher final RW concentrations. To prevent contamination, 0.45 µm syringe filters were added to the air ventilation lines. These filters became blocked within two days and were removed on 17 September, causing the actual RW concentration delivered to the vials to deviate from the theoretical values during the early phase of the experiment.

Contamination occurred despite precautions, and attempts to rescue the cultures were largely unsuccessful. Subsequent plating of vial contents (V2 and V5) on LB agar showed homogeneous colony morphology with no obvious signs of mixed culture, raising the possibility that the observed contamination of the medium may have been *E. coli* rather than an external organism. The data from REP_003 were considered unreliable due to the compounding effects of filter blockage and contamination, and the experiment was not used for quantitative analysis.

4.1.4 REP_004 and REP_005: Parallel Runs and High RW Concentrations

REP_004 (24 September – 3 October 2025, IMC1) and REP_005 (30 September – 10 October 2025, IMC2) ran in parallel, both using cryopreserved adapted strains from REP_002 alongside wild-type controls.

In REP_004, pre-adapted strains (V1–V3) quickly reached approximately 50% RW concentration in LB. Wild-type controls eventually reached similar concentra-

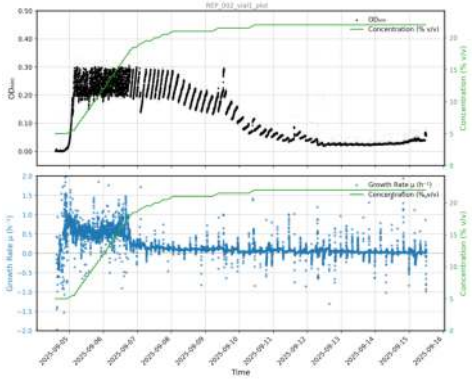

(a) V1 (adapted)

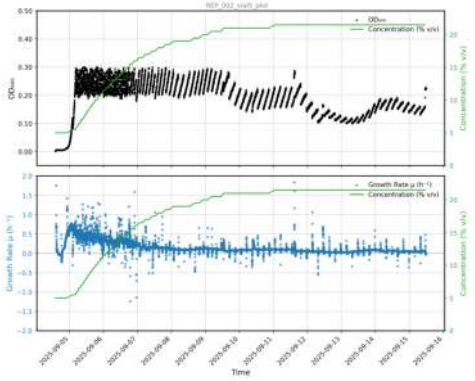

(b) V5 (WT)

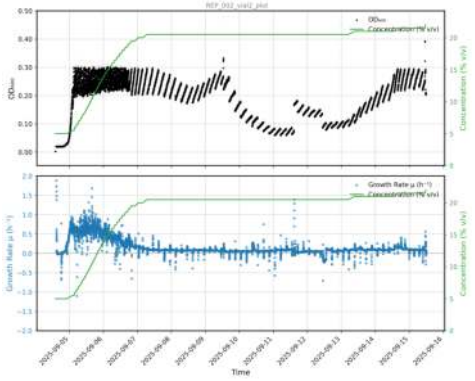

(c) V2 (adapted)

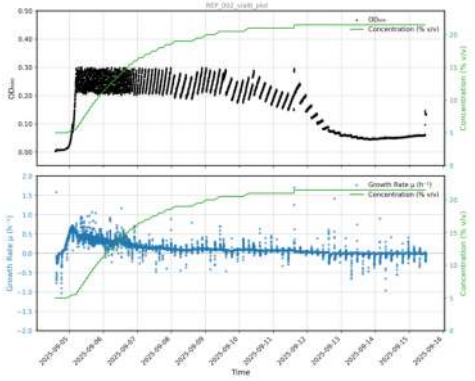

(d) V6 (WT)

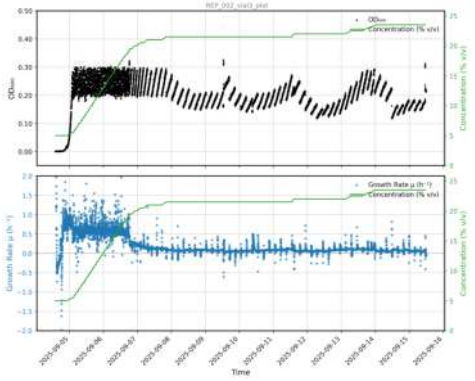

(e) V3 (adapted)

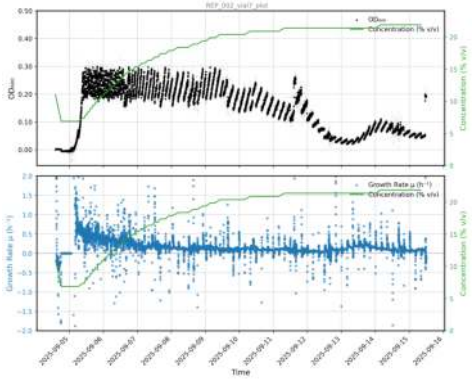

(f) V7 (WT)

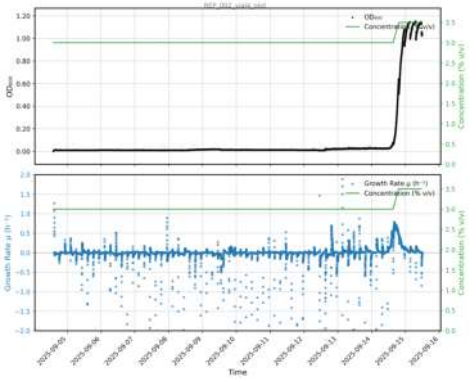

(g) V4 (NC)

Figure 4.2: OD_{600}, RW concentration, and growth rate for REP_002 (3–15 September 2025). V1–V3: pre-adapted from REP_001; V4: NC; V5–V7: WT. First clear evidence of adaptation; V2, V3, V5 reached >21% RW. Contamination from day 12. See Appendix A.

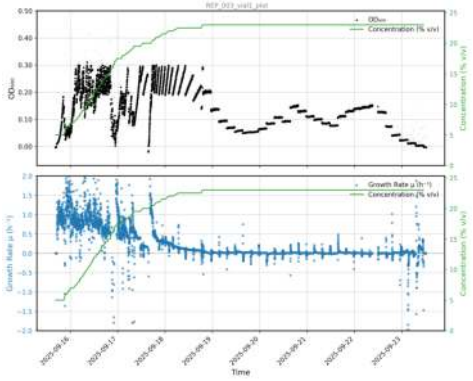

(a) V1 (adapted)

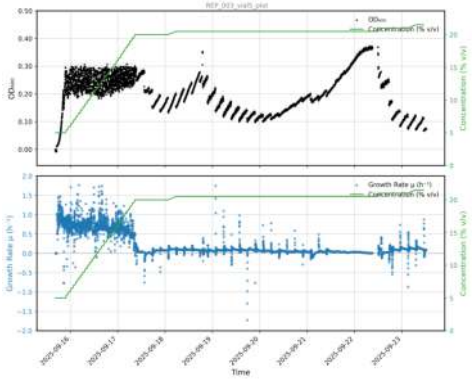

(b) V5 (adapted)

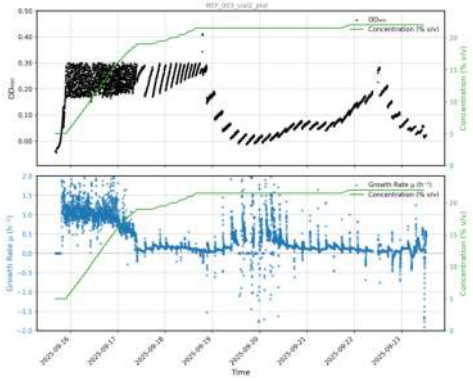

(c) V2 (adapted)

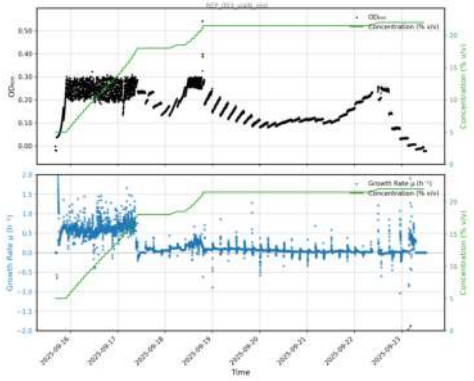

(d) V6 (adapted)

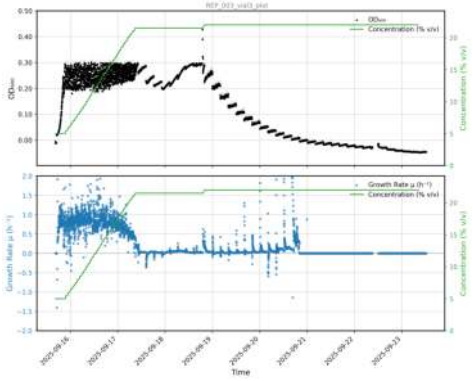

(e) V3 (adapted)

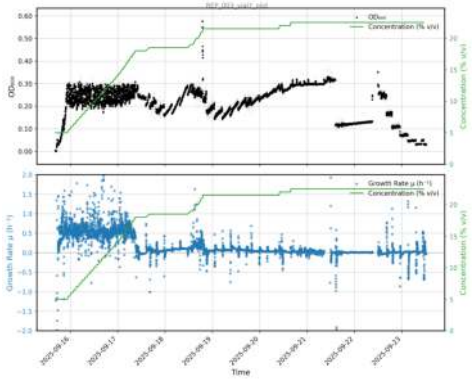

(f) V7 (adapted)

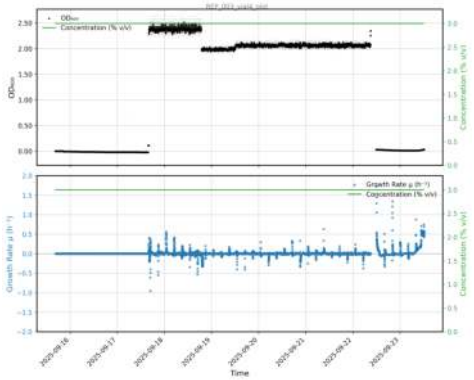

(g) V4 (NC)

Figure 4.3: OD_{600}, RW concentration, and growth rate for REP_003 (15–23 September 2025). Drug stock 50% RW#2. Filter blockage caused OD artefacts in V4 (up to 3.0 in sterile NC). Data unreliable. See Appendix A.

tions after a longer lag period, suggesting that while pre-adapted strains had a kinetic advantage, wild-type *E. coli* 498 retained some capacity for *de novo* adaptation under the morbidostat's escalating stress regime. Contamination was detected in V4 (negative control) on day 4. The OD threshold was adjusted mid-run from the default to 0.6/0.8 on 27 September to better match the growth dynamics observed. Biofilm was observed in V1–V3 and manually removed on 25 September; V4–V7 showed no visible biofilm.

REP_005 achieved the highest RW concentration observed in Phase I: individual vials reached 72% (v/v) RW#2 in LB. Contamination was detected after three days, limiting the duration of reliable data. The 100% pH 7 RW stock used in this experiment allowed the morbidostat to push concentrations substantially higher than in prior runs where the drug stock was diluted.

4.1.5 REP_006: Data Quality Failure

REP_006 (9–24 October 2025, IMC1) was intended to test the transition from LB to M9 medium. The data quality was insufficient for meaningful analysis, and the experiment did not yield usable results. No quantitative conclusions were drawn.

4.1.6 REP_007: Evidence of RW Utilization as Carbon Source

REP_007 (17 October – 5 November 2025, IMC2) was the culminating experiment of Phase I and the first to provide evidence that adapted *E. coli* 498 could utilize RW as a carbon source. Pump 1 delivered M9 with glucose and 5% RW, while Pump 2 delivered M9 without glucose and 5% RW. This design maintained a constant low-level RW background while allowing the morbidostat to vary the glucose supply through the ratio of Pump 1 to Pump 2 in each dilution event.

The experiment achieved its stated goal: growth patterns were consistent with RW utilization as a supplementary carbon source. The conclusion was qualified as requiring further validation because the experimental design did not fully eliminate glucose as a confounding carbon source. Cultures from V1 and V3 were harvested on 31 October 2025, cryopreserved in LB/glycerol, and carried forward as the adapted lineage for Phase II.

An operational incident occurred on the night of 2–3 November when the waste

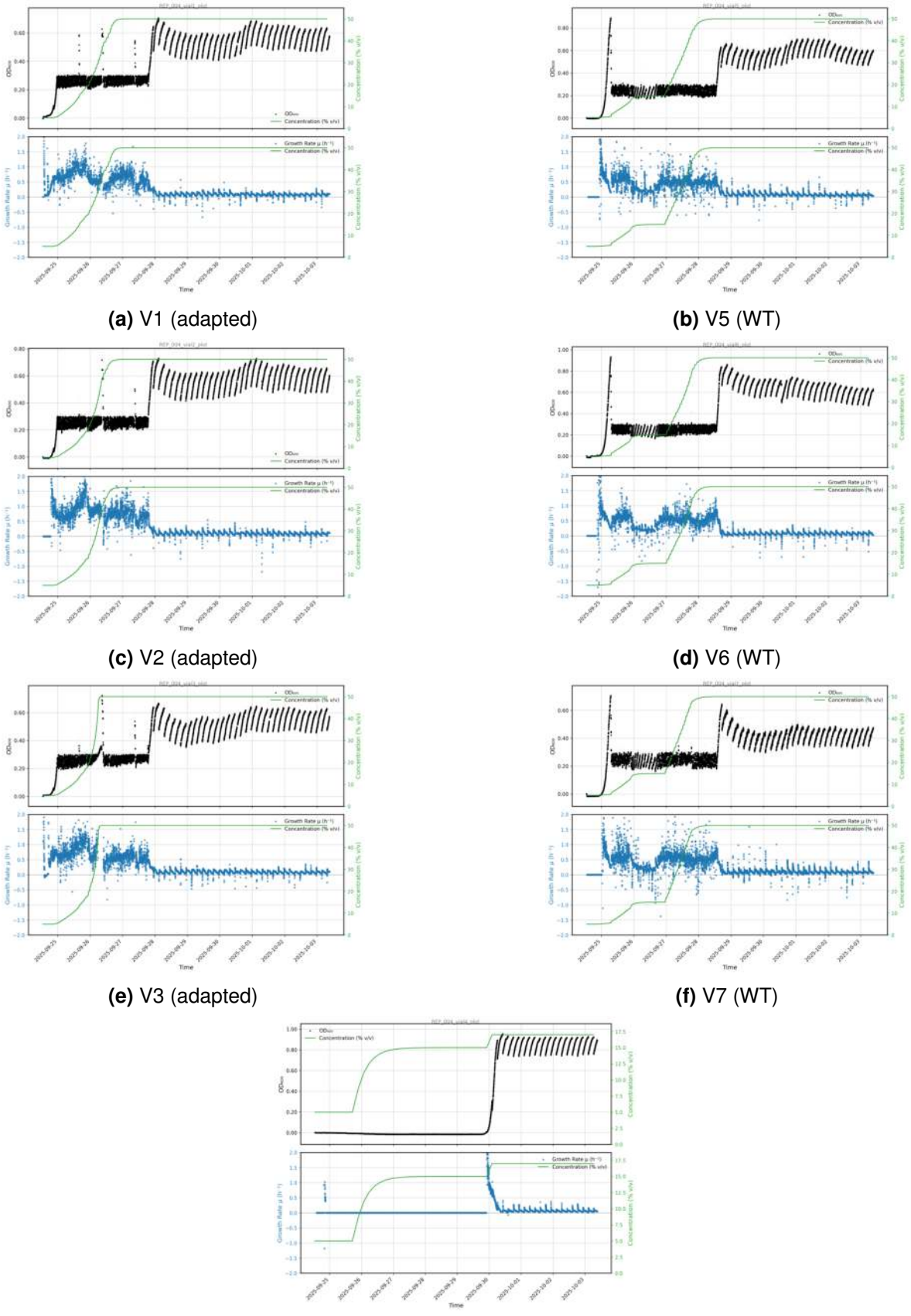

(a) V1 (adapted)

(b) V5 (WT)

(c) V2 (adapted)

(d) V6 (WT)

(e) V3 (adapted)

(f) V7 (WT)

(g) V4 (NC)

Figure 4.4: OD_{600}, RW concentration, and growth rate for REP_004 (24 Sep – 3 Oct 2025, IMC1). All six inoculated vials reached 50% RW#2 with sustained sawtooth dilution cycles for >5 days. NC contaminated day 5. See Appendix A.

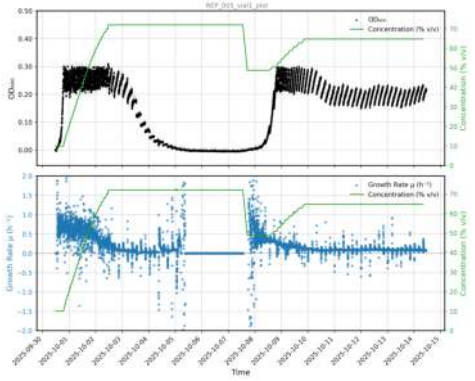

(a) V1 (adapted)

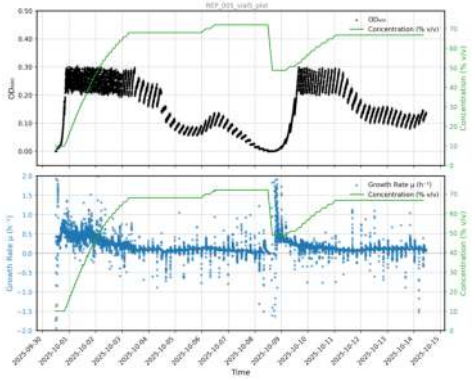

(b) V5 (WT)

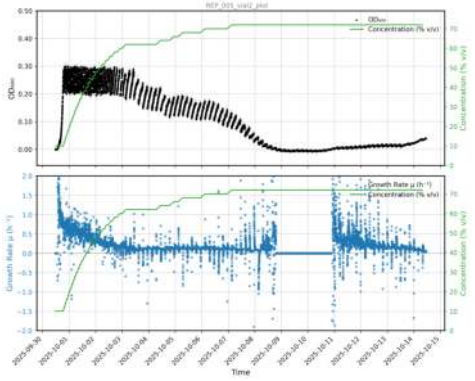

(c) V2 (adapted)

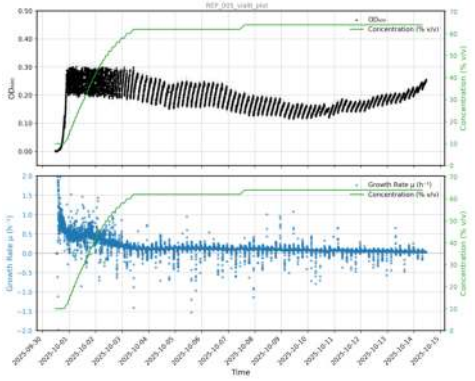

(d) V6 (WT)

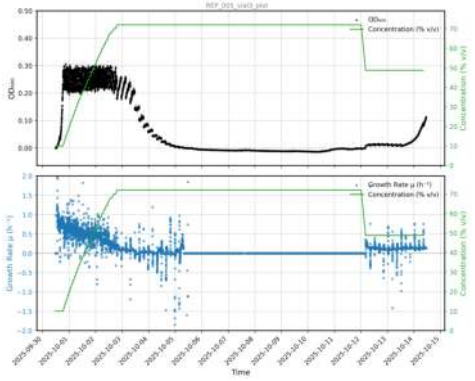

(e) V3 (adapted)

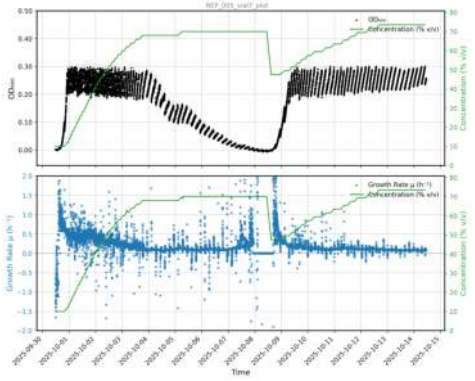

(f) V7 (WT)

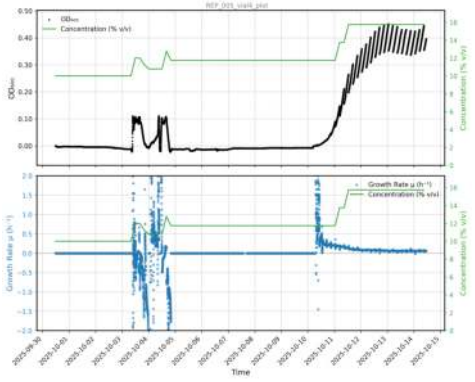

(g) V4 (NC)

Figure 4.5: OD_{600}, RW concentration, and growth rate for REP_005 (30 Sep – 10 Oct 2025, IMC2). Drug stock 100% RW#2. Highest Phase I concentration: 72% (v/v). V6 (WT) never crashed; V7 reached ∼75%. See Appendix A.

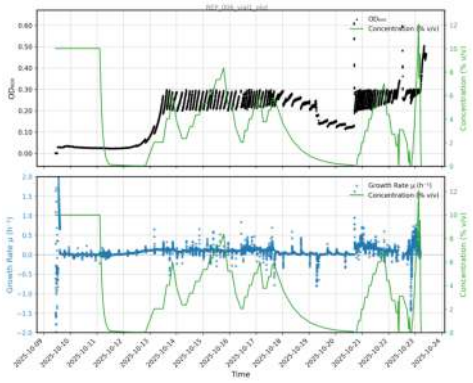

(a) V1 (adapted)

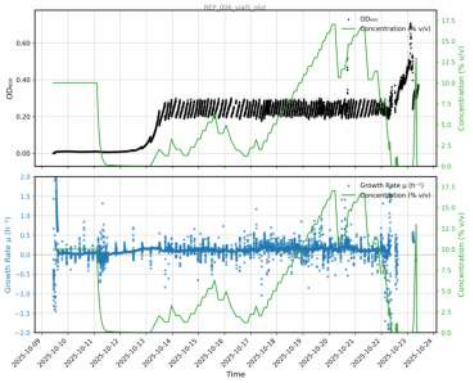

(b) V5 (WT)

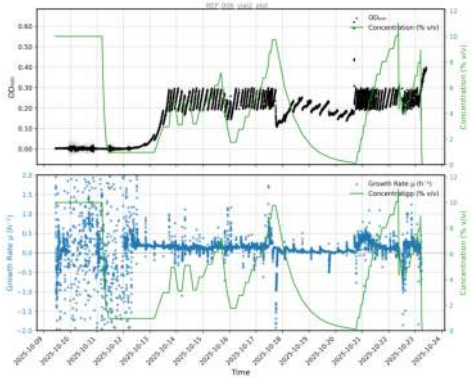

(c) V2 (adapted)

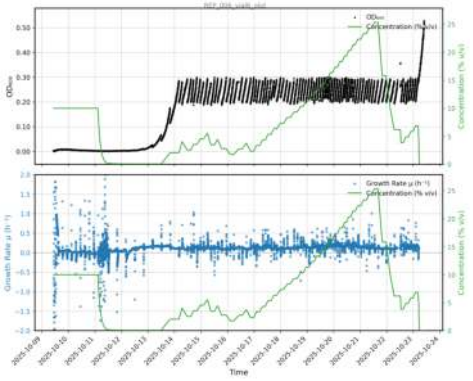

(d) V6 (WT)

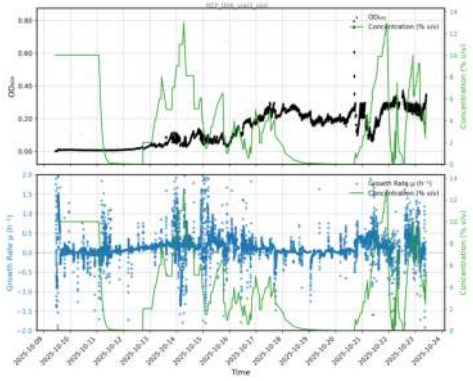

(e) V3 (adapted)

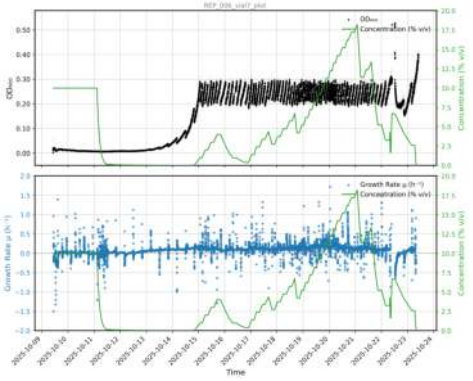

(f) V7 (WT)

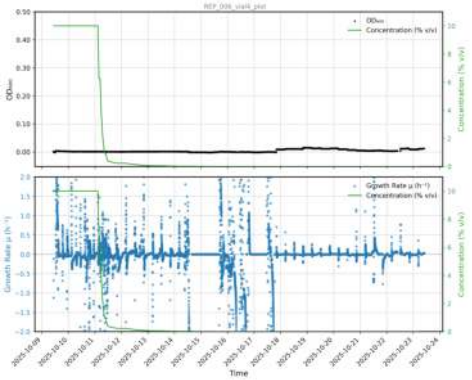

(g) V4 (NC)

Figure 4.6: OD_{600}, RW concentration, and growth rate for REP_006 (9–24 Oct 2025, IMC1). Concentration tracking malfunctioned; erratic curves. V6 and V7 (WT) showed cleanest data with smooth escalation to ∼23% and ∼18%. See Appendix A.

pump clamp opened, causing flooding. The experiment was paused for 20 minutes to allow cells to settle, and excess medium was pumped out. Data from this period were excluded from analysis.

4.1.7 Phase I Summary

Phase I established that *E. coli* 498 cannot tolerate high concentrations of RW#2 without prior adaptation (REP_001), and that morbidostat-driven ALE produces measurable adaptation within 12 days, with adapted strains tolerating $>$21% RW in REP_002 and up to 72% RW in REP_005 under LB-based conditions. Contamination was the dominant cause of experiment termination in this phase, affecting REP_002, REP_003, REP_004, and REP_005. Preliminary evidence from REP_007 suggests that adapted strains can use RW constituents as a carbon source, although this finding required validation under defined medium conditions. The propagation lineage established in Phase I was: REP_002 (V2, V3, V5) $\rightarrow$ REP_004/005 $\rightarrow$ REP_007 (V1, V3).

4.2 Phase II: Defined Medium and Carbon Source Testing (REP_008–REP_015)

4.2.1 REP_008: Transition to Minimal Medium

REP_008 (24 October – 3 November 2025) was the first experiment using M9 minimal medium with glucose. Growth was significantly slower compared to LB-based experiments, and the maximum tolerated RW concentration was substantially lower. This result demonstrated that the RW tolerance observed in Phase I was partly dependent on the nutritional richness of LB broth, which provides amino acids, vitamins, and other metabolites that may buffer against RW toxicity or support cellular repair mechanisms. Under the nutrient-limited conditions of M9, the adaptive capacity of *E. coli* 498 was reduced but not eliminated.

4.2.2 REP_009 and REP_010: Technical Failures

REP_009 (6–13 November 2025, IMC1) suffered from extensive OD measurement deviations and data loss, rendering the results unusable.

REP_010 (6 November – 1 December 2025) was compromised by insufficient

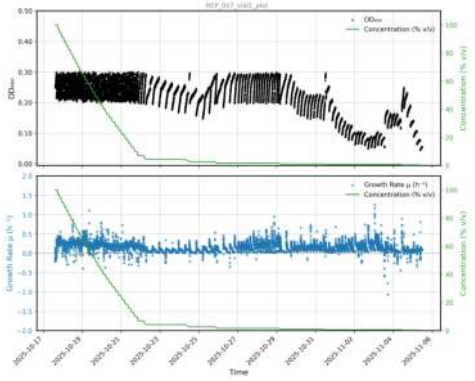

(a) V1 (adapted)

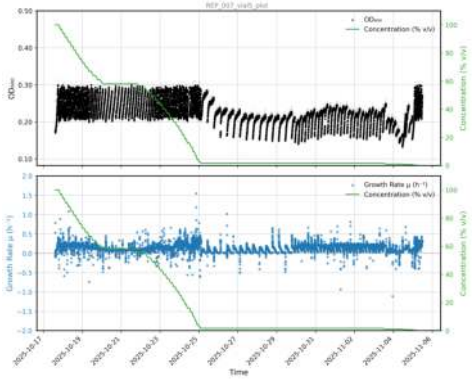

(b) V5 (WT)

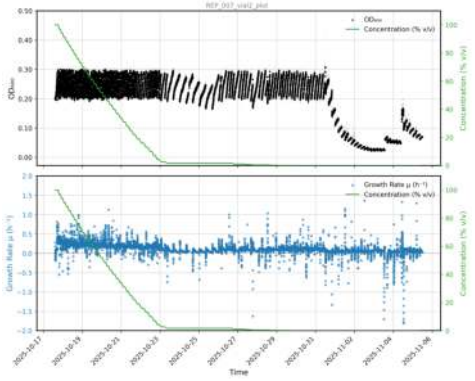

(c) V2 (adapted)

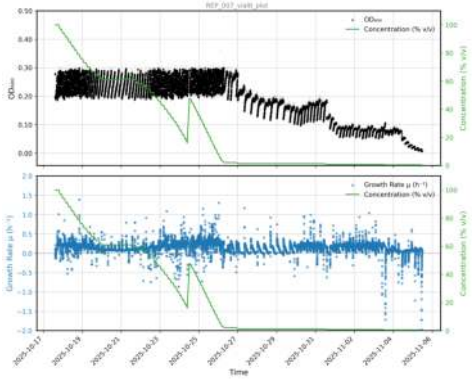

(d) V6 (WT)

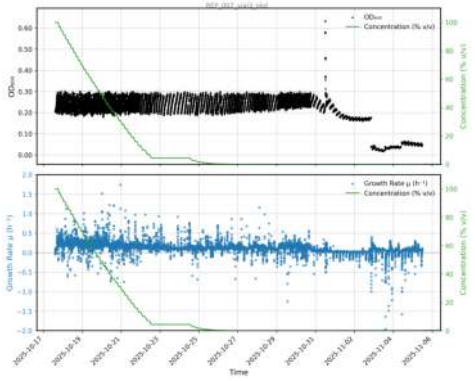

(e) V3 (adapted)

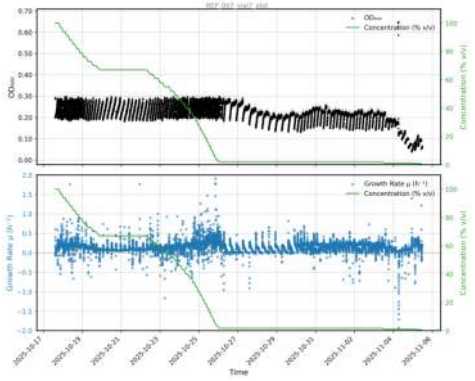

(f) V7 (WT)

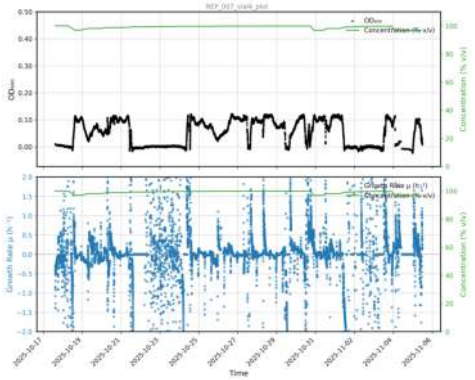

(g) V4 (NC)

Figure 4.7: OD_{600}, RW concentration, and growth rate for REP_007 (17 Oct – 5 Nov 2025, IMC2). M9 + glucose + 5% RW in both pumps. All vials grew; concentration axis tracks drug pump ratio, not actual RW exposure. Waste pump flooding 2–3 Nov crashed V2/V3 but not V5 (WT). See Appendix A.

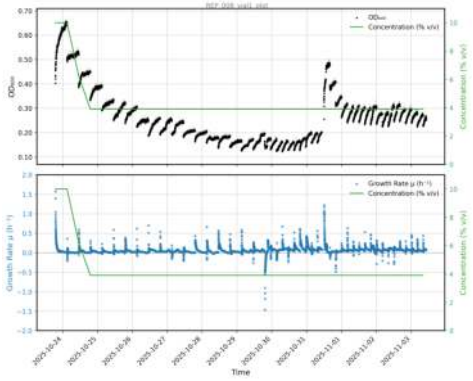

(a) V1 (adapted)

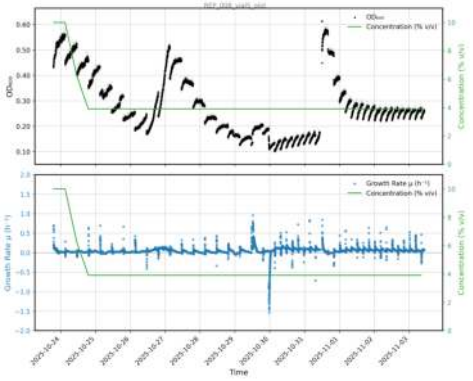

(b) V5 (WT)

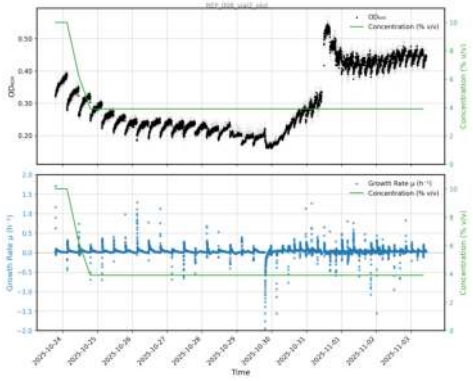

(c) V2 (adapted)

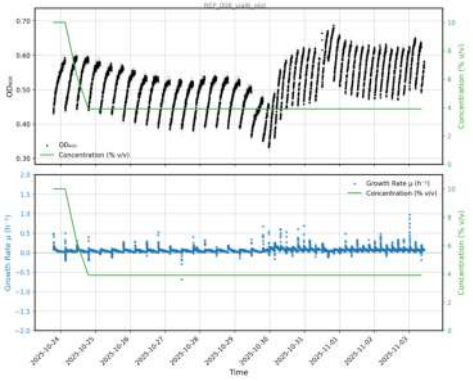

(d) V6 (WT)

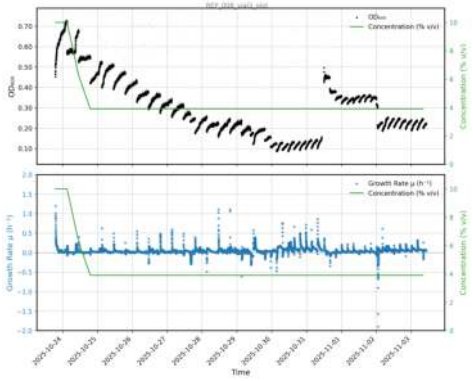

(e) V3 (adapted)

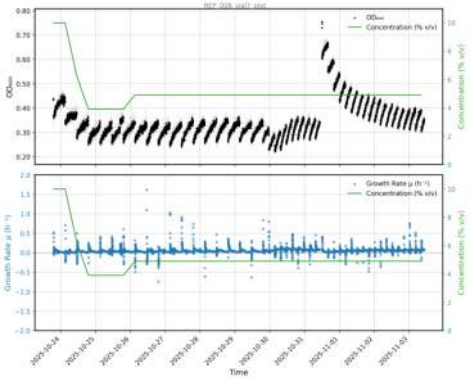

(f) V7 (WT)

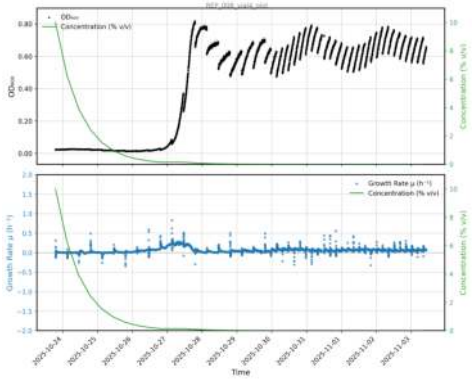

(g) V4 (NC)

Figure 4.8: OD_{600}, RW concentration, and growth rate for REP_008 (24 Oct – 3 Nov 2025, IMC1). Continuation of REP_006 vials without cleaning. RW concentration plateaued at ∼4%. NC (V4) contaminated from 27 Oct. See Appendix A.

inoculum density at startup and prolonged biofilm accumulation that progressively interfered with OD measurements over the 25-day run. The experiment demonstrated that inoculum density is a critical parameter: if the starting OD is too low, the morbidostat's feedback algorithm cannot reliably distinguish growth from noise, leading to erratic dilution behaviour.

4.2.3 REP_011: Growth Without Glucose: First Confirmation

REP_011 (18–30 November 2025, IMC1) tested whether adapted *E. coli* 498 could grow using RW as the sole carbon and energy source, without glucose supplementation (M9 − glucose). This was the key experiment for distinguishing between co-metabolic tolerance and catabolic utilization.

Growth was observed in the absence of glucose, with RW as the only available carbon source. This result provided direct evidence that adapted *E. coli* 498 could metabolize one or more RW constituents (presumably neopentyl glycol and/or ethylene glycol) sufficiently to support cell division. The experiment was affected by multiple deviations: the pH meter was not functioning reliably, the inoculum was not sufficiently dense, and biofilm interference with OD measurements increased over the 12-day run.

4.2.4 REP_012 and REP_013: Equipment Failures

REP_012 (4–9 December 2025) suffered a complete data loss due to a software bug in the Replifactory system. No experimental data were recoverable.

REP_013 (4–11 December 2025) was aborted after it was discovered that Pump 2 (M9/glucose) had an air leak and was not delivering any medium to the vials. All dilution volumes, RW concentrations, and growth data were incorrect.

4.2.5 REP_014: Growth Without Glucose: Extended Confirmation

REP_014 (11 December 2025 – 5 January 2026, IMC2) repeated the carbon source test of REP_011 over an extended period of 25 days. M9 medium was used with a glucose gradient: Pump 1 delivered M9 with glucose, while Pump 2 delivered M9 without glucose but with 5% RW (non-autoclaved). This design allowed the morbidostat to gradually shift the carbon source balance from glucose toward RW as stress escalated.

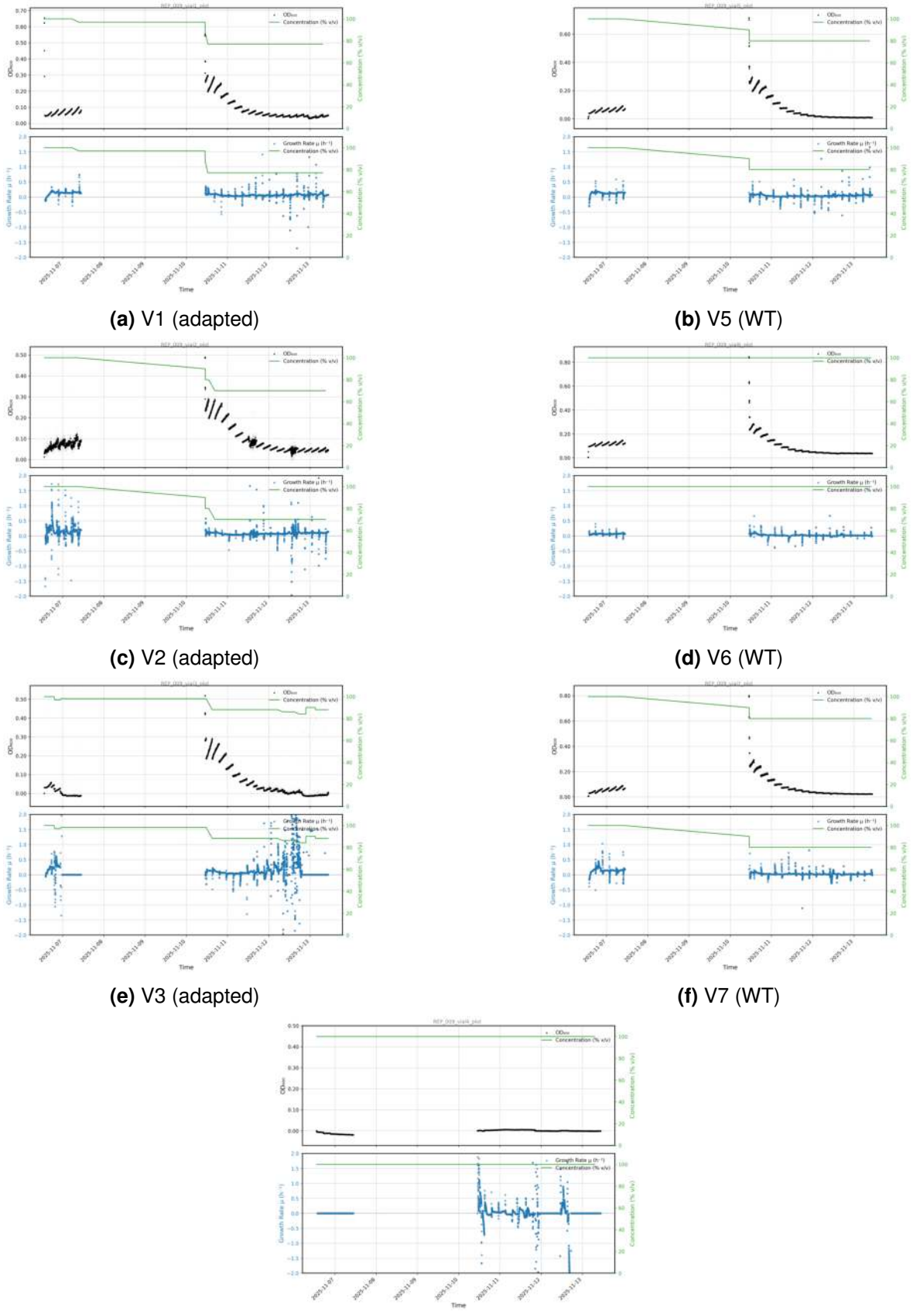

(a) V1 (adapted)

(b) V5 (WT)

(c) V2 (adapted)

(d) V6 (WT)

(e) V3 (adapted)

(f) V7 (WT)

(g) V4 (NC)

Figure 4.9: OD_{600}, RW concentration, and growth rate for REP_009 (6–13 Nov 2025, IMC1). OD sensor miscalibration (read 0.00X while external OD was 0.9–1.6); 3-day data gap. NC sterile. Data unusable. See Appendix A.

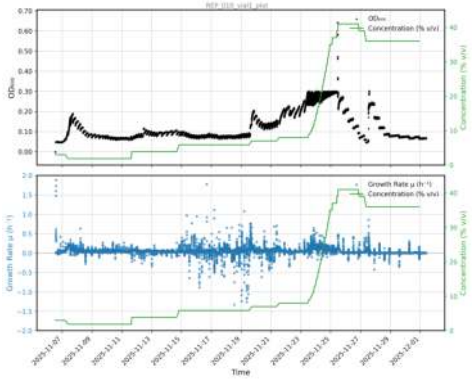

(a) V1 (adapted)

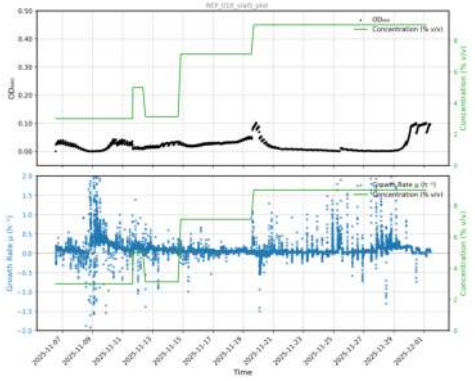

(b) V5 (WT)

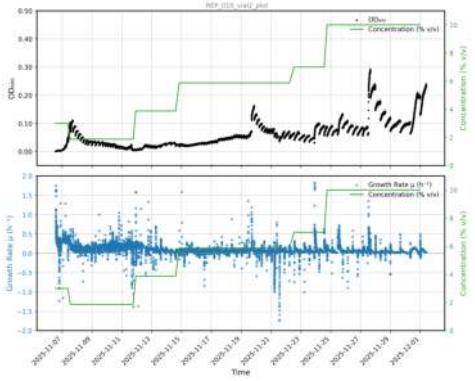

(c) V2 (adapted)

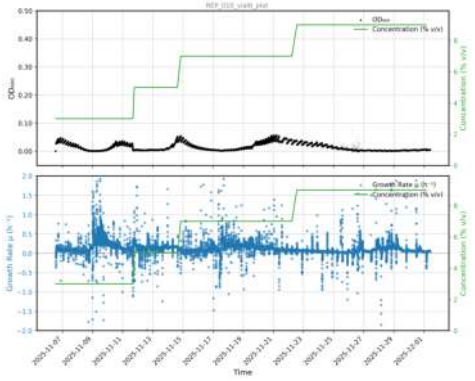

(d) V6 (WT)

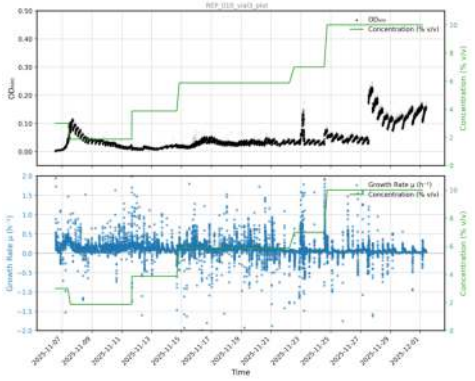

(e) V3 (adapted)

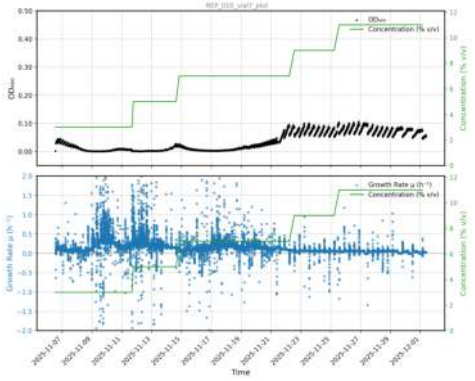

(f) V7 (WT)

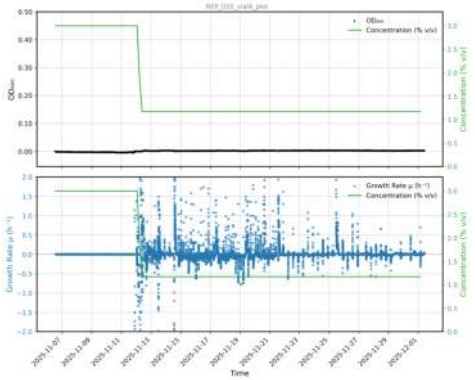

(g) V4 (NC)

Figure 4.10: OD_{600}, RW concentration, and growth rate for REP_010 (6 Nov – 1 Dec 2025, IMC2). M9 without glucose. Adapted V1 reached ∼40% RW; WT V5/V6 showed no growth over 21 days. First clear adapted vs. WT differential. See Appendix A.

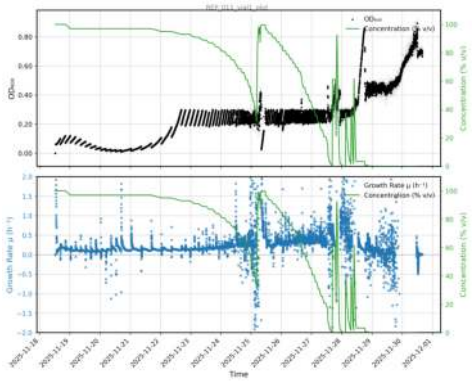

(a) V1 (adapted)

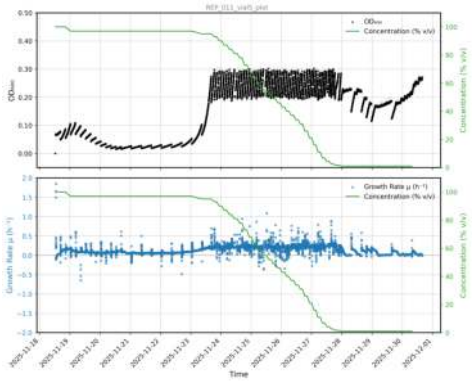

(b) V5 (WT)

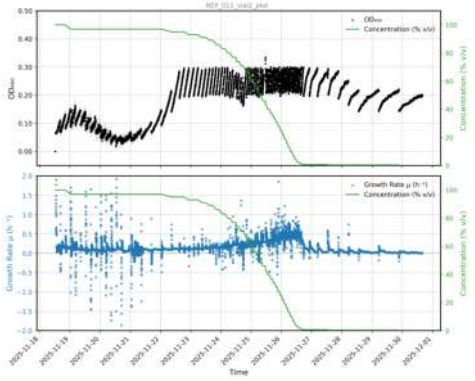

(c) V2 (adapted)

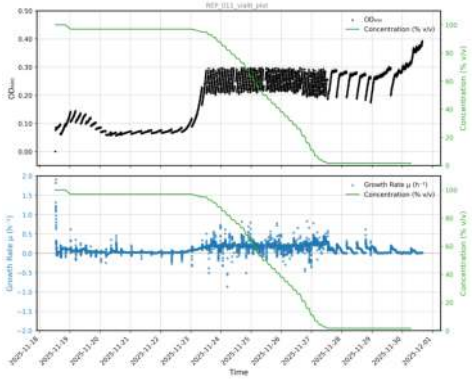

(d) V6 (WT)

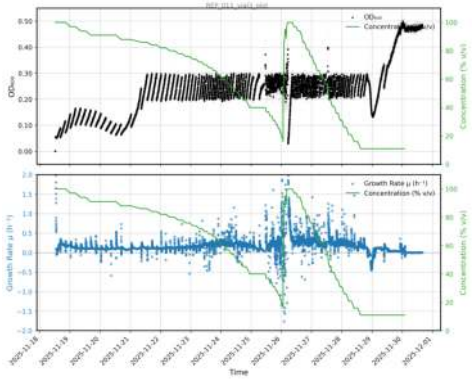

(e) V3 (adapted)

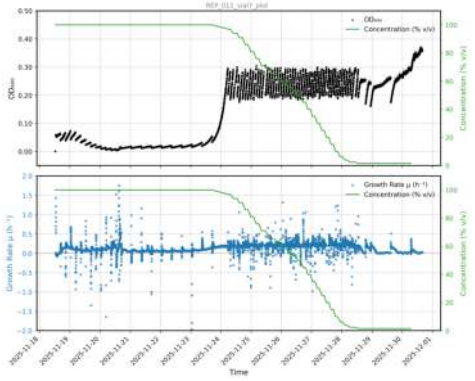

(f) V7 (WT)

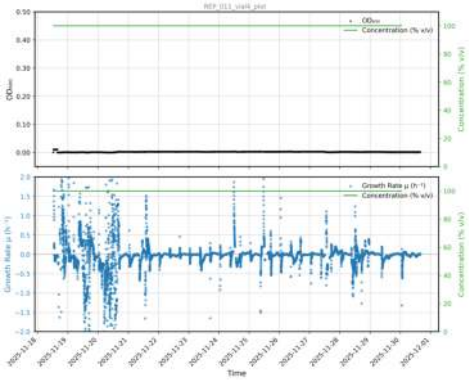

(g) V4 (NC)

Figure 4.11: OD_{600}, RW concentration, and growth rate for REP_011 (18–30 Nov 2025, IMC1). M9 without glucose + 5% RW. All six vials grew: first confirmation of catabolic growth on RW. Adapted V1–V3 showed immediate onset; WT V5–V7 lagged 4–6 days. NC sterile. See Appendix A.

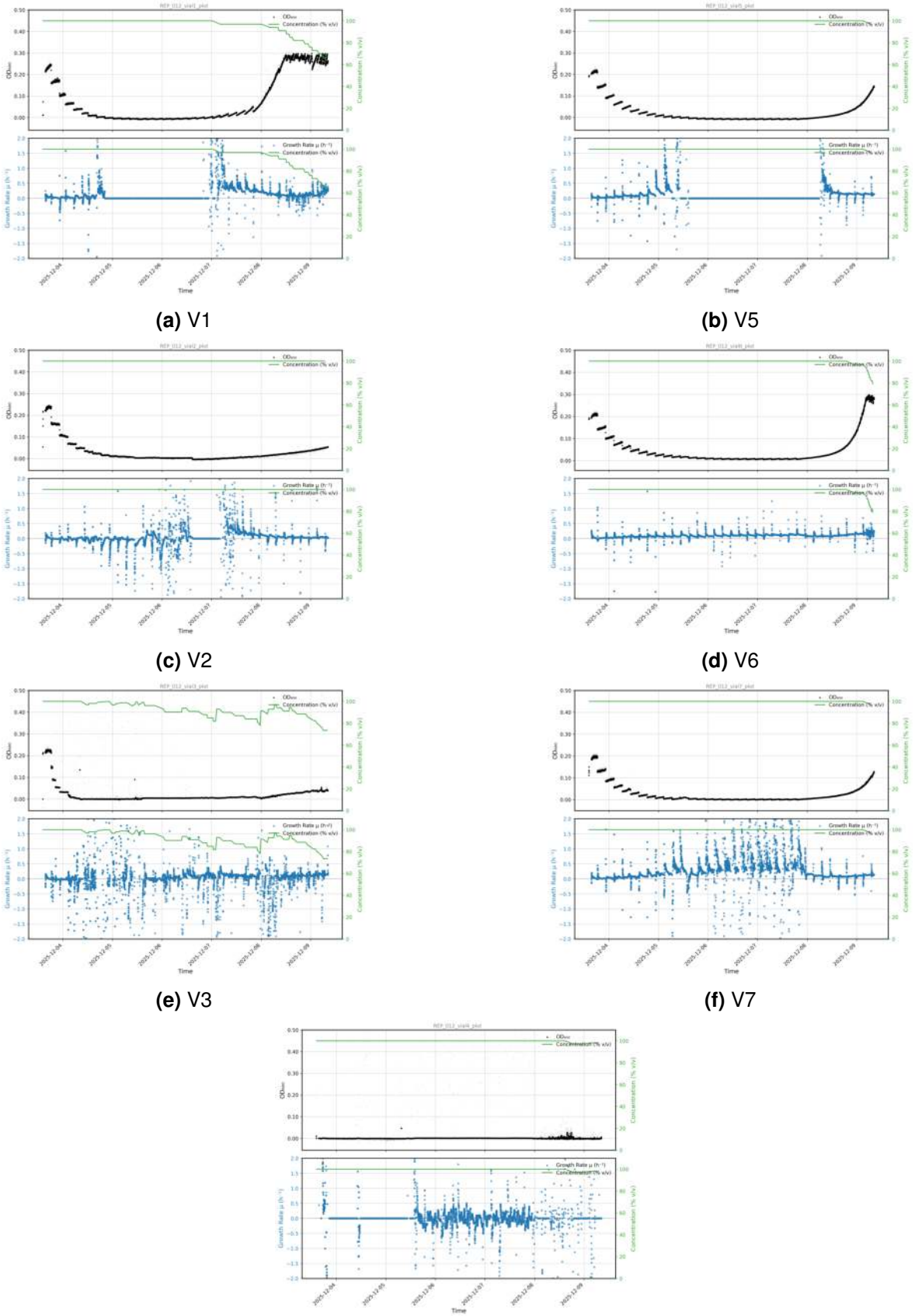

(a) V1

(b) V5

(c) V2

(d) V6

(e) V3

(f) V7

(g) V4 (NC)

Figure 4.12: OD_{600}, RW concentration, and growth rate for REP_012 (4–9 Dec 2025, IMC1). Software bug caused data loss and corruption (false OD outliers in sterile NC). Only V1 showed late recovery. See Appendix A.

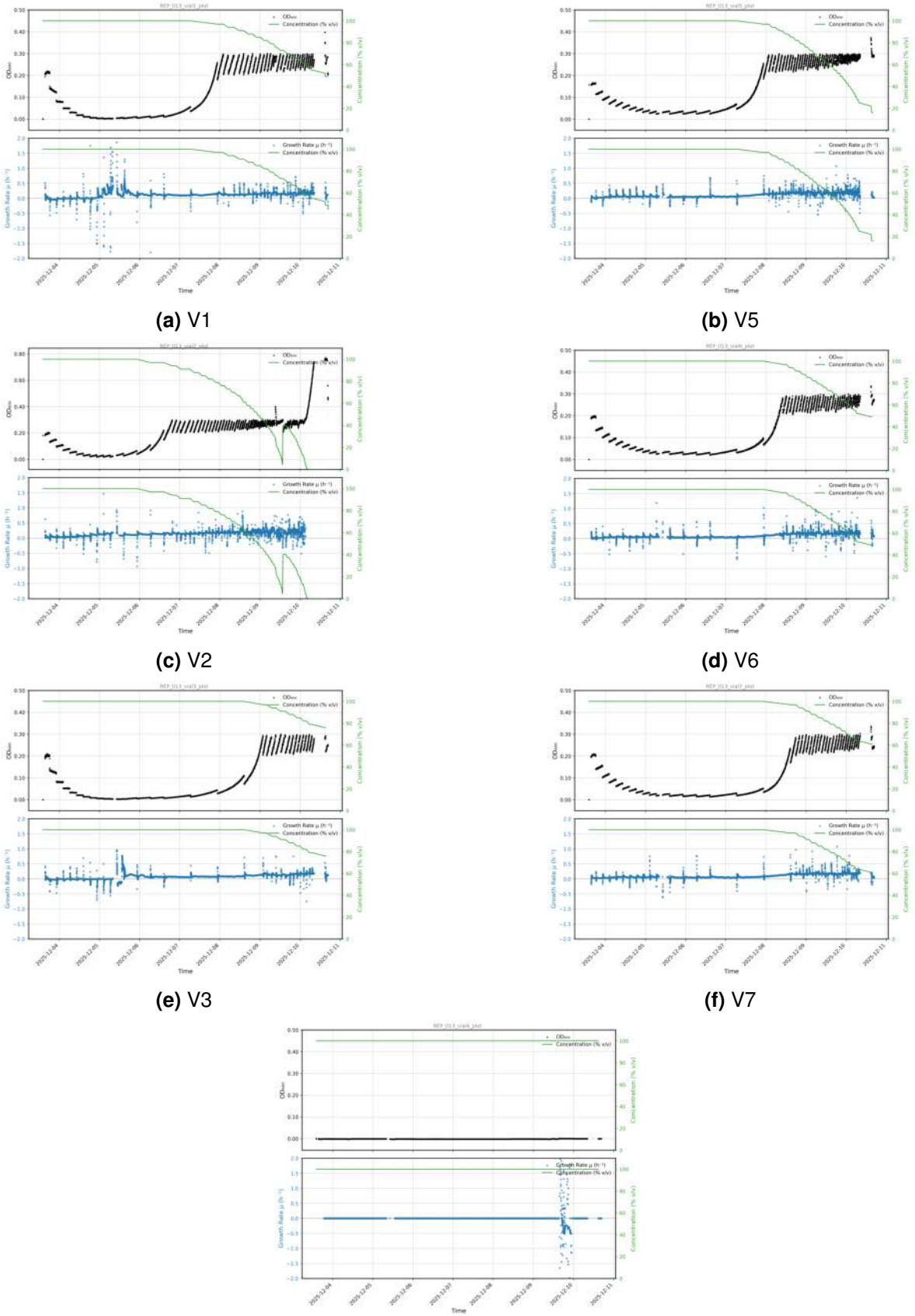

(a) V1

(b) V5

(c) V2

(d) V6

(e) V3

(f) V7

(g) V4 (NC)

Figure 4.13: OD_{600}, RW concentration, and growth rate for REP_013 (4–11 Dec 2025, IMC2). Pump 2 air leak: no medium delivered. All concentration data incorrect. Hardware reused for REP_015 without cleaning. See Appendix A.

Growth without glucose was confirmed over the extended run period. The adapted strains (inoculated at OD_{600} approximately 0.19 after 1:10 dilution) sustained positive growth rates, while wild-type controls showed no measurable growth (OD_{600} = 0 at 1:10 dilution). An operational deviation occurred when the stirrer stopped working from the night of 18–19 December, and V2 received no dilutions from 19–22 December due to a valve failure.

REP_014 confirmed the REP_011 finding with greater confidence: adapted *E. coli* 498 can sustain growth using RW constituents as a carbon and energy source, though the growth rate is substantially lower than under glucose-supplemented conditions.

4.2.6 REP_015: Co-metabolic Variability

REP_015 (11 December 2025 – 5 January 2026) ran concurrently with REP_014 but used M9 with glucose. The experiment was characterised by high variability between replicate vials. The deviation between replicates made it difficult to draw firm quantitative conclusions about the maximum tolerated RW concentration under co-metabolic conditions in M9.

4.2.7 Phase II Summary

Phase II showed that RW tolerance is reduced in M9 minimal medium relative to LB, confirming that the nutritional background influences the adaptive capacity (REP_008). Adapted *E. coli* 498 nevertheless grew using RW as the sole carbon source in REP_011 and REP_014, providing direct evidence for catabolic utilisation of RW constituents. Technical failures (data loss, equipment malfunction, software bugs) affected four of eight experiments in Phase II (REP_009, REP_010, REP_012, REP_013), which reflects the operational challenges of morbidostat-based ALE on open-source prototype hardware.

4.3 Phase III: Cross-Tolerance to RW#3 (REP_016–REP_020)

Following the completion of the RW#2 adaptation series (REP_001–REP_015), five additional morbidostat experiments were conducted using a second batch of reaction water, RW#3 (native pH 5.56), from the same Količevo production process. RW#3 was used without pH neutralisation. All Phase III experiments used LB

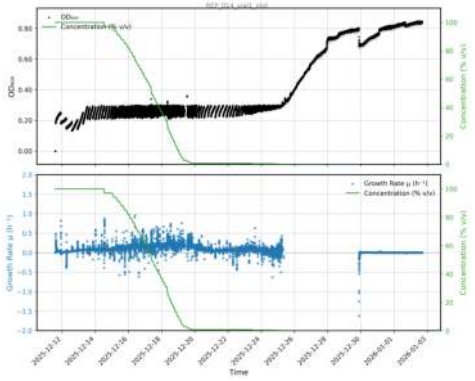

(a) V1 (adapted)

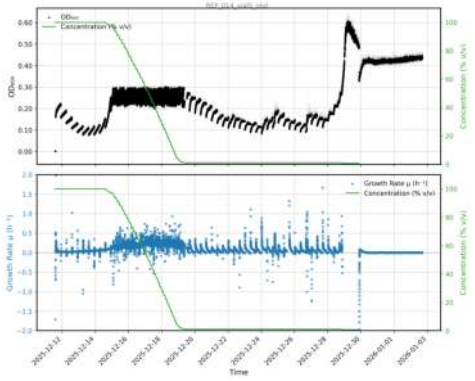

(b) V5 (WT)

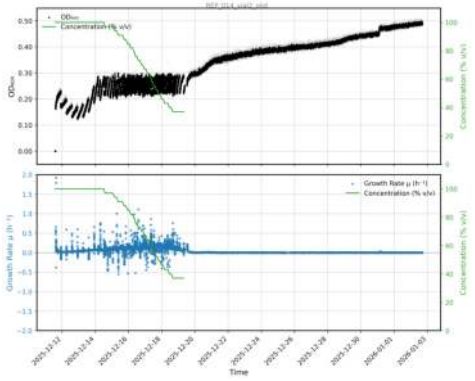

(c) V2 (adapted)

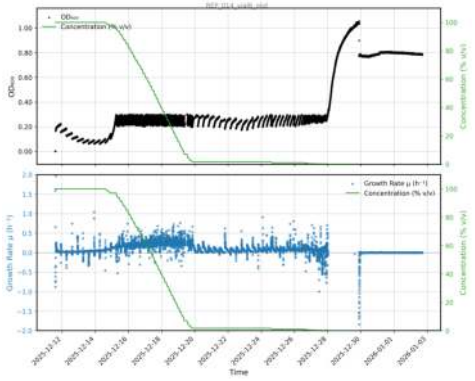

(d) V6 (WT)

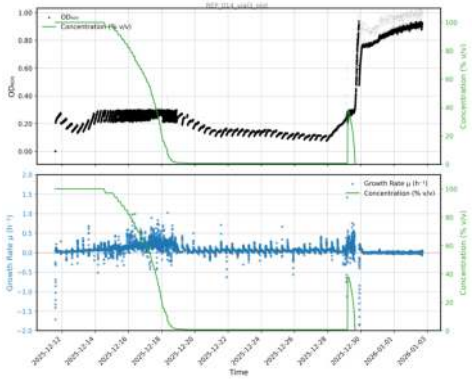

(e) V3 (adapted)

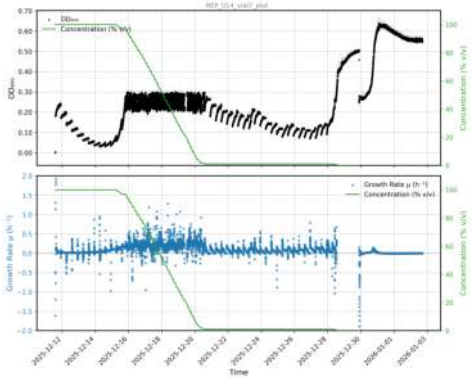

(f) V7 (WT)

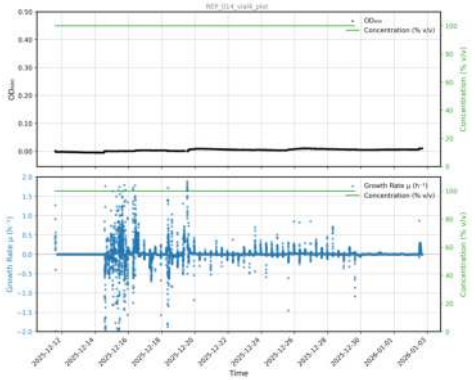

(g) V4 (NC)

Figure 4.14: OD_{600}, RW concentration, and growth rate for REP_014 (11 Dec 2025 – 5 Jan 2026, IMC2). M9 glucose gradient → 0% glucose by day 8. All six vials sustained growth after glucose elimination. V1 showed clearest catabolic signal (OD 0.30, sawtooth at 0% glucose). NC sterile. See Appendix A.

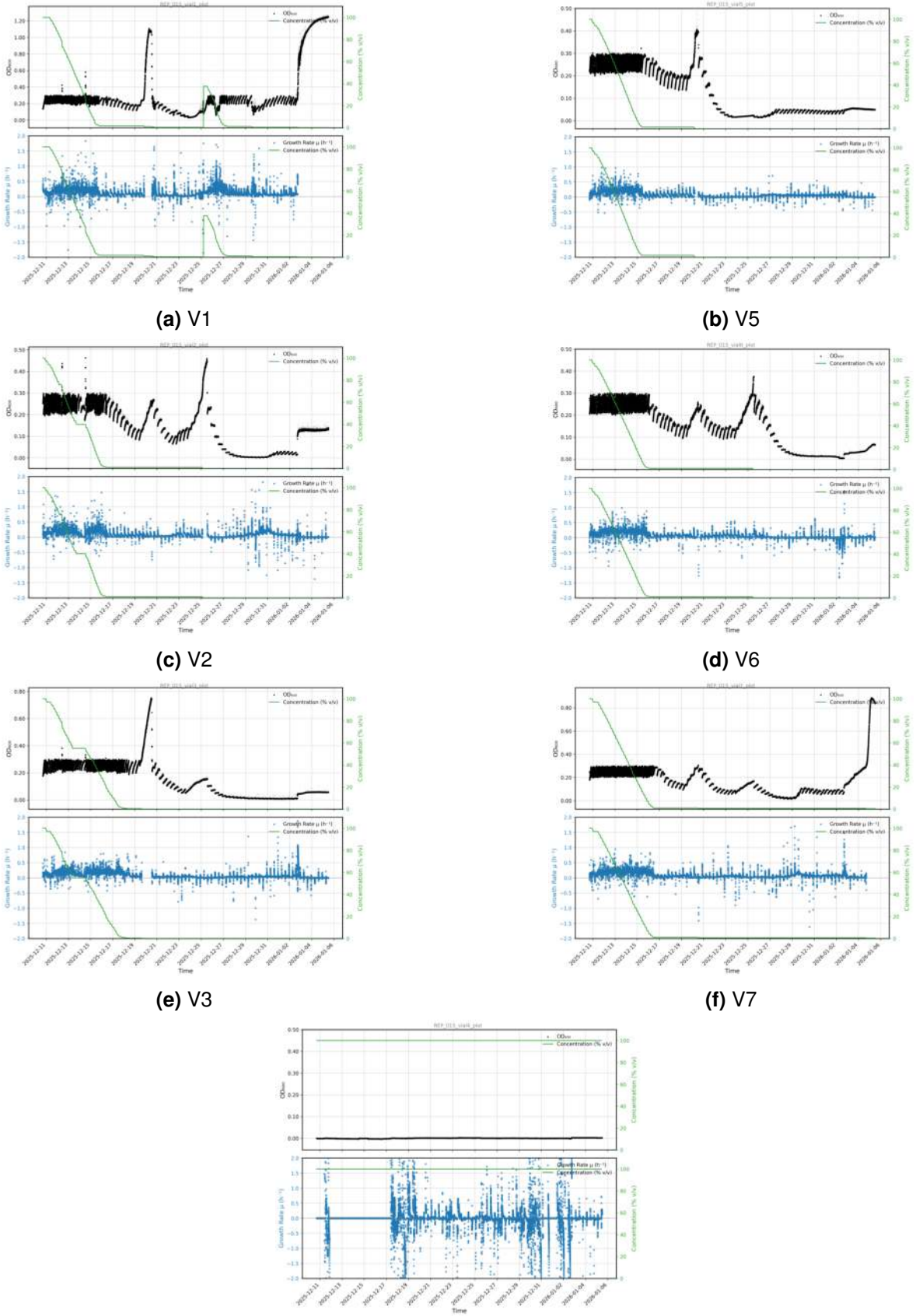

(a) V1

(b) V5

(c) V2

(d) V6

(e) V3

(f) V7

(g) V4 (NC)

Figure 4.15: OD_{600}, RW concentration, and growth rate for REP_015 (11 Dec 2025 – 5 Jan 2026, IMC2). Hardware reused from REP_013 without cleaning. Concentration reached 0% within 4–7 days. OD spikes to 0.75–1.15 around day 9 (biofilm). Suction tube incident 22 Dec invalidated late data. NC sterile. See Appendix A.

medium. The primary objective was to determine whether strains adapted to RW#2 retained their tolerance when exposed to a chemically distinct RW batch, and to explore the upper concentration limits achievable with the adapted lineage.

RW#3 differed from RW#2 in two experimentally relevant respects: (1) a higher native pH (5.56 vs. 1.88), meaning that the proton-driven component of toxicity was reduced; and (2) a darker colour (OD_{600} of 0.21–0.26 for the blank), which interfered with the morbidostat's photodiode-based growth monitoring at high concentrations. Direct comparison of concentration values between RW#2 and RW#3 experiments is therefore not appropriate without accounting for these differences.

4.3.1 REP_016: Equipment Failure

REP_016 (13–14 January 2026, IMC1) was the first experiment using RW#3. The drug pump (Pump 2) did not deliver RW to the vials, rendering all concentration data incorrect. The experiment was terminated after one day. No usable data were obtained.

4.3.2 REP_017: Cross-Tolerance Confirmed

REP_017 (12–19 January 2026, IMC3) tested pre-adapted strains from the REP_007 lineage (V1–V3) and wild-type controls (V5–V7) in LB medium with 50% (v/v) RW#3 as the drug stock. Inoculation was performed by placing frozen glycerol stock crystals into 1.5 mL LB for 2 h and transferring directly to the morbidostat, without an overnight culture step.

The results demonstrated that adaptation to RW#2 conferred cross-tolerance to RW#3:

- Pre-adapted strains reached the maximum drug stock concentration (50%) faster than wild-type controls. Biofilm was observed on pre-adapted vials but not wild-type vials on the second day.
- Wild-type *E. coli* 498 also adapted to RW#3, reaching approximately 50% concentration, but with a longer lag period: reproducing the same pattern observed with RW#2 in Phase I.
- The best-performing vial was V3 (pre-adapted), which was selected for further

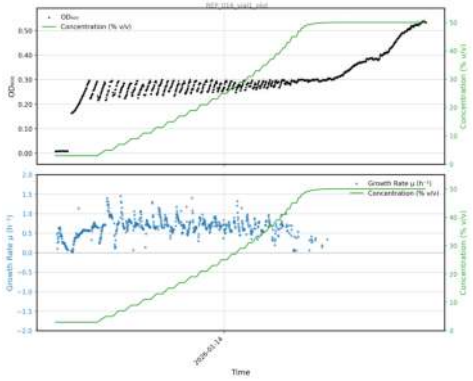

(a) V1 (adapted)

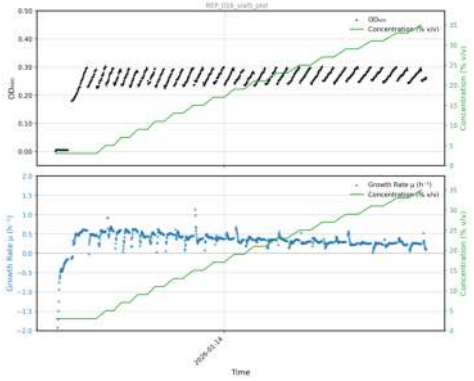

(b) V5 (WT)

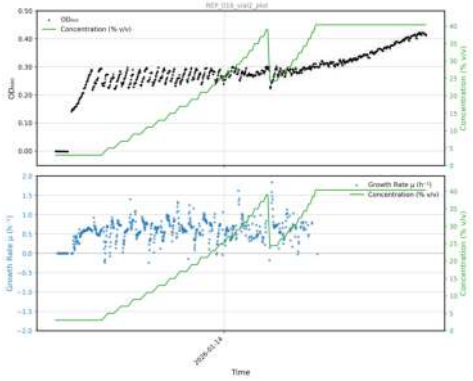

(c) V2 (adapted)

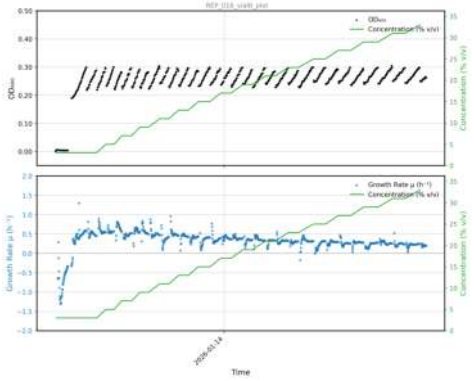

(d) V6 (WT)

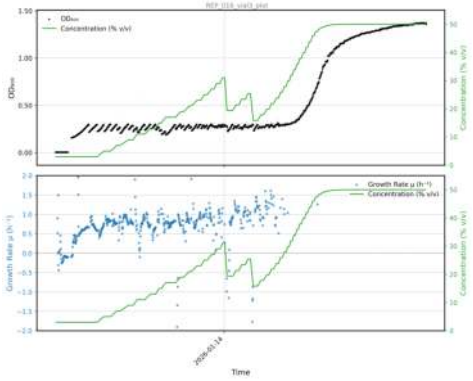

(e) V3 (adapted)

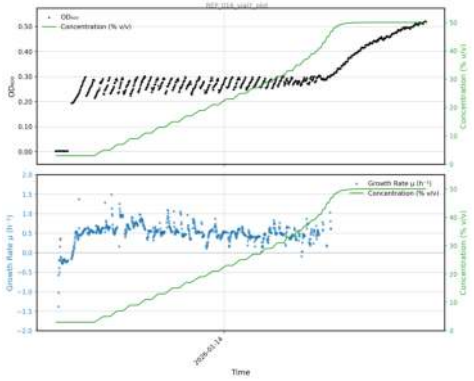

(f) V7 (WT)

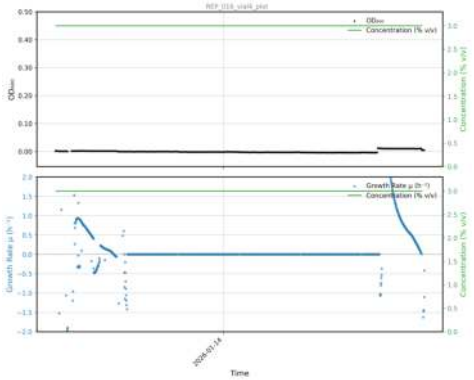

(g) V4 (NC)

Figure 4.16: OD_{600}, RW concentration, and growth rate for REP_016 (13–14 Jan 2026, IMC1). Drug pump failure: Pump 2 did not deliver RW#3 to any vial. OD rise in V1–V3 reflects growth on LB only. Experiment terminated after ∼1 day. See Appendix A.

adaptation in REP_018.

- The negative control (V4) remained sterile throughout, confirming the absence of contamination.
- An operational deviation occurred on 17 January when media ran out. Dilutions were paused, allowing cells to grow to an OD_{600} of approximately 1.1.

This result confirms that the adaptive phenotype acquired through morbidostat evolution with RW#2 is not specific to a single batch of reaction water but transfers to a different batch from the same production process, despite differences in native pH (RW#2: 1.88; RW#3: 5.56) and potentially in detailed composition.

4.3.3 REP_018: Highest RW Tolerance and OD Feedback Loop Discovery

REP_018 (21–26 January 2026, IMC3) was the final LB-based fermentation before the planned switch to M9 medium for the RW#3 series. Pre-adapted strains from the REP_017_V3 lineage (V1–V3) and wild-type controls (V5–V7) were tested with 100% (v/v, undiluted) RW#3 as the drug stock, without pH neutralisation.

REP_018 produced two key findings:

1. V3 achieved 91% RW#3 with genuine growth. Among the pre-adapted vials, V3 exhibited sustained proliferation with OD_{600} rising to 1.20–1.25 and active sawtooth dilution oscillations. The RW#3 concentration in V3 rose steadily to approximately 91% (v/v): the highest confirmed RW tolerance across the entire experimental series (Phases I–III). This demonstrates that the REP_007 $\rightarrow$ REP_017_V3 adaptation lineage can tolerate near-undiluted RW#3 with active cell proliferation.

2. V1 and V2 revealed a critical OD feedback loop artefact. In V1 and V2, the RW#3 concentration rose to 100% without any actual bacterial growth. The mechanism was a positive feedback loop: at high concentrations, the dark colour of RW#3 increased the OD_{600} reading measured by the morbidostat's photodiode sensor. The system interpreted this absorbance increase as cell growth and responded by further escalating the RW concentration, which further increased the background absorbance. This cycle drove V1 and V2 to 100% RW#3 concentration while the vials contained no detectable turbidity from cells (confirmed by camera images). After dilutions were stopped on 24 January and 2 mL LB was added, the OD_{600} in V1

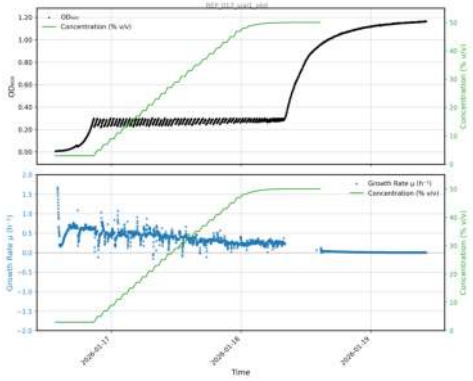

(a) V1 (adapted)

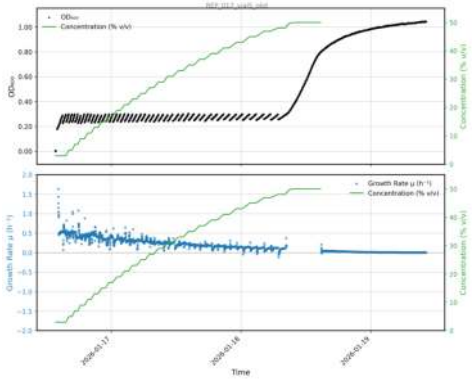

(b) V5 (WT)

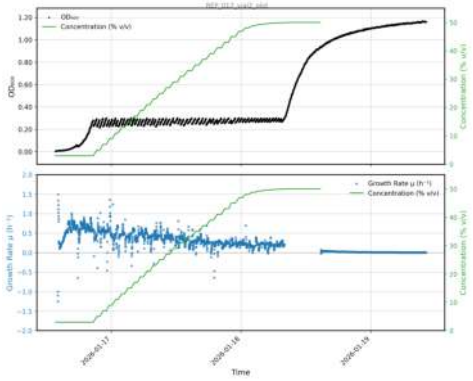

(c) V2 (adapted)

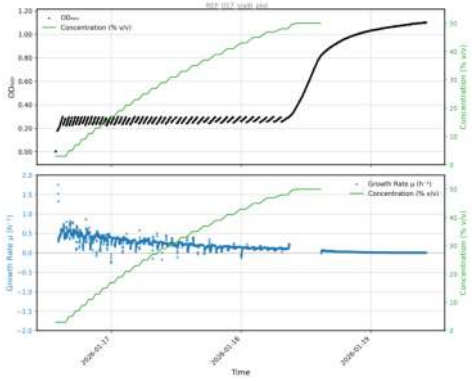

(d) V6 (WT)

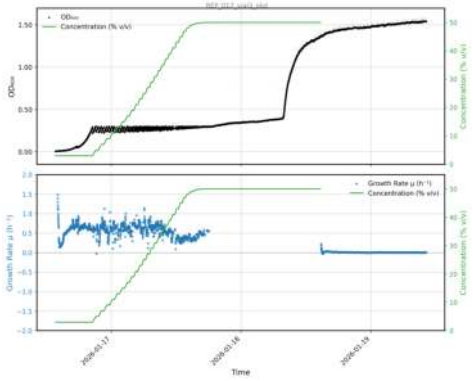

(e) V3 (adapted)

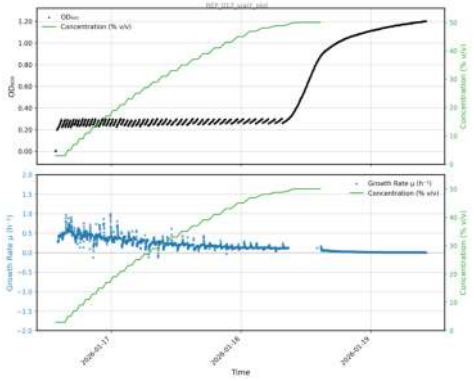

(f) V7 (WT)

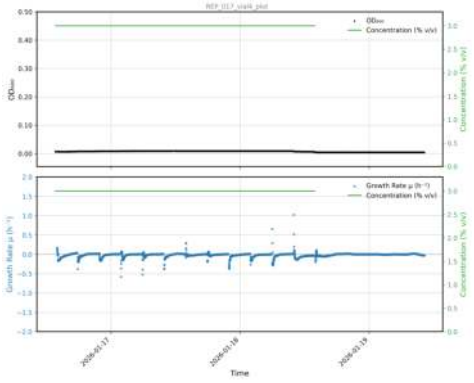

(g) V4 (NC)

Figure 4.17: OD_{600}, RW concentration, and growth rate for REP_017 (12–19 Jan 2026, IMC3). Drug stock 50% RW#3 (no pH neutralisation). Cross-tolerance confirmed: pre-adapted V1–V3 reached 50% RW#3 faster than WT V5–V7. V3 selected for REP_018. NC sterile. See Appendix A.

and V2 settled at a flat 0.37, matching the background absorbance of concentrated RW#3, with no subsequent growth.

The distinction between genuine adaptation (V3) and the measurement artefact (V1, V2) was clear: V3 showed dense, high-amplitude sawtooth oscillations at OD_{600} 1.0–1.25, while V1 and V2 showed flat OD at 0.37 after the feedback loop reached saturation.

The wild-type vials reached individual final RW#3 concentrations of 59%, 61%, and 53% (v/v) respectively (mean $\approx$57.6%), consistent with the $\sim$50% ceiling observed for wild-type *E. coli* 498 in REP_017 and in the RW#2 Phase I experiments. OD_{600} in wild-type vials rose to 0.80–1.05 with genuine sawtooth oscillations.

Contamination was detected in the negative control (V4) on 25 January. The experiment was terminated and frozen on 26 January.

The OD feedback loop represents an inherent limitation of photodiode-based growth monitoring in coloured media. Any future morbidostat work with dark-coloured feedstocks requires either OD baseline correction for the intrinsic absorbance of the medium, or an alternative growth-monitoring method.

4.3.4 REP_019: Contamination

REP_019 (28 January – 5 February 2026, IMC3) attempted to replicate REP_017 with modifications to address the OD interference. Pre-adapted strains from REP_018_V3 and wild-type controls were tested with 100% RW#3 in LB. An attempt to filter RW#3 to reduce the background OD produced no relevant change. Contamination occurred during a media refill under the Bunsen burner, contaminating the LB media flask. The experiment was terminated. No usable adaptation data were obtained.

4.3.5 REP_020: Maximum Concentration Attempt

REP_020 (12–19 February 2026, IMC3) was a replicate of the contaminated REP_019, using pre-adapted strains from REP_018_V3 and wild-type controls with 100% (undiluted) RW#3 in LB. The growth rate threshold for stress escalation was increased to 0.06 h^{-1} to accelerate concentration ramp-up, and the dose increase amount was raised from 2 to 4 percentage points during the run.

Growth stagnated: by 25 February, cells were not growing despite continued

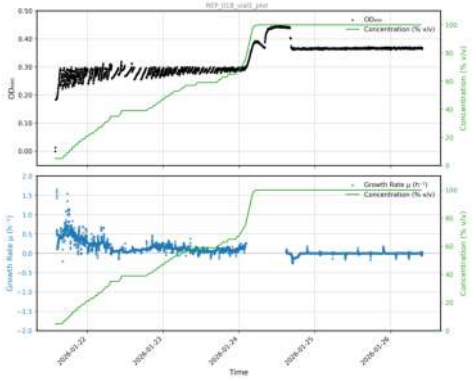

(a) V1 (adapted)

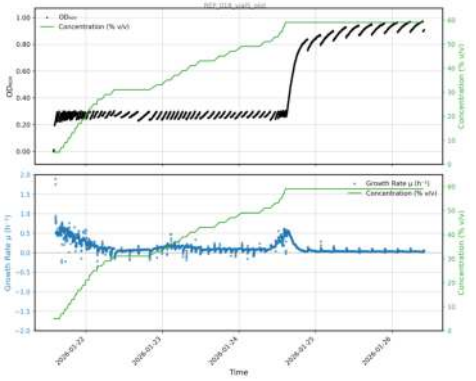

(b) V5 (WT)

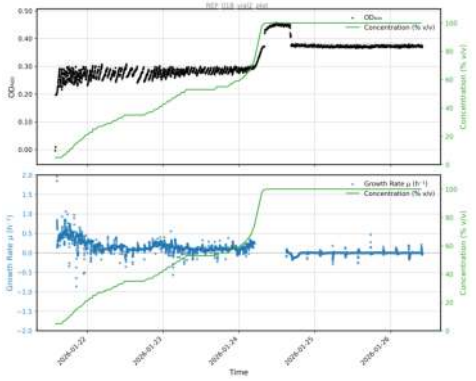

(c) V2 (adapted)

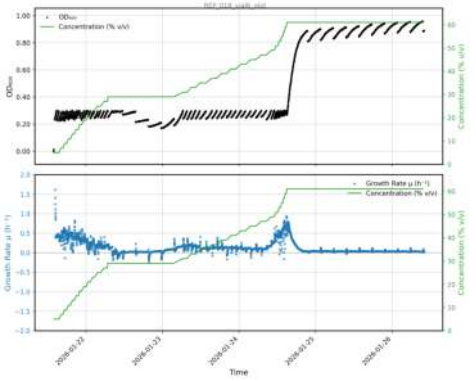

(d) V6 (WT)

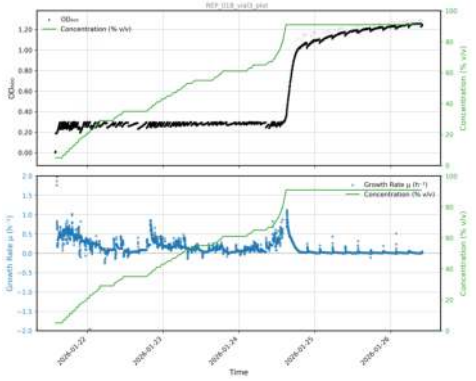

(e) V3 (adapted)

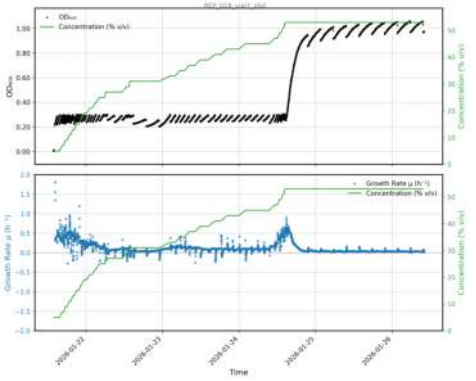

(f) V7 (WT)

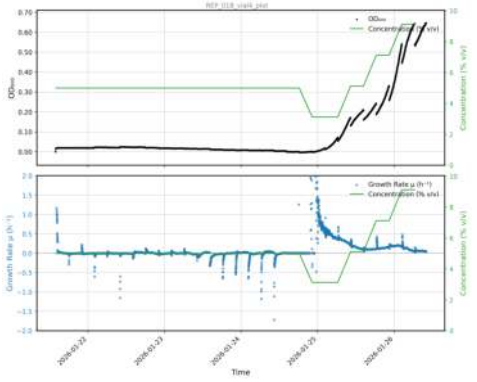

(g) V4 (NC)

Figure 4.18: OD_{600}, RW concentration, and growth rate for REP_018 (21–26 Jan 2026, IMC3). Drug stock 100% RW#3. V3 reached 91% with genuine sawtooth growth (OD 1.20–1.25). V1/V2 reached 100% via OD feedback loop artefact (no actual growth). WT V5–V7 plateaued at ∼57%. NC contaminated 25 Jan. See Appendix A.

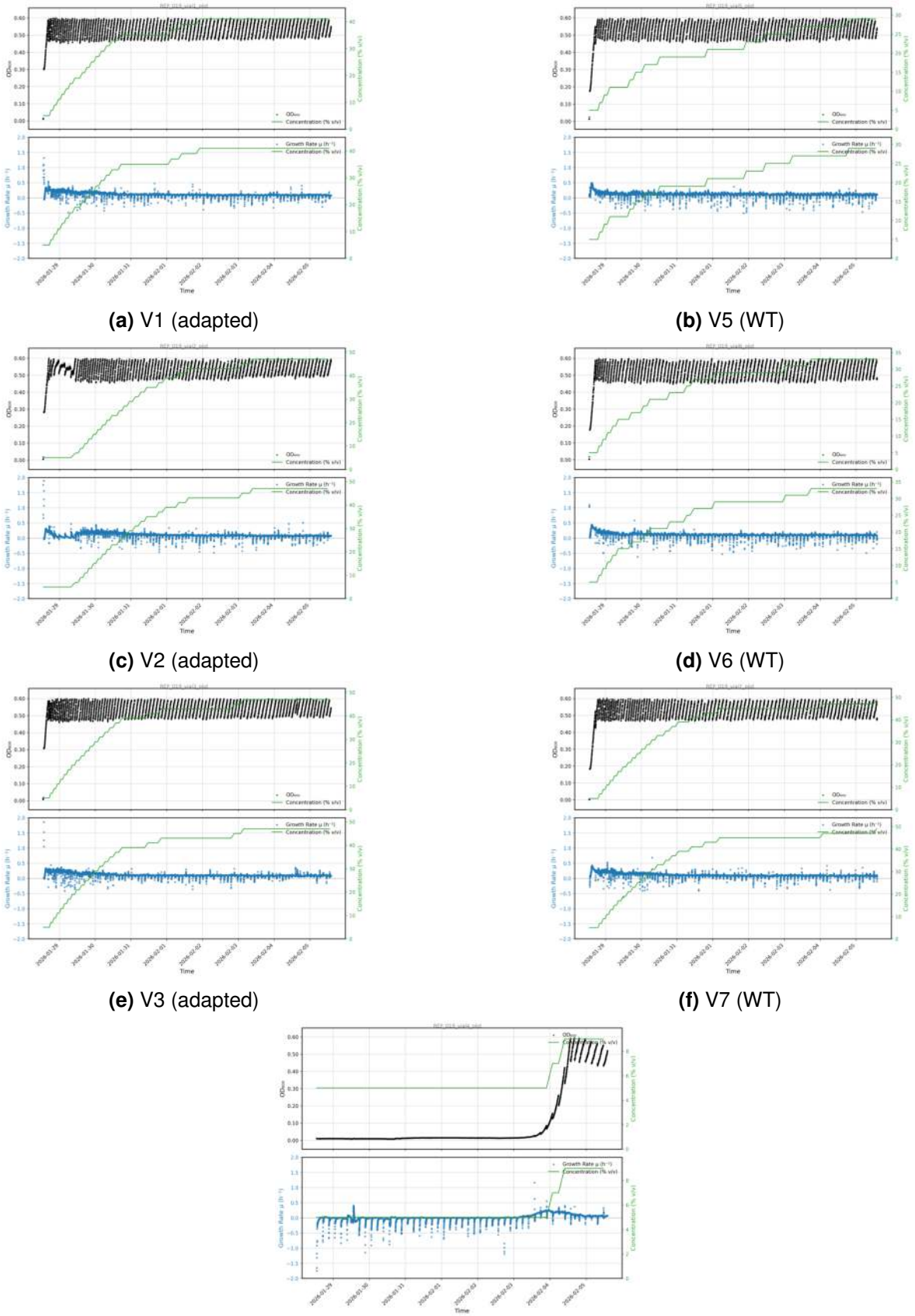

(a) V1 (adapted)

(b) V5 (WT)

(c) V2 (adapted)

(d) V6 (WT)

(e) V3 (adapted)

(f) V7 (WT)

(g) V4 (NC)

Figure 4.19: OD_{600}, RW concentration, and growth rate for REP_019 (28 Jan – 5 Feb 2026, IMC3). Drug stock 100% RW#3 (filtered, no OD change). LB contaminated during media refill. V1–V3 and V5–V7 show contamination artefacts from ∼31 Jan. See Appendix A.

incubation. An operational deviation occurred when the morbidostat settings for V3 were not adjusted in time, causing the drug concentration to be decreased in that vial. The experiment was kept running in the hope of adaptation, but no sustained growth recovery was observed.

REP_020 represents the upper limit of the RW#3 LB-based experiments. The combination of high starting concentration (100% drug stock), aggressive escalation parameters, and the unresolved OD feedback loop issue from REP_018 limited the interpretability of the data.

4.3.6 Phase III Summary

Phase III demonstrated that adaptation to RW#2 confers cross-tolerance to RW#3 (REP_017), showing that the adaptive phenotype is not batch-specific. The highest confirmed RW tolerance across the entire experimental series reached 91% (v/v) RW#3 in REP_018_V3, with genuine cell proliferation. Photodiode-based OD_{600} measurement in the Replifactory was shown to create a positive feedback loop with dark-coloured feedstocks (REP_018 V1/V2), a key limitation for future morbidostat work with industrial waste streams. Two of five Phase III experiments produced no usable data due to equipment failure (REP_016) and contamination (REP_019), consistent with the operational failure rate observed in Phases I and II. The propagation lineage for Phase III was: REP_007 (V1, V3) $\rightarrow$ REP_017 (V3) $\rightarrow$ REP_018 (V3) $\rightarrow$ REP_019/020.

4.4 Technical Challenges and Operational Observations

4.4.1 Contamination

Contamination was the most frequent cause of experiment termination in Phase I, affecting REP_002, REP_003, REP_004, and REP_005. Measures taken to address contamination included the addition of air filters (which caused blockage), improved aseptic technique during inoculation (use of Bunsen burners and laminar flow), and the transition from LB to M9 medium (which provides a less favourable environment for contaminants). No contamination events were recorded in the M9-based experiments of Phase II (REP_008 onward), suggesting that the medium switch was the most effective mitigation strategy.

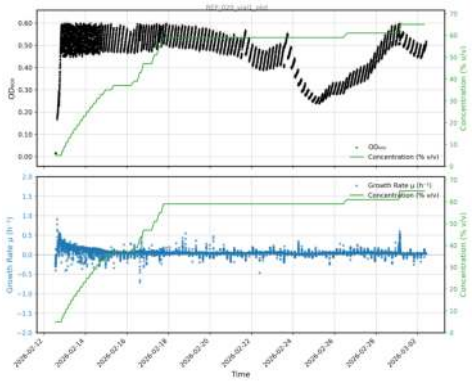

(a) V1 (adapted)

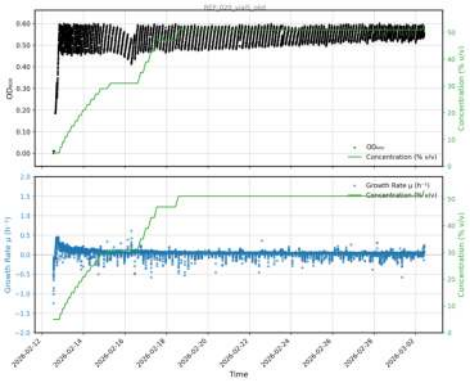

(b) V5 (WT)

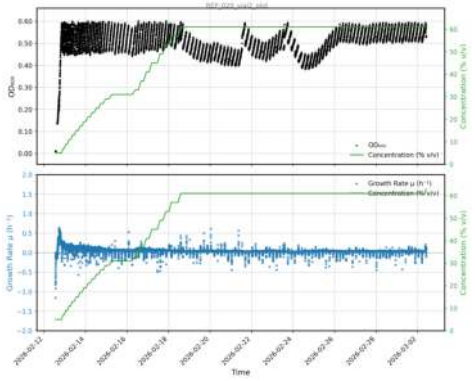

(c) V2 (adapted)

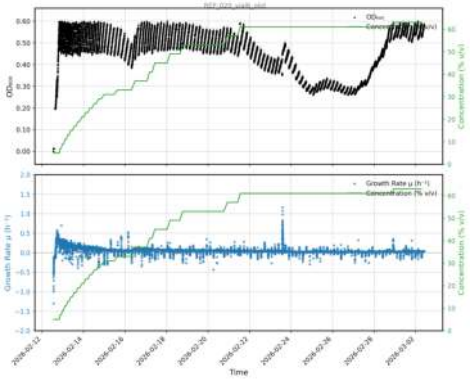

(d) V6 (WT)

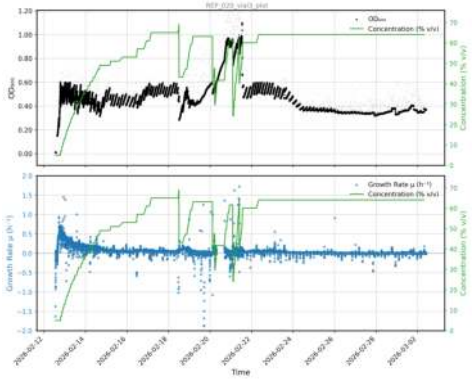

(e) V3 (adapted)

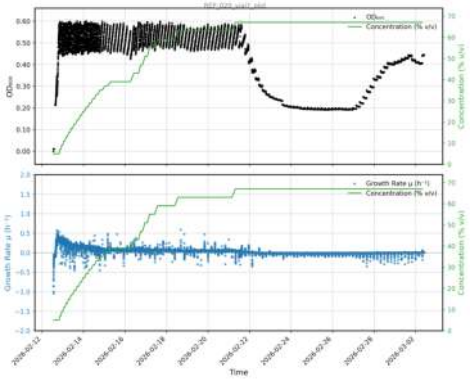

(f) V7 (WT)

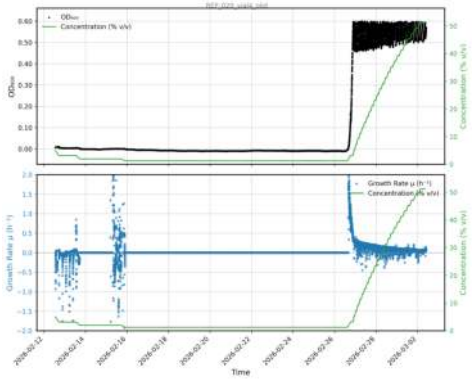

(g) V4 (NC)

Figure 4.20: OD_{600}, RW concentration, and growth rate for REP_020 (12–19 Feb 2026, IMC3). Drug stock 100% RW#3. Growth stagnation in all vials; V5 most stable (OD 0.65). NC contaminated ∼26 Feb. Aggressive escalation (0.06 h^{-1} threshold) did not overcome plateau. See Appendix A.

4.4.2 Biofilm Interference

Biofilm formation on vial walls and stirring bars was observed in multiple experiments, particularly in prolonged runs (REP_004, REP_010, REP_011). Biofilm inflated the OD_{600} readings, causing the morbidostat to overestimate planktonic cell density and trigger inappropriate dilution events.

4.4.3 OD Interference at High RW Concentrations

At RW concentrations exceeding approximately 50% (v/v), the intrinsic colour of the RW contributed to the OD_{600} reading independently of cell density. This artefact was most clearly demonstrated in REP_018 (Section 4.3.3), where V1 and V2 reached 100% RW#3 concentration through a positive feedback loop between the dark colour of the medium and the morbidostat's dose-escalation algorithm, without any actual bacterial growth. This artefact is more pronounced with RW#3 (blank OD_{600} 0.21–0.26) than with RW#2, and represents an inherent limitation of photodiode-based OD measurement in coloured media.

4.4.4 Equipment and Software Failures

The Replifactory platform, as an open-source prototype, exhibited several operational failures:

- Pump malfunction: Pump 2 air leak in REP_013; drug pump failure in REP_016.
- Valve failure: V2 in REP_014 received no dilutions for three days.
- Stirrer failure: REP_014 stirrer stopped overnight (18–19 December).
- Software bug: Complete data loss in REP_012.
- Waste pump failure: Clamp opened in REP_007, causing flooding.

In practice, the open-source hardware proved accessible and inexpensive but lacked the reliability needed for unattended long-duration experiments.

4.5 Summary of Key Results

Table 4.1: Summary of key findings from the morbidostat experimental series.

Finding	Evidence	Experiments
WT cannot tolerate high RW#2 without adaptation	No growth at high initial concentrations	REP_001
Morbidostat ALE produces RW tolerance within days	Adapted strains tolerated $>$21% (REP_002) and up to 72% (REP_005) in LB	REP_002, REP_005
RW tolerance is reduced in M9 vs. LB	Slower growth and lower max RW in M9	REP_008
Adapted strains grow on RW as sole carbon source	Positive growth in M9 $-$ glucose + RW	REP_011, REP_014
RW#2 adaptation transfers to RW#3	Pre-adapted strains outperformed WT on RW#3	REP_017
Biofilm interferes with OD monitoring	Inflated OD, inappropriate dilutions	REP_004, REP_010, REP_011
RW colour causes OD artefact above $\sim$50%	False-high OD, feedback loop to 100% in V1/V2	REP_018 (RW#3)
Highest confirmed tolerance: 91% RW#3	Genuine growth at OD 1.2 in V3	REP_018 (RW#3)
Cross-tolerance RW#2 $\rightarrow$ RW#3	Pre-adapted outperformed WT	REP_017 (RW#3)
Growth stagnation at max. RW#3 stress	No recovery at aggressive escalation	REP_020 (RW#3)

CHAPTER 5

DISCUSSION & CONCLUSIONS

5.1 Adaptation Trajectory and Tolerance Thresholds

The 20-experiment series demonstrated that *E. coli* 498 can be evolved via morbidostat-based ALE to tolerate industrially relevant concentrations of pH-neutralized reaction water from polyester resin production. Starting from a baseline of zero tolerance (REP_001), adapted strains reached RW#2 concentrations exceeding 21 % within 12 days (REP_002) and up to 72 % in individual vials within 10 days (REP_005). These results are consistent with the general finding that morbidostat culture accelerates adaptive evolution by maintaining continuous selective pressure near the population's tolerance limit (Toprak et al., 2012, 2013).

The adaptation trajectory followed a characteristic pattern: an initial lag phase of approximately 10 hours following inoculation, a period of rapid concentration escalation driven by the morbidostat's feedback loop, and an eventual plateau at which growth rate and stress intensity reached a dynamic equilibrium. This pattern mirrors the stepwise resistance acquisition described in antibiotic morbidostat studies (Toprak et al., 2012), though the selective agent in this case is a complex chemical mixture rather than a single defined compound. Because RW contains many toxic components, adaptation requires several tolerance mechanisms to evolve concurrently. This co-evolutionary demand may explain the variability between replicate vials and the difficulty of reproducing exact concentration trajectories across experiments.

The observation that wild-type *E. coli* 498 also achieved moderate adaptation under morbidostat selection (reaching approximately 50 % RW#3 in REP_017, although with a longer lag than pre-adapted strains) suggests that the morbidostat's feedback mechanism is sufficiently powerful to drive *de novo* adaptation from a naive starting population. In practical terms, maintaining a pre-adapted stock culture may

not be necessary for industrial applications if sufficient time is allowed for initial adaptation.

5.2 Evidence for Catabolic Utilization of RW

Adapted *E. coli* 498 grew using RW constituents as the sole carbon and energy source (REP_011, REP_014), which is the main result of this thesis. The adapted strain did not simply survive in the presence of RW; it metabolized organic components to support cell division.

The experimental argument for catabolism is based on a comparison of three metabolic conditions:

- In LB + RW (Phase I), growth was robust but could be attributed entirely to LB nutrients, with RW tolerance reflecting passive detoxification or efflux.
- In M9 + glucose + RW (REP_008, REP_015), growth was slower, and tolerance was reduced relative to LB, confirming that the nutritional background contributes to apparent tolerance.
- In M9 − glucose + RW (REP_011, REP_014), growth occurred in the absence of any alternative carbon source, with RW as the only available substrate.

Growth under the third condition can only be explained by enzymatic degradation of one or more RW constituents. The most plausible substrates are the glycols (neopentyl glycol and ethylene glycol), which are the major organic constituents of the RW (Pirman, 2025). *E. coli* possesses the enzymatic machinery for ethylene glycol oxidation via the *fucO–aldA* pathway, which converts EG to glycolaldehyde and then to glycolate, feeding into central metabolism via the glyoxylate shunt (Boronat et al., 1983). To the author's knowledge, no reports of neopentyl glycol degradation by *E. coli* were identified in the literature surveyed; if confirmed, this would represent a novel metabolic capability, possibly acquired through mutation during ALE.

The growth rate under catabolic conditions was substantially lower than under co-metabolic or LB-supplemented conditions, and REP_014 demonstrated that more time is required for catabolic growth than initially expected. This is consistent with the energetic constraints of metabolizing sub-optimal carbon sources and the likely

incomplete degradation of the more recalcitrant RW components (resin oligomers, catalysts).

5.3 Cross-Tolerance, Transferability, and Concentration Limits

The Phase III experiments (REP_016–REP_020) tested whether adaptation to RW#2 transfers to a different RW batch and how far the adapted phenotype can be pushed.

Two points follow from the REP_017 cross-tolerance result:

1. The adaptive phenotype is not specific to a single RW batch. RW#2 (native pH 1.88, neutralised to 7.0) and RW#3 (native pH 5.56, used without neutralisation) differ in pH, optical properties, and potentially in detailed composition, yet the adaptation transfers. This suggests that the tolerance mechanisms evolved during the RW#2 series target broadly shared toxic components rather than batch-specific contaminants.

2. Adaptation to the worst-case feedstock (RW#2, the untreated full-stream reaction water sampled before any on-site cleaning process, with lower native pH) provides a conservative baseline. If adapted strains tolerate RW#2, they can be expected to tolerate any less contaminated RW batch from the same production process, which is relevant for practical deployment where batch-to-batch variability is inevitable.

REP_018 went further: the REP_017_V3 lineage tolerated up to 91 % (v/v) RW#3 with genuine cell proliferation, the highest confirmed RW tolerance across all 20 experiments. Direct comparison of this value with the 72 % (v/v) RW#2 achieved in REP_005 (Phase I) requires caution: RW#3 has a higher native pH, was used without neutralisation, and has different optical properties. The 91 % value nevertheless demonstrates that the adaptation ceiling had not been reached in the RW#2 series and that continued evolution under morbidostat selection can drive tolerance to near-undiluted industrial waste.

The subsequent experiments (REP_019, contaminated; REP_020, growth stagnation) suggest that pushing beyond 91 % with the current experimental setup and strain lineage encounters diminishing returns. Whether this reflects a biological ceil-

ing or an operational limitation of the morbidostat at extreme concentrations (OD feedback loop, aggressive escalation parameters) remains an open question.

5.4 The Role of Biofilm

Biofilm formation was observed as a recurring phenomenon across the experimental series, with documented interference in REP_004, REP_010, and REP_011. In the context of this thesis, biofilm played a predominantly disruptive role: it inflated OD_{600} readings, triggered inappropriate dilution events, and complicated the quantitative interpretation of growth rate data.

At the same time, biofilm may have contributed positively to the adaptation process. Cells embedded in a biofilm matrix are partially shielded from toxic compounds by diffusion limitation through the EPS layer, and biofilm communities harbour phenotypic heterogeneity that can buffer against lethal stress. In several experiments, the planktonic population recovered rapidly after washout events, a pattern consistent with re-seeding from a surface-attached biofilm reservoir. Whether the biofilm served as a protected niche that preserved adapted variants during high-stress periods, or whether it merely confounded the OD measurements, cannot be definitively resolved with the available data.

In a scale-up context, biofilm formation would be an advantage rather than a problem. Fixed-film bioreactors such as trickling filters and moving bed biofilm reactors rely on surface-attached biomass to maintain high cell densities and resist washout, and the adapted *E. coli* 498 strains could be deployed in such systems.

5.5 Limitations

The results of this study are subject to several limitations that affect their interpretation.

5.5.1 OD_{600} as the Sole Growth Metric

All growth monitoring relied on OD_{600} measured by the Replifactory's built-in photodiode sensor, with periodic validation by external spectrophotometry. OD_{600} is a proxy for cell density and does not distinguish between viable and non-viable cells, nor between planktonic cells and biofilm-associated biomass. At high RW concen-

trations (>50 % v/v), the intrinsic absorbance of the coloured RW contributed to the OD reading independently of cell density, producing a systematic positive bias.

The absence of complementary analytical methods (colony-forming unit counts, flow cytometry, or dry cell weight measurements) means that the absolute cell densities reported are estimates, and the growth rates calculated from OD time-series data carry an inherent uncertainty that increases with RW concentration.

5.5.2 No Marking of Dilution Events in OD Data

The Replifactory's OD time-series data do not explicitly mark when dilution events occurred. This complicates the post-hoc analysis of growth rates, because OD drops caused by dilution must be distinguished from OD drops caused by cell death or washout.

5.5.3 Technical Failure Rate

Of the 15 experiments targeting RW#2 adaptation (REP_001–REP_015), seven produced data of limited or no value: REP_001 (failed design), REP_003 (contamination + filter issues), REP_006 (poor data quality), REP_009 (data loss), REP_010 (insufficient inoculum), REP_012 (software bug), and REP_013 (pump failure). This failure rate of approximately 47 % reflects the limitations of the Replifactory as an open-source prototype and reduces the statistical power of the dataset.

5.5.4 Absence of Chemical Analysis

This study did not include chemical analysis of the RW before and after biological treatment. Chemical characterisation of the RW constituents and quantitative measurement of degradation products are addressed in the parallel master thesis by David Klingholz, which covers genetic analysis, COD measurement, cytotoxicity testing, and HPLC characterisation of the same RW batches used in this work. Without independent analytical data in the present study, the extent of actual pollutant removal by the adapted strain cannot be quantified. The evidence for catabolic degradation is indirect: growth in the absence of glucose implies carbon assimilation from RW, but the specific compounds degraded, the degradation products, and the fraction of total organic load removed remain unknown.

5.5.5 Unanswered Ecotoxicity Question

The original scope of this thesis included a research question on whether biological treatment of RW reduces acute ecotoxicity, as measured by the Microtox bioassay (*Aliivibrio fischeri*, EC_{50}) (Abbas et al., 2018; Soupilas et al., 2008). The Microtox assay was not performed during the experimental period due to equipment and time constraints. Consequently, the question of whether the adapted strain reduces the ecotoxicity of treated RW remains unanswered and is deferred to future work.

5.5.6 Single Organism

All experiments used a single strain (*E. coli* 498, a K-12 derivative). *E. coli* is not traditionally considered a strong degrader of complex organic pollutants. The choice of *E. coli* was motivated by its genetic tractability and suitability as an ALE model organism, but the degradation efficiency achieved may not represent the upper bound of what biological treatment could accomplish with more specialised organisms.

5.6 Comparison with Literature

The morbidostat-based ALE approach used here builds on the work of Toprak et al. (2012) and Toprak et al. (2013), who used the same platform to evolve antibiotic resistance. The adaptation timescales observed in the present study (measurable tolerance within 12 days, high-level tolerance within weeks) are comparable to those reported for antibiotic resistance, even though RW is chemically far more complex than a single antibiotic.

A direct numerical comparison is limited by the novelty of applying morbidostat ALE to complex industrial waste. Toprak et al. (2012) reported stepwise increases in the minimum inhibitory concentration (MIC) for chloramphenicol, trimethoprim, and doxycycline over approximately 25 days, with final MIC values rising several-fold relative to the wild type. The RW system resists this form of quantification because no single MIC can be defined for a mixture of unknown composition; tolerance is instead expressed as percent volume of RW tolerated. The 12-day timeline to $>$21 % RW#2 (REP_002) and the subsequent escalation to 91 % RW#3 in a pre-adapted lineage (REP_018) place the present work within the same order of magnitude as the timescales reported for antibiotic ALE, although the underlying

phenotype (multi-component chemical tolerance combined with carbon assimilation) differs from single-compound MIC shifts. No prior morbidostat study identified in the literature surveyed has targeted complex industrial process water as the selective pressure, and direct numerical benchmarks are therefore sparse.

The observation that adapted *E. coli* 498 grew on RW as a sole carbon source fits within the broader ALE literature, which has repeatedly shown that laboratory evolution can produce novel metabolic phenotypes, including growth on non-native substrates (Dragosits & Mattanovich, 2013; Hirasawa & Maeda, 2022). To the best of the author's knowledge, the specific finding that *E. coli* can be evolved to grow on glycol-containing industrial wastewater has not been reported before.

5.7 Future Directions

Several lines of follow-up work would strengthen and extend the findings reported here:

1. **Catabolism vs. detoxification — the central open question.** The glucose-free growth observed in REP_011 and REP_014 is consistent with assimilation of carbon from RW, but the data presented here do not exclude the alternative interpretation that adapted *E. coli* 498 primarily *detoxifies* RW constituents (e.g. via efflux, sequestration, or partial oxidation that does not yield net biomass carbon) while obtaining the carbon required for division from intracellular reserves, regenerated cofactors, or trace carry-over substrates. Distinguishing genuine mineralisation from detoxification is the first task for follow-up work and should combine: (i) ^{13}C-labelled NPG and EG fed to adapted cultures with isotope tracking into biomass and CO_2 (Boronat et al., 1983); (ii) a closed COD/TOC carbon balance across the morbidostat (input minus output) to quantify the fraction of organic carbon removed; and (iii) targeted metabolomics for glycolaldehyde, glycolate, and NPG-derived intermediates. Identifying this thesis as a tolerance and catabolism-screening result rather than a remediation result is appropriate; the detoxification-versus-degradation question is the immediate next step, not a side issue.

2. Chemical characterisation of degradation: HPLC and COD measurements of RW before and after biological treatment to quantify pollutant removal and identify specific degradation products (Tripathy et al., 2025; Viktoryová et al., 2022).

3. Genomic analysis of adapted strains: Whole-genome sequencing of adapted isolates from key experiments (REP_007, REP_014) to identify the mutations responsible for RW tolerance and catabolic capacity (Tenaillon et al., 2016).

4. Scale-up to bioreactor format: Transition from the 12 mL morbidostat vials to bench-scale continuous bioreactors (e.g., moving bed biofilm reactors) to assess treatment performance at higher volumes and flow rates.

5. Multi-organism consortia: Testing mixed cultures or defined consortia including *Pseudomonas* or *Rhodococcus* species alongside adapted *E. coli* 498 to improve degradation breadth and efficiency (Larkin et al., 2005; Wynands et al., 2023).

6. Ecotoxicity assessment: Microtox bioassay (EC_{50}, *Aliivibrio fischeri*) of biologically treated RW to determine whether biological treatment reduces the acute ecotoxicity of the treated effluent (Abbas et al., 2018; Soupilas et al., 2008).

7. OD correction algorithms: Development of RW-concentration-dependent OD correction factors to improve monitoring accuracy at high RW concentrations.

8. Long-term stability: Assessment of whether the adapted phenotype is genetically stable over extended cultivation without selective pressure, or whether it reverts to wild-type sensitivity.

The development of a biological treatment process for industrial reaction water aligns with several United Nations Sustainable Development Goals (SDGs): SDG 6 (Clean Water and Sanitation), by reducing the discharge of hazardous chemicals into water systems; SDG 9 (Industry, Innovation and Infrastructure), by providing a sustainable alternative to incineration for industrial waste management; and SDG 12 (Responsible Consumption and Production), by converting a waste stream into a

substrate for microbial biomass rather than releasing its carbon content as CO_2. The positive environmental impact of replacing high-temperature incineration with ambient-temperature bioprocessing provides further motivation for continued research in this direction.

5.8 Conclusions

Escherichia coli 498 was successfully evolved by morbidostat-based adaptive laboratory evolution to tolerate near-undiluted, pH-neutralised industrial reaction water from polyester resin polycondensation. Maximum confirmed tolerance reached 72 % (v/v) RW#2 in LB (REP_005) and 91 % (v/v) RW#3 in a cross-tolerant pre-adapted lineage (REP_018), with concurrent wild-type controls limited to approximately 50–60 % (v/v). Adapted strains sustained growth in the absence of glucose with RW as the only added carbon source (REP_011, REP_014), consistent with assimilation of carbon from one or more RW constituents. Adaptation acquired against RW#2 transferred to RW#3 without re-adaptation. Biofilm formation and the optical interference of dark RW with photodiode-based OD_{600} measurement were identified as the principal operational confounders. Whether the observed glucose-free growth reflects genuine catabolic mineralisation of RW carbon or reactor-level detoxification with limited carbon assimilation cannot be resolved from the data presented and is the central question for follow-up work. Quantification of pollutant removal (COD, glycol, NPG), identification of degradation pathways, and ecotoxicity assessment of treated effluent are required before biological treatment can be evaluated as a process-level alternative to incineration of polyester reaction water.

LIST OF REFERENCES

Abbas, M., Adil, M., Ehtisham-ul-Haque, S., Munir, B., Yameen, M., Ghaffar, A., Shar, G. A., Asif Tahir, M., & Iqbal, M. (2018). Vibrio fischeri bioluminescence inhibition assay for ecotoxicity assessment: A review. *Science of The Total Environment*, *626*, 1295–1309. https://doi.org/10.1016/j.scitotenv.2018.01.066

Arregui, L., Ayala, M., Gómez-Gil, X., Gutiérrez-Soto, G., Hernández-Luna, C. E., Herrera De Los Santos, M., Levin, L., Rojo-Domínguez, A., Romero-Martínez, D., Saparrat, M. C. N., Trujillo-Roldán, M. A., & Valdez-Cruz, N. A. (2019). Laccases: Structure, function, and potential application in water bioremediation. *Microbial Cell Factories*, *18*(1), 200. https://doi.org/10.1186/s12934-019-1248-0

Asgher, M., Bhatti, H. N., Ashraf, M., & Legge, R. L. (2008). Recent developments in biodegradation of industrial pollutants by white rot fungi and their enzyme system. *Biodegradation*, *19*(6), 771–783. https://doi.org/10.1007/s10532-008-9185-3

Biko, O. D., Viljoen-Bloom, M., & Van Zyl, W. H. (2020). Microbial lignin peroxidases: Applications, production challenges and future perspectives. *Enzyme and Microbial Technology*, *141*, 109669. https://doi.org/10.1016/j.enzmictec.2020.109669

Boronat, A., Caballero, E., & Aguilar, J. (1983). Experimental evolution of a metabolic pathway for ethylene glycol utilization by *Escherichia coli*. *Journal of Bacteriology*, *153*(1), 134–139. https://doi.org/10.1128/jb.153.1.134-139.1983

Dragosits, M., & Mattanovich, D. (2013). Adaptive laboratory evolution – principles and applications for biotechnology. *Microbial Cell Factories*, *12*(1), 64. https://doi.org/10.1186/1475-2859-12-64

Falade, A. O., Nwodo, U. U., Iweriebor, B. C., Green, E., Mabinya, L. V., & Okoh, A. I. (2017). Lignin peroxidase functionalities and prospective applications. *MicrobiologyOpen*, *6*(1), e00394. https://doi.org/10.1002/mbo3.394

Gopalakrishnan, V., Crozier, D., Card, K. J., Chick, L. D., Krishnan, N. P., McClure, E., Pelesko, J., Williamson, D. F., Nichol, D., Mandal, S., Bonomo, R. A., & Scott, J. G. (2022). A low-cost, open-source evolutionary bioreactor and its educational use. *eLife*, *11*, e83067. https://doi.org/10.7554/eLife.83067

Hirasawa, T., & Maeda, T. (2022). Adaptive laboratory evolution of microorganisms: Methodology and application for bioproduction. *Microorganisms*, *11*(1), 92. https://doi.org/10.3390/microorganisms11010092

Jee, J., Rasouly, A., Shamovsky, I., Akivis, Y., Steinman, S., Mishra, B., & Nudler, E. (2016). Rates and mechanisms of bacterial mutagenesis from maximum-depth sequencing. *Nature*, *534*(7609), 693–696. https://doi.org/10.1038/nature18313

Konan, D., Ndao, A., Koffi, E., Elkoun, S., Robert, M., Rodrigue, D., & Adjallé, K. (2024). Biodecomposition with phanerochaete chrysosporium: A review. *AIMS Microbiology*, *10*(4), 1068–1101. https://doi.org/10.3934/microbiol.2024046

Larkin, M. J., Kulakov, L. A., & Allen, C. C. (2005). Biodegradation and rhodococcus – masters of catabolic versatility. *Current Opinion in Biotechnology*, *16*(3), 282–290. https://doi.org/10.1016/j.copbio.2005.04.007

Liu, S., Xu, X., Kang, Y., Xiao, Y., & Liu, H. (2020). Degradation and detoxification of azo dyes with recombinant ligninolytic enzymes from aspergillus sp. with secretory overexpression in pichia pastoris. *Royal Society Open Science*, *7*(9), 200688. https://doi.org/10.1098/rsos.200688

Majumder, S., Raghuvanshi, S., & Gupta, S. (2014). Estimation of kinetic parameters for bioremediation of cr(VI) from wastewater using *Pseudomonas taiwanensis* **,** an isolated strain from enriched mixed culture. *Bioremediation Journal*, *18*(3), 236–247. https://doi.org/10.1080/10889868.2014.889075

Nair K, S., Manu, B., & Azhoni, A. (2021). Sustainable treatment of paint industry wastewater: Current techniques and challenges. *Journal of Environmental Management*, *296*, 113105. https://doi.org/10.1016/j.jenvman.2021.113105

Phulpoto, A. H., Qazi, M. A., Mangi, S., Ahmed, S., & Kanhar, N. A. (2016). Biodegradation of oil-based paint by bacillus species monocultures isolated from the paint warehouses. *International Journal of Environmental Science and Technology*, *13*(1), 125–134. https://doi.org/10.1007/s13762-015-0851-9

Pirman, T. (2025). Waste reduction in KHSI [Kansai Helios Slovenija d.o.o., internal document].

Q-A samples of reaction water [Kansai Helios Slovenija d.o.o., internal quality assurance document]. (2025).

Ravikumar, H., Rao, S., & Karigar, C. (2012). Biodegradation of paints: A current status. *Indian Journal of Science and Technology*, *5*, 1977–1987. https://doi.org/10.17485/ijst/2012/v5i1.33

RD project order — reduction of waste-water and waste-solvent from resin production [Kansai Helios, internal project document]. (2025).

Rusnac, C. (2024). Replifactory: A multiplexed, automated, and scalable platform for continuous evolution experiments [Open-source hardware project, documentation and design files available on GitHub]. https://catalin-rusnac.github.io/replifactory_docs/

S., P. (2001). Feasibility of bioremediation by white-rot fungi. *Applied Microbiology and Biotechnology*, *57*(1), 20–33. https://doi.org/10.1007/s002530100745

Shindhal, T., Rakholiya, P., Varjani, S., Pandey, A., Ngo, H. H., Guo, W., Ng, H. Y., & Taherzadeh, M. J. (2021). A critical review on advances in the practices and perspectives for the treatment of dye industry wastewater. *Bioengineered*, *12*(1), 70–87. https://doi.org/10.1080/21655979.2020.1863034

Singh, A. K., Fernandez-Lafuente, R., Schmidt, J. E., Boczkaj, G., & Bilal, M. (2024). Biocatalytic functionalities of lignin peroxidase-based systems in lignin depolymerization and pollutants removal from environmental matrices. *Current Pollution Reports*, *10*(3), 345–361. https://doi.org/10.1007/s40726-024-00310-0

Sivapuratharasan, V., Lenzen, C., Michel, C., Muthukrishnan, A. B., Jayaraman, G., & Blank, L. M. (2022). Metabolic engineering of *Pseudomonas taiwanensis* VLB120 for rhamnolipid biosynthesis from biomass-derived aromatics.

Metabolic Engineering Communications, *15*, e00202. https://doi.org/10.1016/j.mec.2022.e00202

Soupilas, A., Papadimitriou, C., Samaras, P., Gudulas, K., & Petridis, D. (2008). Monitoring of industrial effluent ecotoxicity in the greater thessaloniki area. *Desalination*, *224*(1), 261–270. https://doi.org/10.1016/j.desal.2007.07.003

Tenaillon, O., Barrick, J. E., Ribeck, N., Deatherage, D. E., Blanchard, J. L., Dasgupta, A., Wu, G. C., Wielgoss, S., Cruveiller, S., Médigue, C., Schneider, D., & Lenski, R. E. (2016). Tempo and mode of genome evolution in a 50,000-generation experiment. *Nature*, *536*(7615), 165–170. https://doi.org/10.1038/nature18959

Tenaillon, O., Rodríguez-Verdugo, A., Gaut, R. L., McDonald, P., Bennett, A. F., Long, A. D., & Gaut, B. S. (2012). The molecular diversity of adaptive convergence. *Science*, *335*(6067), 457–461. https://doi.org/10.1126/science.1212986

Thanavel, M., Bankole, P. O., Selvam, R., Govindwar, S. P., & Sadasivam, S. K. (2020). Synergistic effect of biological and advanced oxidation process treatment in the biodegradation of remazol yellow RR dye. *Scientific Reports*, *10*(1), 20234. https://doi.org/10.1038/s41598-020-77376-5

Tian, J., Deng, W., Zhang, Z., Xu, J., Yang, G., Zhao, G., Yang, S., Jiang, W., & Gu, Y. (2023). Discovery and remodeling of vibrio natriegens as a microbial platform for efficient formic acid biorefinery. *Nature Communications*, *14*(1), 7758. https://doi.org/10.1038/s41467-023-43631-2

Toprak, E., Veres, A., Michel, J.-B., Chait, R., Hartl, D. L., & Kishony, R. (2012). Evolutionary paths to antibiotic resistance under dynamically sustained drug selection. *Nature Genetics*, *44*(1), 101–105. https://doi.org/10.1038/ng.2269

Toprak, E., Veres, A., Yildiz, S., Pedraza, J. M., Chait, R., Paulsson, J., & Kishony, R. (2013). Building a morbidostat: An automated continuous-culture device for studying bacterial drug resistance under dynamically sustained drug inhibition. *Nature Protocols*, *8*(3), 555–567. https://doi.org/10.1038/nprot.nprot.2013.021

Tripathy, S., Kar, O. P., & Pradhan, A. (2025). Challenges and innovations in industrial wastewater treatment: Safeguarding water resources and promoting sustainable practices. *Water, Air, & Soil Pollution*, *236*(2), 92. https://doi.org/10.1007/s11270-025-07742-4

Viktoryová, N., Szarka, A., & Hrouzková, S. (2022). Recent developments and emerging trends in paint industry wastewater treatment methods [Publisher: Multidisciplinary Digital Publishing Institute]. *Applied Sciences*, *12*(20), 10678. https://doi.org/10.3390/app122010678

Wynands, B., Wierckx, N., Heipieper, H. J., & Eberlein, C. (2023). Pseudomonas taiwanensis VLB120 als Plattform für die Biotechnologie. *BIOspektrum*, *29*(6), 686–688. https://doi.org/10.1007/s12268-023-2015-7

APPENDIX A

DETAILED FIGURE DESCRIPTIONS

This appendix contains the detailed per-vial figure descriptions for all 20 morbidostat experiments (REP_001 through REP_020). Each section corresponds to one experiment and provides individual vial-level interpretation of the OD_{600}, RW concentration, and growth rate time-series shown in the corresponding figure in Chapter 4, followed by a collective summary.

A.1 REP_001 (1–3 September 2025)

> *Experimental context:* REP_001 (1–3 September 2025). Medium: LB broth. Drug stock: 30% (v/v) RW#2 (pH 7.0) in LB, starting concentration approximately 16% (v/v) in vials. Duration: 3 days. Vials 1–3: *E. coli* 498 designated for adaptation. Vial 4: sterile negative control. Vials 5–7: wild-type *E. coli* 498 controls. Device: Replifactory morbidostat. RW batch: RW#2.

Figure REP_001-V1 (adaptation group, *E. coli* 498). The upper panel shows OD_{600} remaining near baseline throughout the 3-day run, with scattered outlier readings reaching up to approximately 0.5 (around 3 September) but no sustained increase. The RW concentration (green line) rose rapidly from approximately 11% to 16% (v/v) within the first hours and remained flat thereafter, indicating that the morbidostat growth-rate threshold for dose escalation was never reached. The lower panel shows growth rate μ values predominantly clustered at zero, with isolated positive and negative spikes (± 1.5 h^{-1}) reflecting sensor noise at near-zero OD. No sustained growth was observed.

Figure REP_001-V2 (adaptation group, *E. coli* 498). OD_{600} remained flat at baseline throughout the entire run, with values slightly below zero due to calibration offset. The RW concentration rose from approximately 11% to 16% (v/v) and

remained constant. The growth rate μ panel shows initial negative spikes (down to -1.5 h^{-1}) during the first hours, followed by a completely flat trace at zero for the remainder of the experiment. This vial exhibited the cleanest non-growth signal of all REP_001 vials, confirming complete growth inhibition at the applied RW concentration.

Figure REP_001-V3 (adaptation group, *E. coli* 498). OD_{600} remained very close to zero in a tight band throughout the run, with no detectable increase. The RW concentration followed the same pattern as V1 and V2, rising to approximately 16% (v/v) and holding constant. The growth rate μ panel, however, shows persistent oscillation: initial high positive values (up to 1.8 h^{-1}) that decayed over the first 12 hours, followed by sustained low-amplitude oscillation around zero for the remainder of the run. These μ oscillations are attributed to noise amplification from very low OD values rather than genuine growth activity, as no corresponding OD increase was observed.

Figure REP_001-V4 (sterile negative control). OD_{600} remained at baseline throughout the run, with only a few isolated outlier points (up to approximately 0.03) around 3 September. The RW concentration was held constant at approximately 3% (v/v) — substantially lower than the inoculated vials — consistent with negative control configuration. Growth rate μ remained flat at zero, with only two outlier data points in the initial phase. The sterile control confirms the absence of contamination and establishes that RW#2 at the applied concentrations does not generate a measurable OD_{600} artefact in LB medium.

Figure REP_001-V5 (wild-type *E. coli* 498). OD_{600} remained near baseline for the majority of the run; however, multiple isolated high-amplitude OD spikes were recorded throughout the experiment, reaching values of 0.5–1.0. These spikes were transient (single data points or short clusters) and did not lead to sustained OD elevation, indicating measurement artefacts or transient cellular events rather than active proliferation. The RW concentration rose to approximately 16% (v/v) and remained constant. The growth rate μ panel shows continuous noisy oscillation (± 2.0 h^{-1}) throughout the entire run, more scattered than in other vials, consistent with the sporadic OD spikes generating unstable μ calculations.

Figure REP_001-V6 (wild-type *E. coli* 498). OD_{600} remained near baseline with minimal noise throughout the run. The RW concentration rose to approximately 16% (v/v) and remained flat. The growth rate μ panel shows moderate oscillation, with initial positive spikes (up to 1.2 h^{-1}) during the first 12 hours that attenuated over time, and sporadic negative outliers (down to -2.0 h^{-1}) interspersed throughout. No sustained positive growth rate was recorded. The pattern is consistent with complete growth inhibition.

Figure REP_001-V7 (wild-type *E. coli* 498). This vial was the only one in REP_001 to show a transient OD increase that was not reproduced in subsequent experiments at the same starting concentration. The upper panel shows OD_{600} near baseline for the first approximately 30 hours, followed by a sharp onset of apparent growth around 3 September. OD_{600} rose from approximately 0.05 to 0.15–0.30, stabilising at 0.20–0.30 with considerable scatter for the remainder of the run. The RW concentration trace responded dynamically: it initially rose to approximately 16% (v/v), then dropped sharply to approximately 6% (v/v) around 2–3 September as the morbidostat detected growth failure, before gradually recovering to approximately 12–13% (v/v). The lower panel shows growth rate μ initially highly variable ($\pm$2.0 h^{-1}), followed by a negative dip around the onset of the OD rise, and then persistently positive values (0.2–1.0 h^{-1}) from 3 September onward. While the morbidostat response and positive μ values are consistent with bacterial proliferation, the pattern could not be reproduced in REP_002 or later runs at comparable starting concentrations, and the main text (Section 4.1.1) therefore treats this event as transient rather than as confirmed adaptation.

Collective summary. REP_001 demonstrated that the initial RW#2 drug stock concentration of 30% (v/v), delivering approximately 16% (v/v) starting concentration to the vials, exceeded the tolerance threshold of *E. coli* 498 for most conditions. Six of seven vials showed no sustained growth. The sole exception, V7 (wild-type), exhibited clear growth onset after approximately 30 hours, with the morbidostat responding by first reducing and then re-escalating the RW concentration — the expected feedback behaviour during successful adaptation. The transient OD spikes observed in V5 were not reproducible and did not lead to sustained proliferation. The

growth in V7 could not be reproduced in subsequent experiments at the same high starting concentration, establishing that a lower initial RW concentration with gradual morbidostat-driven escalation was required for consistent adaptation in REP_002.

A.2 REP_002 (3–15 September 2025)

Experimental context: REP_002 (3–15 September 2025). Medium: LB broth. Drug stock: 30% (v/v) RW#2 (pH 7.0) in LB. Starting concentration: 5% (v/v) for V1–V6; 11% (v/v) for V7. Duration: 12 days. Vials 1–3: pre-adapted *E. coli* 498 inocula from REP_001 (V1 from REP_001-V1, V2 from REP_001-V3, V3 from REP_001-V7). Vial 4: sterile negative control. Vials 5–7: wild-type *E. coli* 498. Device: Replifactory morbidostat. RW batch: RW#2. Contamination detected from 12 September onward; data after this date should be interpreted with caution.

Figure REP_002-V1 (pre-adapted *E. coli* 498, inoculum from REP_001-V1). Growth was established within approximately 10 hours of inoculation. The upper panel shows OD_{600} rising sharply from near zero to 0.20–0.35, with a dense sawtooth oscillation pattern reflecting morbidostat-driven dilution cycles clearly visible from 5–7 September. The RW concentration (green line) escalated progressively from approximately 5% to 22% (v/v) by 9 September. After 8 September, OD_{600} began a gradual decline, falling to approximately 0.10 by 10–11 September and approaching baseline by 14–16 September. The lower panel shows growth rate μ initially high (0.5–1.5 h^{-1}) during the active growth phase, progressively declining toward zero and becoming predominantly negative in the final days. V1 was not selected for cryopreservation due to loss of growth toward the end of the run.

Figure REP_002-V2 (pre-adapted *E. coli* 498, inoculum from REP_001-V3). Rapid growth onset comparable to V1, with OD_{600} reaching 0.20–0.30 and establishing clear dilution cycle oscillations from 5–7 September. The RW concentration rose progressively from approximately 5% to 20–21% (v/v) by 8 September. OD_{600} was maintained at oscillating levels through approximately 10 September, with the dilution sawtooth pattern persisting longer than in V1. A cluster of elevated OD data points appeared around 15–16 September, coinciding with the contamination period.

Growth rate μ was initially 0.5–1.0 h^{-1}, gradually declining but remaining intermittently positive through most of the usable run. V2 was selected for cryopreservation (25% glycerol, -80 °C) and carried forward in the propagation lineage.

Figure REP_002-V3 (pre-adapted *E. coli* 498, inoculum from REP_001-V7). Growth established rapidly, with dense OD_{600} oscillations of 0.20–0.30 visible from 5 September onward. Several high outlier OD spikes (0.8–0.9) were recorded in the first two days. The RW concentration escalated from approximately 5% to 22% (v/v) by 8 September and continued to rise, reaching the highest value observed in REP_002 at approximately 24% (v/v) by 15 September. Growth rate μ was initially elevated (0.5–1.0 h^{-1}) and remained intermittently positive throughout the run, though declining in magnitude after 8 September. V3 was selected for cryopreservation and carried forward in the propagation lineage. The high maximum RW concentration suggests that the inoculum from REP_001-V7 — the only vial in REP_001 that exhibited sustained growth — may have carried a partial adaptation advantage.

Figure REP_002-V4 (sterile negative control). OD_{600} remained at baseline (near zero) for the first 10 days of the experiment. The RW concentration was held constant at approximately 3% (v/v). Around 14–15 September, a dramatic OD_{600} increase was observed, with values rising rapidly from near zero to approximately 1.2, exhibiting a classic exponential growth curve. This event coincides with the contamination reported from 12 September onward and confirms that the negative control was compromised. Growth rate μ was near zero with moderate noise for the first 10 days, followed by increasingly positive values around 14 September. The contamination of V4 provides a clear biomarker for when contamination reached all vials in this experiment.

Figure REP_002-V5 (wild-type *E. coli* 498). Growth was established after a lag phase, with OD_{600} rising to 0.20–0.30 and maintaining dense dilution cycle oscillations from 5 September through approximately 12 September. The RW concentration escalated progressively from approximately 5% to 20% (v/v) by 10–11 September. Growth rate μ was initially high (0.5–1.0 h^{-1}), declining gradually but remaining largely positive through the usable run period. The growth kinetics of V5 (wild-type) were broadly comparable to the pre-adapted vials, indicating that *de novo* adap-

tation under the morbidostat's escalating stress regime was effective even without prior exposure. V5 was selected for cryopreservation alongside V2 and V3.

Figure REP_002-V6 (wild-type *E. coli* 498). Growth established with dynamics similar to V5. OD_{600} oscillated around 0.20–0.30 with clear dilution cycles. The RW concentration rose progressively from approximately 5% to 20% (v/v) by 10 September. OD_{600} began declining after approximately 12 September, approaching near-baseline values by 15–16 September. Growth rate μ was initially 0.5–1.0 h^{-1} and declined over time. V6 was not selected for cryopreservation due to reduced growth toward the end of the run.

Figure REP_002-V7 (wild-type *E. coli* 498). This vial started at a higher initial RW concentration of approximately 11% (v/v), compared to 5% for all other vials. Growth was established after a lag phase, with OD_{600} oscillating around 0.15–0.25: slightly lower amplitude than V5 and V6, consistent with the higher initial stress. The RW concentration rose progressively to approximately 20% (v/v) by 11 September. After 11–12 September, OD_{600} declined significantly, with increasingly irregular and scattered data points coinciding with the contamination period. Growth rate μ was initially positive (0.5–1.0 h^{-1}) but became predominantly negative from 12 September onward. V7 was not selected for cryopreservation. A procedural note documented that the vial lid came off during sampling and was rinsed with ethanol, which may have contributed to contamination susceptibility.

Collective summary. REP_002 provided the first clear evidence that *E. coli* 498 can adapt to RW#2 under morbidostat selection pressure in LB medium. All six inoculated vials (V1–V3 pre-adapted, V5–V7 wild-type) established growth within approximately 10 hours and tolerated progressively escalating RW concentrations, with the best-performing vials (V2, V3, V5) reaching $>$21% (v/v) RW#2. The pre-adapted inoculum from REP_001-V7 (carried in V3) achieved the highest maximum concentration ($\sim$24% v/v), suggesting a partial adaptation advantage from the prior exposure. Wild-type vials adapted *de novo* under the morbidostat regime with comparable kinetics, though V7's higher starting concentration (11% vs 5%) resulted in slightly lower OD amplitudes. Contamination from 12 September onward ultimately terminated the experiment and was confirmed by the dramatic growth event in the

negative control (V4). Cultures from V2, V3, and V5 were cryopreserved and formed the propagation lineage for subsequent experiments.

A.3 REP_003 (15–23 September 2025)

Experimental context: REP_003 (15–23 September 2025). Medium: LB broth. Drug stock: 50% (v/v) RW#2 (pH 7.0) in LB (increased from 30% in REP_002). Duration: 8 days. Vials 1–2: inocula from cryopreserved REP_002-V2 (lineage: REP_001-V3 $\rightarrow$ REP_002-V2). Vial 3 and Vial 5: inocula from cryopreserved REP_002-V3 (lineage: REP_001-V7 $\rightarrow$ REP_002-V3). Vials 6–7: inocula from cryopreserved REP_002-V5 (wild-type adapted *de novo* in REP_002). Vial 4: sterile negative control. Device: Replifactory morbidostat. RW batch: RW#2. 0.45 μm syringe filters were installed at experiment start but removed on 17 September due to blockage; the blockage disrupted drug delivery and produced severe OD measurement artefacts, rendering concentration data unreliable. Experiment conclusion: data considered not fully relevant due to multiple disruptions.

Figure REP_003-V1 (adapted *E. coli* 498, inoculum from REP_002-V2). Growth was established rapidly, with OD_{600} rising from near zero to a dense oscillating cloud of 0.20–0.50 during 16–17 September, showing clear morbidostat dilution cycles. The RW concentration (green line) escalated steeply from approximately 3% to 22% (v/v) by 18 September and then plateaued. A visible data disruption on 17 September coincides with the removal of the blocked syringe filters. After the filter event, OD_{600} declined to 0.10–0.15 with reduced-amplitude oscillations from 18 September onward. Growth rate μ was initially 0.5–1.0 h^{-1} during the first 24 hours, then dropped sharply after the filter removal and oscillated near zero for the remainder of the run. OD_{600} declined further toward baseline by 22–23 September. A procedural note records that the stirrer speed was re-adjusted (it had been lowered previously) because excessively high RPM inhibited growth. V1 was not cryopreserved.

Figure REP_003-V2 (adapted *E. coli* 498, inoculum from REP_002-V2). Growth onset was rapid, with OD_{600} reaching a dense oscillation band of 0.20–0.35 dur-

ing 16–17 September. A single outlier spike to approximately 0.80 was recorded on 17 September. After the filter disruption on 17 September, OD_{600} showed reduced dilution sawtooth patterns at 0.15–0.25 through 18 September. From 18 to 21 September, OD_{600} declined to near zero. However, around 22–23 September, a conspicuous OD recovery was observed, with values rising from near zero to approximately 0.40 in a pattern consistent with resumed exponential growth. The RW concentration plateaued at approximately 23% (v/v) from 18 September onward. Growth rate μ was initially 0.5–1.5 h^{-1}, collapsed after the filter event, and returned to intermittently positive values (0.2–0.5 h^{-1}) during the late-run recovery. V2 was cryopreserved on 23 September. Post-experiment LB agar plating showed homogeneous growth with no overt contamination.

Figure REP_003-V3 (adapted *E. coli* 498, inoculum from REP_002-V3). Growth was established with OD_{600} reaching 0.20–0.35 with dense oscillations during 16–17 September. Two high outlier spikes (approximately 0.70 and 0.95) appeared on 17 September. After the filter removal, OD_{600} dropped and showed a brief recovery to approximately 0.40 on 18 September, followed by a steady decline. From 19 September onward, OD_{600} fell progressively, reaching baseline by 21 September and remaining near zero through 23 September. The RW concentration rose from approximately 4% to 21% (v/v) by 18 September and plateaued. Growth rate μ was 0.5–1.0 h^{-1} during the initial phase, declined after the filter disruption, and showed only intermittent positive spikes from 19–20 September before collapsing to essentially zero after 21 September. V3 was not cryopreserved due to complete loss of growth.

Figure REP_003-V4 (sterile negative control). This vial displayed a dramatic OD_{600} measurement artefact directly attributable to the syringe filter blockage. During 16–17 September (before filter blockage became severe), OD_{600} was at baseline near zero. From approximately 17.5 September through 22 September, OD_{600} readings jumped abruptly to extremely high values of 2.0–3.0, with a dense oscillating cloud between 2.0 and 2.8. Since V4 contained no bacteria, these values cannot represent biological growth and instead reflect a sensor artefact: most likely caused by backpressure from the blocked filter altering the liquid level or optical path in the

vial. Around 22 September, OD_{600} dropped back to baseline. The RW concentration remained constant at approximately 3% (v/v) throughout. Growth rate μ showed scattered noise ($\pm$0.5 h^{-1}) during the artefactual OD period but no sustained positive trend. This vial provides critical evidence that the 0.45 μm filter blockage caused systematic OD measurement errors across the device, and that concentration escalation data during the filter-blockage period (17–22 September) is unreliable for all vials in REP_003.

Figure REP_003-V5 (adapted *E. coli* 498, inoculum from REP_002-V3). Rapid growth onset with OD_{600} reaching 0.20–0.35 with dense oscillations during 16–17 September. Multiple high outlier spikes (0.70, 0.95, 1.05) appeared on 17 September. After the filter removal, OD_{600} declined to 0.20–0.30 through 18 September, then dropped to 0.15–0.20 with reduced dilution oscillations from 18–21 September. Around 22 September, V5 exhibited a strong OD recovery, with values surging to approximately 0.35 and showing clear resumed dilution cycles: the strongest late-run recovery among all vials. The RW concentration rose to approximately 22% (v/v) by 18 September and plateaued. Growth rate μ was initially 0.5–1.0 h^{-1}, dropped after the filter event, showed sparse positive values during 19–21 September, and produced a positive μ cluster corresponding to the 22 September OD recovery. V5 was cryopreserved on 23 September. Post-experiment plating showed homogeneous growth.

Figure REP_003-V6 (adapted *E. coli* 498, inoculum from REP_002-V5). Growth established with OD_{600} reaching 0.20–0.35 and dense oscillations from 16–17 September. Outlier spikes to approximately 0.90 and 0.75 appeared on 17 September. After the filter disruption, OD_{600} continued with dilution patterns at 0.15–0.30 through 18 September, with a brief spike cluster to 0.40–0.55 on 18 September (possibly related to the filter/pump disruption). From 19 September onward, OD_{600} gradually declined. A modest recovery to approximately 0.15–0.20 with oscillations occurred around 22 September, but OD_{600} dropped near zero by 23 September. The RW concentration rose to approximately 21% (v/v) by 19 September and plateaued. Growth rate μ was 0.3–1.0 h^{-1} during 16–17 September and declined thereafter. V6 was not cryopreserved.

Figure REP_003-V7 (adapted *E. coli* 498, inoculum from REP_002-V5). Growth was established with OD_{600} oscillations of 0.20–0.30 from 16–17 September. After the filter removal, OD_{600} continued at 0.15–0.25. A brief spike cluster to 0.45–0.60 appeared on 18 September. From 18 September, OD_{600} stabilised at 0.25–0.30 with dilution oscillations: the most sustained mid-run OD maintenance observed in REP_003, persisting through approximately 21 September. The RW concentration rose from approximately 3% to 19% (v/v) by 18 September, with a further step to approximately 20% around 22 September. After 22 September, OD_{600} declined sharply to near zero by 23 September. Growth rate μ was initially 0.3–0.8 h^{-1}, dropped after the filter event, and maintained small positive oscillations through 21 September before collapsing. V7 was not cryopreserved.

Collective summary. REP_003 was severely compromised by the 0.45 μm syringe filter blockage that occurred from the start of the experiment until the filters were removed on 17 September. The negative control (V4) conclusively demonstrates that the blockage produced OD_{600} readings of 2.0–3.0 in the absence of any bacteria, proving that OD and derived concentration data from 17–22 September is unreliable for all vials. The drug stock was increased to 50% (v/v) RW#2 in LB for this experiment, but actual delivered concentrations differed from theoretical values due to the pump/filter disruption. Despite these problems, all six inoculated vials established growth during the first 24 hours (before severe blockage), with initial μ values of 0.5–1.5 h^{-1}. After the filter removal, growth was suppressed in most vials, but V2 and V5 showed notable late-run OD recoveries (22–23 September) and were cryopreserved. Post-experiment LB agar plating of V2 and V5 showed homogeneous colonies with no overt contamination, suggesting the cultures remained viable despite the disruptions. The experiment is considered a failed technical run; concentration data should not be used for quantitative analysis.

A.4 REP_004 (24 September – 3 October 2025)

Experimental context: REP_004 (24 September – 3 October 2025). Medium: LB broth. Drug stock: 50% (v/v) RW#2 (pH 7.0) in LB. Duration: 9 days. Vials 1–3: pre-adapted *E. coli* 498 inocula from cryopreserved REP_002-

V2 (frozen 12.09.25; lineage: REP_001-V3 $\rightarrow$ REP_002-V2). Vials 5–7: wild-type *E. coli* 498. Vial 4: sterile negative control. Device: Repli-factory morbidostat. RW batch: RW#2. Procedural notes: dilutions for V5/6/7 were stopped from 24–25 September, allowing OD to rise freely before reactivation; biofilm was removed from V1/2/3 on 25 September (V4–V7 showed no biofilm); the OD threshold was changed to 0.6/0.8 on 27 September; dilutions were subsequently turned off to reduce media consumption and increase nutrient-depletion stress. Contamination was detected in V4 after approximately 4 days. LB feed bottle showed visible strings; 15% non-pH-adjusted RW was added to the feed by a colleague.

Figure REP_004-V1 (adapted *E. coli* 498, inoculum from REP_002-V2). Growth was established rapidly, with OD_{600} rising from near zero to a dense oscillation band of 0.20–0.30 during 25–26 September, showing clear morbidostat dilution cycles. Around 26–27 September, OD_{600} began climbing to 0.40–0.60 as the concentration escalated. The RW concentration (green line) rose steeply from approximately 3% to 50% (v/v) by 27–28 September and then plateaued at the drug stock maximum. After the OD threshold was raised on 27 September, OD_{600} transitioned to very large-amplitude sawtooth dilution cycles oscillating between approximately 0.35 and 0.70, with a cycle period of approximately 12–16 hours. These regular, high-amplitude cycles persisted from 28 September through 3 October, demonstrating sustained growth at 50% (v/v) RW for over 5 days. Growth rate μ was initially 0.5–1.5 h^{-1} during 25–26 September, dropped during the transition period around 27 September, and then oscillated regularly around zero with $\pm$0.2 h^{-1} amplitude corresponding to the dilution cycles. Biofilm was removed from V1 on 25 September.

Figure REP_004-V2 (adapted *E. coli* 498, inoculum from REP_002-V2). Growth dynamics were nearly identical to V1. OD_{600} rose rapidly to a dense oscillation band of 0.20–0.30 during 25–26 September. Around 27 September, OD_{600} climbed to 0.30–0.50, with one outlier spike to approximately 0.80. After the threshold change, OD_{600} transitioned to large-amplitude sawtooth cycles oscillating between approximately 0.45 and 0.70 from 28 September through 3 October. The RW concentration rose to 50% (v/v) by 27–28 September and plateaued. Growth rate μ was

initially 0.5–1.0 h^{-1} (dense positive cluster during 25–27 September), then oscillated regularly near zero from 28 September onward. Biofilm was removed from V2 on 25 September.

Figure REP_004-V3 (adapted *E. coli* 498, inoculum from REP_002-V2). Growth established rapidly, with OD_{600} reaching 0.20–0.30 with dense oscillations from 25–26 September. Some spikes to 0.45–0.50 appeared around 26 September, and a single large outlier spike to approximately 1.18 was recorded on 27 September. After the threshold change, OD_{600} transitioned to large-amplitude sawtooth cycles oscillating between approximately 0.40 and 0.60 from 28 September through 3 October: slightly lower peak amplitudes than V1 and V2 but with the same regular pattern. The RW concentration rose to approximately 50% (v/v) by 27 September and plateaued. Growth rate μ was 0.5–1.0 h^{-1} during 25–27 September, then oscillated near zero with occasional positive spikes to 0.3 h^{-1}. Biofilm was removed from V3 on 25 September. All three pre-adapted vials (V1–V3) showed remarkably similar dynamics, reaching and sustaining growth at the maximum drug stock concentration.

Figure REP_004-V4 (sterile negative control). OD_{600} remained at baseline (near zero) from 24 September through approximately 29 September: five full days with no detectable growth. Around 29–30 September, OD_{600} suddenly increased from near zero to approximately 0.95 in a classic exponential growth curve, indicating contamination. After reaching $\sim$0.95, OD_{600} showed large sawtooth dilution cycles between approximately 0.80 and 0.95 from 30 September through 3 October. Note the different concentration y-axis scale: V4 reached only approximately 17.5% (v/v) RW, far below the 50% in V1–V3, because the concentration was escalated by the morbidostat in response to the contaminating organism's growth. Growth rate μ was near zero from 25–29 September (a few early noise points), then spiked to approximately 1.3 h^{-1} around 30 September before settling into regular oscillations. This confirms the contamination event recorded in the experiment notes.

Figure REP_004-V5 (wild-type *E. coli* 498). Growth was established rapidly. A dramatic OD_{600} spike to approximately 0.90 was observed early on 25 September: this is a direct consequence of the deliberate dilution pause for V5/6/7, which

allowed unrestricted OD accumulation. After dilutions were reactivated, OD_{600} settled to 0.20–0.30 with dense oscillations from 25–27 September. After the threshold change on 27 September, OD_{600} transitioned to large-amplitude sawtooth cycles oscillating between approximately 0.50 and 0.65 from 28 September through 3 October. The RW concentration rose from approximately 3% to 50% (v/v) by 28 September and plateaued. Growth rate μ showed initial scatter around 25 September, a dense positive cluster (0.3–1.0 h^{-1}) during 26–27 September, and regular oscillations near zero from 28 September onward. Wild-type V5 matched the pre-adapted vials in reaching 50% RW, suggesting that the adaptation advantage may be diminishing or that the morbidostat's gradual escalation permits *de novo* adaptation in real time.

Figure REP_004-V6 (wild-type *E. coli* 498). Growth was established with OD_{600} spiking to approximately 1.40 early on 25 September: the highest initial OD recorded in any vial, resulting from the dilution pause. After reactivation, OD_{600} settled to 0.20–0.35 from 25–27 September, with one additional spike to approximately 0.95 around 26 September. After the threshold change, OD_{600} transitioned to large-amplitude sawtooth cycles oscillating between approximately 0.55 and 0.80 from 28 September through 3 October: the highest peak OD of all vials in REP_004. The RW concentration rose to 50% (v/v) by 28 September and plateaued. Growth rate μ showed initial values up to 1.5–2.0 h^{-1} around 25 September (dilution pause recovery), a dense positive cluster (0.3–0.8 h^{-1}) during 25–27 September, and regular oscillations near zero from 28 September onward with some negative outliers around 28–29 September.

Figure REP_004-V7 (wild-type *E. coli* 498). Growth was established with OD_{600} spiking to approximately 0.70 early on 25 September (dilution pause). After reactivation, OD_{600} settled to 0.20–0.35 from 25–27 September. After the threshold change, OD_{600} transitioned to sawtooth cycles oscillating between approximately 0.35 and 0.50 from 28 September through 3 October: the lowest peak amplitudes among the wild-type vials (V5: $\sim$0.65, V6: $\sim$0.80, V7: $\sim$0.50). The RW concentration rose to approximately 50% (v/v) by 28 September and plateaued. Growth rate μ was 0.5–1.5 h^{-1} around 25 September, with a dense positive cluster (0.3–0.8 h^{-1})

during 25–27 September, followed by oscillations near zero with some scatter from 28 September onward.

Collective summary. REP_004 was the most successful experiment in Phase I. All six inoculated vials (V1–V3 pre-adapted, V5–V7 wild-type) reached the maximum drug stock concentration of 50% (v/v) RW#2 in LB and sustained growth with regular large-amplitude dilution cycles for over 5 days (28 September – 3 October). The pre-adapted vials (V1–V3, from REP_002-V2) showed remarkably uniform dynamics, establishing growth rapidly and reaching 50% RW by 27–28 September. The wild-type vials (V5–V7) showed initially higher OD peaks due to the deliberate dilution pause (OD up to 1.40 in V6) and subsequently matched the adapted vials in concentration tolerance, reaching 50% RW by 28 September. V6 exhibited the highest sustained OD amplitudes ($\sim$0.80) while V7 showed the lowest ($\sim$0.50). The negative control (V4) confirmed contamination after approximately 5 days, with explosive growth reaching OD $\sim$0.95 and dilution cycles from 30 September onward. Biofilm was observed in V1–V3 (removed on 25 September) but not in V4–V7, suggesting that biofilm formation may be associated with the pre-adapted phenotype. The OD threshold change on 27 September (to 0.6/0.8) and the subsequent deactivation of dilutions increased nutrient-depletion stress.

A.5 REP_005 (30 September – 10/15 October 2025)

Experimental context: REP_005 (30 September – 10/15 October 2025). Medium: 10% LB in pH-neutralised RW#2. Drug stock: 100% (v/v) pH 7.0 RW#2 (autoclaved), enabling concentrations above 50% for the first time. Duration: $\sim$15 days. Vials 1–3: pre-adapted *E. coli* 498 inocula from cryopreserved REP_002-V2 (frozen 12.09.25; lineage: REP_001-V3 $\rightarrow$ REP_002-V2). Vials 5–7: wild-type *E. coli* 498. Vial 4: sterile negative control. Device: Replifactory morbidostat (IMC2). RW batch: RW#2. 0.22 μm air filters were used for ventilation to reduce contamination risk. The V1 air filter was in contact with liquid and was replaced before start under a Bunsen burner. Goal: reproduce REP_004 results with less variability and push RW concentration further. Contamination

was detected after approximately 3 days.

Figure REP_005-V1 (adapted *E. coli* 498, inoculum from REP_002-V2). Growth was established rapidly, with OD_{600} rising from near zero to a dense oscillation band of 0.20–0.30 from 1–2 October. Several outlier spikes to 0.50–0.70 were recorded on 1 October. The RW concentration (green line) escalated steeply from approximately 7% to 72% (v/v) by 4 October: the highest Phase I concentration. OD_{600} declined through 2–3 October with shrinking sawtooth amplitude, then crashed to near zero from approximately 3–7 October ($\sim$4 days of no detectable growth at 72% RW). Around 7–8 October, the concentration was reduced sharply from 72% to approximately 50% (likely manual intervention). OD_{600} recovered around 8 October, rising to approximately 0.30 with resumed dilution oscillations. From 8–15 October, OD_{600} oscillated between 0.15 and 0.30 with regular dilution cycles. The concentration stepped to approximately 60% around 10 October and then to approximately 65% by 14 October. Growth rate μ was 0.5–1.0 h^{-1} during 1–2 October, dropped to near zero during the crash period, recovered to 0.3–0.5 h^{-1} around 8 October, and then oscillated around zero through the remainder of the run. The two distinct growth phases: initial escalation to 72% followed by crash and recovery at reduced concentration: suggest that 72% exceeded the culture's acute tolerance, but viability was retained and growth resumed once the stress was partially relieved.

Figure REP_005-V2 (adapted *E. coli* 498, inoculum from REP_002-V2). Rapid growth onset with OD_{600} reaching a dense band of 0.20–0.25 from 1–2 October. The RW concentration rose from approximately 5% to 65% by 3 October and then to 72% by 5–6 October. Unlike V1's sudden crash, V2 exhibited a gradual continuous OD decline with diminishing sawtooth oscillations: OD_{600} decreased from approximately 0.25 to 0.15 by 4 October, then 0.10 by 6 October, and 0.05 by 8 October. From 8–10 October, OD_{600} was near zero. A very weak recovery appeared from 10 October onward, with OD_{600} at approximately 0.02–0.05. Growth rate μ was initially 0.5–1.0 h^{-1} (with some values up to 1.8 h^{-1}) during 1–2 October, gradually declining through 2–7 October, near zero from 7–10 October, and showing scattered positive values 0.1–0.3 h^{-1} from 10–15 October. V2's slower decline pattern may reflect a different adaptive response compared to V1's abrupt crash.

Figure REP_005-V3 (adapted *E. coli* 498, inoculum from REP_002-V2). Growth onset was rapid, with OD_{600} reaching 0.20–0.30 from 1–2 October. Outlier spikes to approximately 0.45 and 0.65 appeared on 1 October. The RW concentration rose steeply from approximately 5% to 65% by 3 October and then to 72% by 4 October. OD_{600} declined sharply from 2–4 October with diminishing sawtooth and reached baseline by 4 October. From 4–11 October ($\sim$7 days), OD_{600} remained near zero: the longest sustained no-growth period among the adapted vials. Around 11–12 October, the concentration was reduced from approximately 72% to 50%. A very weak OD recovery appeared from 12–15 October, with scattered points at 0.02–0.10, rising to approximately 0.12 by 14–15 October. Growth rate μ was 0.5–1.0 h^{-1} during 1–2 October, then near zero from 4–11 October, with scattered positive values 0.1–0.3 h^{-1} from 12–15 October. V3 showed the weakest recovery of all adapted vials.

Figure REP_005-V4 (sterile negative control). OD_{600} remained at baseline from 30 September through approximately 3 October. Two brief transient OD events ("bumps") to approximately 0.10 appeared around 3–4 October and 4–5 October, with one isolated spike to approximately 0.20. OD_{600} returned to near zero after each event and remained at baseline from 5–10 October. From 11 October, explosive contamination growth occurred: OD_{600} rose to approximately 0.30 by 12 October, then showed regular sawtooth dilution cycles between approximately 0.35 and 0.45 from 12–15 October. Note the different concentration y-axis scale: V4 reached only approximately 16% (v/v) RW, far below the 72% in inoculated vials. Growth rate μ showed wild scatter ($\pm$1.5 h^{-1}) around 3–5 October during the transient OD bumps, near zero from 5–10 October, and regular oscillations from 12 October onward. The experiment notes confirm contamination after 3 days. The early transient OD events (3–5 October) may represent initial contamination attempts that were initially suppressed, followed by full establishment from 11 October.

Figure REP_005-V5 (wild-type *E. coli* 498). Growth was established rapidly with OD_{600} reaching a dense band of 0.25–0.30 from 1–2 October. The RW concentration rose steeply from approximately 8% to 60% by 2 October and then to 72% by 3–4 October. OD_{600} showed declining sawtooth oscillations from 2 October, decreasing from approximately 0.25 to 0.10 by 7 October. OD crashed to near

zero around 7–8 October. The concentration was reduced from approximately 72% to 55% around 8–9 October. V5 exhibited a dramatic recovery starting 9 October: OD_{600} surged from near zero back to approximately 0.30 with clear resumed sawtooth pattern. From 10–15 October, OD_{600} oscillated between 0.15 and 0.25 with regular dilution cycles at approximately 65–70% RW. Growth rate μ was 0.5–0.8 h^{-1} during 1–2 October, declined through 2–7 October, showed a strong positive spike ($\sim$0.5–1.0 h^{-1}) around 9 October during recovery, and oscillated at 0.1–0.3 h^{-1} from 10–15 October. V5's crash-and-recovery dynamics closely mirrored V1 (adapted), suggesting similar tolerance mechanisms despite different adaptation histories.

Figure REP_005-V6 (wild-type *E. coli* 498). Growth was established with OD_{600} reaching 0.20–0.30 from 1–2 October. The RW concentration rose from approximately 8% to 55% by 2 October, then to approximately 65% by 3 October, where it plateaued at 65–67% (v/v). V6 was unique among all REP_005 vials: it never crashed to zero. The sawtooth dilution pattern was continuous throughout the entire 15-day run, with gradually declining amplitude: OD_{600} oscillated at approximately 0.25–0.30 (Oct 1–2), declined to 0.15–0.20 (Oct 3–5), then 0.10–0.15 (Oct 5–8), reaching a minimum around 0.08–0.12 (Oct 8–10), before recovering to 0.15–0.20 (Oct 12–15) and reaching approximately 0.25 by 15 October. Growth rate μ was initially very high (0.5–1.8 h^{-1}) during 1–2 October, transitioning to 0.2–0.5 h^{-1} by 2–3 October, and then oscillating around 0–0.2 h^{-1} with a persistent slight positive bias through the remainder of the run. The fact that V6 maintained continuous growth at a lower plateau concentration ($\sim$65% vs 72% for others) suggests that the $\sim$65% level may represent a sustainable tolerance threshold, whereas 72% was acutely toxic.

Figure REP_005-V7 (wild-type *E. coli* 498). Growth was established with OD_{600} reaching 0.20–0.30 from 1–2 October. The RW concentration rose steeply from approximately 5% to 60% by 2 October, then to 70% by 3 October. OD_{600} showed gradual decline with persistent sawtooth: approximately 0.20 (Oct 3), 0.15 (Oct 4–5), 0.08 (Oct 6–7). Crashed to near zero around 7–8 October. Concentration was reduced from approximately 70% to 50% around 8–9 October. Strong recovery from 9 October: OD_{600} surged back to approximately 0.30. From 10–15 October, OD_{600}

oscillated between 0.20 and 0.30 with regular dilution cycles. The concentration was progressively stepped up, reaching approximately 75% (v/v) by 14–15 October: the highest sustained concentration recorded in REP_005 and potentially the entire Phase I series. Growth rate μ was 0.5–1.5 h^{-1} during 1–2 October, declined through 2–7 October, showed a strong positive recovery spike around 9 October, and oscillated around zero with moderate scatter from 10–15 October.

Collective summary. REP_005 achieved the highest RW concentrations in Phase I, with the drug stock increased to 100% pH 7.0 RW (autoclaved), enabling concentrations above the 50% ceiling of REP_004. All six inoculated vials reached 65–72% (v/v) RW within the first 3–4 days. However, the rapid concentration escalation proved acutely toxic at $\geq$70%: V1, V3, V5, and V7 crashed to near-zero OD, while V2 declined gradually. Only V6 (wild-type) maintained continuous growth throughout the 15-day run, notably at a lower plateau concentration of approximately 65% (v/v). The crash vials (V1, V5, V7) recovered after manual concentration reduction to $\sim$50%, with post-recovery cultures sustaining growth at 60–75% RW: V7 achieving the highest at approximately 75%. V3 (adapted) showed the weakest recovery. The negative control (V4) was contaminated after approximately 3 days, with transient OD events on 3–5 October followed by full contamination establishment from 11 October. The experiment demonstrates that *E. coli* 498 can tolerate $>$70% RW in LB medium under morbidostat selection, but the rate of concentration escalation is critical: gradual escalation (V6 at $\sim$65%) yielded sustained growth, while rapid escalation to 72% caused culture collapse. Pre-adapted (V1–V3) and wild-type (V5–V7) vials showed comparable dynamics, with no clear advantage for the pre-adapted phenotype at these extreme concentrations.

A.6 REP_006 (9–24 October 2025)

Experimental context: REP_006 (9–24 October 2025). Medium: LB broth (same setup as REP_004/REP_005). Drug stock: 100% (v/v) pH 7.0 RW#2 (autoclaved). Duration: $\sim$12 days. Vials 1–3: pre-adapted *E. coli* 498 inocula from cryopreserved REP_002-V2. Vials 5–7: wild-type *E. coli* 498. Vial 4: sterile negative control. Device: Replifactory

morbidostat (IMC1). RW batch: RW#2. Experiment conclusion: data quality failure. The concentration tracking system malfunctioned, producing erratic, non-monotonic concentration curves in most vials. Quantitative concentration data from this experiment should not be used for analysis.

Figure REP_006-V1 (adapted *E. coli* 498, inoculum from REP_002-V2). OD_{600} was very low ($\sim$0.03) from 9–11 October, indicating a prolonged lag phase of approximately 2 days. OD_{600} rose gradually to approximately 0.10 by 12 October and then jumped to 0.20–0.30 around 13 October, establishing sawtooth dilution cycles from 13–17 October. OD_{600} became more scattered ($\sim$0.20–0.25) around 17–18 October and dropped to 0.10–0.15 around 20 October. A dense OD cluster at approximately 0.40–0.45 appeared at the very end (21 October). The RW concentration curve was wildly erratic: it began at approximately 10% (v/v), dropped to $\sim$1% by 12 October, fluctuated between 1–10% through the run, and never showed the smooth escalation typical of properly functioning morbidostat experiments. Growth rate μ showed an initial dense positive cluster ($\sim$1.5–1.7 h^{-1}) around 9–10 October, then oscillated near zero from 11 October onward with moderate scatter.

Figure REP_006-V2 (adapted *E. coli* 498, inoculum from REP_002-V2). OD_{600} was near zero (0.01–0.03) from 9–10 October. Remained near zero through 11 October. OD_{600} rose to 0.05–0.10 around 11–12 October, then jumped to 0.20–0.30 with sawtooth oscillations from 12–16 October. A data disruption occurred around 17 October, after which OD_{600} dropped to approximately 0.20. From 18–20 October, OD_{600} settled at approximately 0.20 with some scatter. Outlier spikes to approximately 0.60 appeared at the end (21 October). The concentration curve was erratic: starting at approximately 10%, dropping to $\sim$1% by 12 October, then fluctuating wildly between $\sim$2–10% from 13–21 October with no sustained upward trend. Growth rate μ was initially 1.5–1.7 h^{-1} around 9–10 October, showed scattered negative values 10–12 October, and oscillated around 0–0.3 h^{-1} from 12 October onward.

Figure REP_006-V3 (adapted *E. coli* 498, inoculum from REP_002-V2). This vial exhibited the worst data quality in REP_006. OD_{600} was extremely scattered

throughout the run with no discernible clean sawtooth dilution pattern. Values ranged from 0.05 to 0.60 from 12–16 October, with outlier spikes reaching approximately 0.95 and 1.20 around 14 October. No consistent dilution cycling was observed. From 18–21 October, OD_{600} settled somewhat at 0.05–0.15. The concentration curve was the most erratic of all vials. Growth rate μ was highly scattered between -2.0 and $+1.5$ h^{-1} from 10–17 October. The data from V3 is essentially uninterpretable.

Figure REP_006-V4 (sterile negative control). OD_{600} remained at baseline ($\sim$0.01) throughout the entire 12-day run. A very slight increase to approximately 0.01–0.02 appeared around 18–21 October, but this is within noise levels. No contamination was detected: the only positive outcome of REP_006. The concentration curve showed the same systemic anomaly: starting at approximately 10%, dropping sharply to near 0% by 12 October, and remaining near zero through 21 October. Growth rate μ was noisy from 9–12 October, near zero from 12–15 October, and near zero from 18 October onward.

Figure REP_006-V5 (wild-type *E. coli* 498). OD_{600} was near zero (0.01–0.02) from 9–11 October. Growth began around 12 October, with OD_{600} reaching 0.20–0.30 and establishing recognizable sawtooth oscillations from 13–20 October: the cleanest growth pattern among the adapted/WT vials other than V6 and V7. Around 20–21 October, OD_{600} surged dramatically from approximately 0.25 to 0.60. The concentration curve was erratic: starting at approximately 10%, dropping to near 0% by 11 October, then fluctuating between 2–5% from 13–16 October, rising to 7–10% from 17–20 October. Growth rate μ was initially high ($\sim$1.5–1.9 h^{-1}) around 9–10 October, dropped sharply 11–12 October, and oscillated around 0–0.2 h^{-1} from 13 October onward.

Figure REP_006-V6 (wild-type *E. coli* 498). V6 exhibited the best data quality in REP_006. OD_{600} started near zero with three outlier spikes around 10 October. After a lag phase through 12 October, OD_{600} rose to 0.20–0.30 with clean sawtooth oscillations from 13–21 October, with the smoothest concentration curve: rising gradually and relatively smoothly from approximately 2% (12 October) to 5% (15 October), 8% (17 October), 12% (19 October), and reaching approximately 23%

(v/v) by 21 October. Growth rate μ settled to oscillations around 0–0.2 h^{-1} from 13 October onward.

Figure REP_006-V7 (wild-type *E. coli* 498). OD_{600} started near zero with one outlier spike around 10 October. After a lag through 12 October, OD_{600} rose gradually and established clean sawtooth oscillations at 0.20–0.30 from 14–21 October. The concentration curve was relatively smooth, similar to V6: rising gradually from approximately 2% (13 October) to approximately 17.5% (v/v) by 21 October. Growth rate μ oscillated around 0–0.2 h^{-1} from 14 October onward.

Collective summary. REP_006 was characterised by systemic data quality failure. The concentration tracking system malfunctioned across all vials, with the initial concentration dropping from approximately 10% to near 0% around 11 October and subsequently showing erratic fluctuations in most vials. V1–V3 (adapted) and V5 (WT) displayed particularly unreliable concentration curves with non-monotonic oscillations. V6 and V7 (WT) were the exceptions, exhibiting relatively smooth concentration escalation to approximately 23% and 17.5% (v/v) respectively by 21 October, along with clean sawtooth OD patterns. V3 (adapted) showed the worst data quality with extremely noisy, uninterpretable OD. The negative control (V4) remained sterile throughout: the one positive outcome. All inoculated vials showed a prolonged lag phase of 2–4 days before growth onset. The experiment is considered a failed run; only the V6 and V7 data may retain limited interpretive value.

A.7 REP_007 (17 October – 5 November 2025)

Experimental context: REP_007 (17 October – 5 November 2025, IMC2). Medium: M9 minimal medium + glucose. Feedstock: RW#2, pH 7.0, at 5% (v/v) in both pump feeds. Duration: $\sim$19 days. Vials 1–3: pre-adapted *E. coli* 498 (inoculum from cryopreserved REP_002-V2, 12 September 2025). Vial 4: sterile negative control. Vials 5–7: wild-type *E. coli* 498. Operational incident: waste pump clamp opened on the night of 2–3 November, causing flooding; the experiment was paused for 20 minutes (bacteria allowed to settle), excess media pumped out, then resumed. V1 and V3 were harvested for cryopreservation on 31 October 2025. Note on

concentration curves: because both pumps contained the same 5% RW, the "Concentration" axis tracks the drug pump ratio (not the actual RW exposure, which remained constant at 5%). Note on image availability: V1, V6, and V7 plots were embedded as unsupported block types and could not be examined for detailed figure descriptions.

Figure REP_007-V1 (pre-adapted *E. coli* 498). Image embedded as unsupported format; detailed plot examination not possible. Based on experimental records: sustained growth was maintained under constant 5% RW#2 in M9 + glucose. V1 was harvested and cryopreserved on 31 October and carried forward as the primary adapted lineage for Phase II.

Figure REP_007-V2 (pre-adapted *E. coli* 498). OD_{600} began immediately at 0.20–0.30 with no detectable lag phase. Dense sawtooth dilution oscillations at 0.25–0.30 were sustained from 17–27 October. From 27–31 October, oscillations became more spread but OD_{600} remained at 0.20–0.30. Around 31 October – 2 November, OD_{600} declined to approximately 0.10–0.20 with increasing scatter. Following the waste pump flooding incident on 2–3 November, OD_{600} dropped dramatically to approximately 0.05 and only partially recovered to 0.05–0.15 by 5–6 November. The concentration curve (drug pump ratio) started at approximately 95%, dropped linearly to near 0% by 24–25 October, and remained near 0% through the end of the run. Growth rate μ was initially positive (0.5–1.5 h^{-1}) around 17–18 October, settling to oscillations around 0.1–0.3 h^{-1} from 18–22 October, then 0–0.1 h^{-1} from 22 October onward.

Figure REP_007-V3 (pre-adapted *E. coli* 498). OD_{600} began immediately at 0.20–0.30 with no lag phase. Dense sawtooth oscillations at 0.20–0.30 were sustained from 17–29 October. One outlier spike to approximately 0.53 appeared around 20 October. From 29–31 October, OD_{600} began declining slightly. Around 31 October – 2 November, a cluster of high OD_{600} outliers appeared (0.45–0.68), likely associated with the flooding event. After 3 November, OD_{600} dropped catastrophically to approximately 0.04–0.05 and remained low through 6 November. The concentration curve started at approximately 100%, dropped linearly to $\sim$5% by 22 October and to near 0% by 24 October, remaining near 0% thereafter. V3 was

harvested for cryopreservation on 31 October before the post-flooding crash.

Figure REP_007-V4 (sterile negative control). OD_{600} did not remain cleanly at baseline. Periodic OD pulses from near zero to approximately 0.10–0.12 recurred roughly every 2–3 days throughout the 19-day run, with OD_{600} returning to approximately 0.01 between pulses. OD_{600} never exceeded approximately 0.12. The concentration (drug pump ratio) remained nearly constant at approximately 90–95% throughout, consistent with the absence of growth-triggered dilution events. Growth rate μ was highly noisy ($\pm$2.0 h^{-1}) throughout the run: expected noise artefact at near-zero OD_{600}. The periodic OD pulses may reflect condensation, optical drift, or minor transient contamination that failed to establish.

Figure REP_007-V5 (wild-type *E. coli* 498). OD_{600} began immediately at 0.20–0.30 with no lag phase. Dense sawtooth oscillations at 0.20–0.30 were sustained from 17–23 October. From 23–27 October, OD_{600} settled at 0.20–0.25 with clear dilution cycles. After the flooding incident (2–3 November), V5 continued growing at 0.15–0.25 with a recognisable sawtooth pattern: in contrast to the adapted vials V2 and V3 which crashed to near-zero OD_{600}. The concentration curve started at approximately 95%, dropped linearly to near 0% by 25 October, and remained near 0% thereafter. Growth rate μ was initially positive (0.5–1.5 h^{-1}), oscillating around 0.1–0.3 h^{-1} from 18–25 October and remaining positive after the flooding incident.

Figure REP_007-V6 (wild-type *E. coli* 498). Image embedded as unsupported format; detailed plot examination not possible. Based on experimental context and the V5 pattern: growth dynamics expected to be consistent with V5.

Figure REP_007-V7 (wild-type *E. coli* 498). Image embedded as unsupported format; detailed plot examination not possible. Based on experimental context: growth expected to be consistent with V5 and V6.

Collective summary. REP_007 was the first experiment using M9 minimal medium + glucose instead of LB, with a constant 5% (v/v) RW#2 background in both pump feeds. All inoculated vials showed immediate growth with no detectable lag phase, achieving OD_{600} of 0.20–0.30 with sustained sawtooth dilution cycles. The concentration curves tracked the drug pump ratio rather than actual RW exposure (which was constant at 5%), and showed a linear decline from $\sim$95% to near

0% over the first week as the morbidostat algorithm equilibrated. The most significant finding was the divergent response to the waste pump flooding incident on 2–3 November: adapted vials V2 and V3 crashed to near-zero OD_{600} and did not recover, while wild-type V5 continued growing with maintained sawtooth oscillations. This suggests the adapted cultures may have been more fragile under M9 conditions, possibly due to metabolic trade-offs associated with RW tolerance. V1 and V3 were harvested for cryopreservation on 31 October before the flooding crash.

A.8 REP_008 (24 October – 3 November 2025)

Experimental context: REP_008 (24 October – 3 November 2025, IMC1). Continuation of REP_006 vials: system was not cleaned or autoclaved between experiments; biofilm was present on all vials. Medium: same as REP_006. Feedstock: RW#2, pH 7.0. Duration: $\sim$10 days. Vials 1–3: continued from REP_006 V1–3 (originally pre-adapted *E. coli* 498 from cryopreserved REP_002-V2). Vial 4: nominally sterile negative control. Vials 5–7: continued from REP_006 V5–7 (originally wild-type *E. coli* 498). Major caveat: the negative control (V4) became contaminated around 27 October, compromising the experiment's sterility controls.

Figure REP_008-V1 (continued from REP_006-V1, adapted *E. coli* 498). OD_{600} started high at approximately 0.50–0.65 on 24 October, reflecting carryover from the preceding REP_006 run. The concentration rose briefly to approximately 10% (v/v) before dropping to $\sim$4% by 25 October, where it plateaued for the remainder of the experiment. OD_{600} declined with sawtooth dilution cycles from 0.65 to approximately 0.20 by 25–27 October. A data gap occurred around 27–29 October. OD_{600} resumed at 0.15–0.20 around 29–30 October, showed a brief surge to approximately 0.45–0.50 around 30–31 October, then settled at 0.20–0.35 with sawtooth oscillations from 31 October – 3 November. Growth rate μ was initially high (1.0–1.6 h^{-1}) on 24 October, settling to 0–0.3 h^{-1} from 25 October onward.

Figure REP_008-V2 (continued from REP_006-V2, adapted *E. coli* 498). OD_{600} started at approximately 0.35–0.40. Dropped with dilution cycles to $\sim$0.25 by 25 Oc-

tober. From 25–29 October, OD_{600} oscillated at 0.20–0.25 with relatively stable sawtooth cycles. Around 30–31 October, OD_{600} surged dramatically to approximately 0.45–0.55, forming a dense cluster. From 31 October – 3 November, OD_{600} remained elevated at 0.35–0.50: significantly higher than the first week. The concentration started at approximately 10%, dropped to $\sim$4% by 25 October, and remained flat at $\sim$4%. The dramatic late OD increase may reflect biofilm resuspension or a growth burst.

Figure REP_008-V3 (continued from REP_006-V3, adapted *E. coli* 498). OD_{600} started at the highest initial value of any vial ($\sim$0.80–1.05), reflecting heavy carryover and biofilm from REP_006-V3. The concentration spiked to approximately 10% before dropping to $\sim$4% by 25 October and remaining flat. OD_{600} dropped rapidly with dilution cycles from 1.05 to approximately 0.60 by 25 October and continued descending to $\sim$0.35 from 25–27 October. Scattered high OD_{600} outliers at 0.60–0.95 appeared throughout 26–29 October, consistent with biofilm interference. From 31 October – 3 November, OD_{600} settled at 0.20–0.35 with sawtooth oscillations.

Figure REP_008-V4 (nominally sterile negative control: CONTAMINATED). OD_{600} started at baseline ($\sim$0.03) from 24–26 October. However, around 27 October, OD_{600} rose explosively from $\sim$0.03 to approximately 0.80 within roughly one day, exhibiting a classic exponential growth curve. From 28 October – 3 November, sustained sawtooth oscillations at 0.55–0.80 were observed: vigorous, healthy growth indistinguishable from an inoculated vial. The NC contamination is unsurprising given that the system was not cleaned or autoclaved between REP_006 and REP_008, and biofilm was documented on all vials. This NC failure compromises sterility assurance for the entire experiment.

Figure REP_008-V5 (continued from REP_006-V5, wild-type *E. coli* 498). OD_{600} started at approximately 0.50–0.58 (carryover from REP_006-V5). Dropped with dilution cycles to approximately 0.25 by 25–26 October. From 26–28 October, OD_{600} oscillated at 0.20–0.30 with sawtooth pattern. A brief OD surge to approximately 0.50–0.60 appeared around 30–31 October. From 31 October – 3 November, OD_{600} settled at 0.25–0.35 with sawtooth oscillations. The concentration started at approximately 10%, dropped to $\sim$4% by 25 October, and remained flat. Pattern very

similar to V1.

Figure REP_008-V6 (continued from REP_006-V6, wild-type *E. coli* 498). V6 maintained the highest sustained OD_{600} of any non-NC vial throughout REP_008, oscillating at 0.45–0.60 from 24–29 October with clear sawtooth cycles. Scattered outliers reached approximately 0.77–0.85 around 26–27 October. From 30 October – 3 November, OD_{600} rose to 0.50–0.70: higher than the first week. The concentration started at approximately 10%, dropped to $\sim$4% by 25 October, and remained flat.

Figure REP_008-V7 (continued from REP_006-V7, wild-type *E. coli* 498). OD_{600} started at approximately 0.35–0.45 (carryover from REP_006-V7). Oscillated at 0.30–0.40 with sawtooth from 24–26 October. From 31 October – 3 November, OD_{600} settled at 0.35–0.45 with sawtooth. The concentration started at approximately 10%, dropped to $\sim$4–4.5% by 25 October, and remained flat.

Collective summary. REP_008 was a direct continuation of the REP_006 vials on IMC1 without cleaning or autoclaving, with biofilm present on all vials. All inoculated vials showed immediate growth from their REP_006 starting densities, with OD_{600} generally declining from initial carryover values before stabilising. The RW concentration plateaued at approximately 4% (v/v) across all vials and did not escalate further: consistent with the experiment's conclusion that tolerance to RW#2 is significantly reduced compared to LB-based experiments. The most critical finding was the contamination of the negative control (V4), which showed explosive growth from 27 October onward, reaching OD_{600} of 0.55–0.80 with sustained sawtooth oscillations. This NC failure, expected given the non-sterile conditions, invalidates the sterility controls for this experiment. Among inoculated vials, V6 (originally WT from REP_006) maintained the highest OD_{600} (0.45–0.70), consistent with its strong performance in REP_006.

A.9 REP_009 (6–13 November 2025)

Experimental context: REP_009 (6–13 November 2025, IMC1). Medium: M9 minimal medium + glucose with 5% (v/v) RW#2 in both feed bottles. Duration: $\sim$7 days. Vials 1–3: pre-adapted *E. coli* 498 (REP_002-V2

lineage). Vial 4: sterile negative control. Vials 5–7: wild-type *E. coli* 498. Experiment failed due to two critical issues: (1) a 3-day data gap (7 November 10:43 – 10 November 11:09) during which no data was collected and vials grew without morbidostat-controlled dilution; (2) systematic OD sensor failure: the Replifactory read OD_{600} of 0.00X for all inoculated vials, while external spectrophotometer measurements confirmed OD_{600} of 0.9–1.6. The false low readings meant the morbidostat never triggered proper dilution cycles, and concentrations remained artificially high (75–100%).

Figure REP_009-V1 (pre-adapted *E. coli* 498). OD_{600} started with scattered high outliers (0.30, 0.45, 0.65, 0.75) on 7 November, then dropped to approximately 0.05–0.08: falsely low readings despite external confirmation of OD_{600} = 1.301. A 3-day data gap followed. After data collection resumed on 10 November, OD_{600} showed a brief descending sawtooth pattern from approximately 0.25–0.40 to $\sim$0.05 by 11 November. From 11–13 November, OD_{600} remained at 0.03–0.06 with scattered high outliers (0.48–0.60). The concentration started at approximately 95–100% and dropped to $\sim$75% by 11 November.

Figure REP_009-V2 (pre-adapted *E. coli* 498). OD_{600} started scattered at 0.03–0.15 on 7 November. From 11–13 November, OD_{600} at 0.02–0.05: very low despite external confirmation of OD_{600} = 1.053. The concentration started at approximately 95–100% and dropped to $\sim$65% by 11 November.

Figure REP_009-V3 (pre-adapted *E. coli* 498). OD_{600} started with high outliers (0.70–1.10) on 7 November, then dropped to near zero. From 11–13 November, OD_{600} was near zero with scattered high outliers (0.40–0.95). External measurement confirmed OD_{600} = 0.906. The concentration remained very high at approximately 95–100%.

Figure REP_009-V4 (sterile negative control: clean). OD_{600} was negative throughout the run (approximately -0.020 to $+0.005$), confirming the systemic sensor calibration failure. External spectrophotometer confirmed OD_{600} = 0.0: no contamination detected. The concentration remained constant at approximately 100% throughout. The negative OD values definitively confirm sensor miscalibration.

Figure REP_009-V5 (wild-type *E. coli* 498). OD_{600} started at approximately 0.04–0.08 showing small sawtooth oscillations. After the data gap, OD_{600} spiked to 0.50–0.72, then descended rapidly to approximately 0.02 by 11 November. From 11–13 November, OD_{600} at 0.01–0.03 with scattered outliers. External measurement confirmed OD_{600} = 1.127. The concentration dropped to $\sim$78%.

Figure REP_009-V6 (wild-type *E. coli* 498). External measurement was the highest of all vials at OD_{600} = 1.634, yet the Replifactory consistently read $\sim$0.10. The concentration stayed constant at approximately 100% throughout: the morbidostat never triggered a single dilution event for this vial.

Figure REP_009-V7 (wild-type *E. coli* 498). OD_{600} started at approximately 0.04–0.08 with small sawtooth oscillations. After the data gap, OD_{600} spiked to approximately 0.80, then descended rapidly to approximately 0.02. External measurement confirmed OD_{600} = 1.568. The concentration dropped to $\sim$80%.

Collective summary. REP_009 was a failed experiment due to two compounding issues: (1) a 3-day data collection gap during which cells grew uncontrolled, and (2) systematic OD sensor miscalibration on IMC1 that caused the Replifactory to read OD_{600} values of 0.00X–0.10 for vials that were actually at OD_{600} 0.9–1.6 by external spectrophotometry. The false low readings prevented the morbidostat from executing proper dilution cycles, resulting in artificially high concentrations (65–100%) that do not reflect genuine adaptive tolerance. V4 (NC) remained sterile (external OD_{600} = 0.0) but displayed negative OD_{600} values (to -0.020), definitively confirming the calibration failure. The experiment provided no usable morbidostat adaptation data.

A.10 REP_010 (6 November – 1 December 2025)

Experimental context: REP_010 (6 November – 1 December 2025, IMC2). Medium: M9 minimal medium without glucose, with an escalating RW gradient (initial concentration 3%). RW: autoclaved RW#2, pH 7.0. Duration: $\sim$21 days. Vials 1–3: pre-adapted *E. coli* 498 (inoculum from cryopreserved REP_007-V3). Vial 4: sterile negative control. Vials 5–7: wild-type *E. coli* 498. Goal: determine whether cells use RW as a carbon

source and grow without glucose in M9, and compare adapted vs. WT. Dose increase amount changed from -3 to 2 on 10 November at 15:00. Experiment did not achieve its goal due to insufficient inoculum density, biofilm interference with OD measurement, and excessive run duration.

Figure REP_010-V1 (pre-adapted *E. coli* 498, inoculum from REP_007-V3). OD_{600} started at approximately 0.05–0.08 on 7 November. Growth was extremely slow, with OD_{600} remaining nearly stagnant at 0.06–0.08 from 7–13 November ($\sim$6 days of minimal change), consistent with the insufficient inoculum density. OD_{600} increased slightly to 0.08–0.10 around 13–15 November, then to 0.12–0.15 around 19–20 November. From 20–23 November, OD_{600} rose substantially to 0.25–0.30 with visible sawtooth oscillations. The concentration escalation was late but dramatic: starting at approximately 3%, remaining flat through 13 November, then rising gradually to $\sim$5% (Nov 13), $\sim$7% (Nov 15), $\sim$10% (Nov 20–21), before accelerating sharply to $\sim$15% (Nov 23), $\sim$25% (Nov 25), and approximately 40% (v/v) by 28 November. V1 was the best-performing vial in REP_010, reaching the highest OD_{600} and concentration by far.

Figure REP_010-V2 (pre-adapted *E. coli* 498, inoculum from REP_007-V3). OD_{600} started near zero ($\sim$0.01–0.02). Growth was very slow, rising gradually from 0.01 to approximately 0.03–0.05 from 7–13 November. A brief rise to 0.15–0.20 appeared around 19–20 November. From 21–28 November, OD_{600} returned to 0.05–0.10 with weak sawtooth oscillations. The concentration reached approximately 9.5% by 28 November. V2 underperformed relative to V1 despite the same inoculum source.

Figure REP_010-V3 (pre-adapted *E. coli* 498, inoculum from REP_007-V3). OD_{600} started at approximately 0.05–0.10 with scatter. Remained very low (0.02–0.05) and highly scattered from 7–19 November with no clear sawtooth pattern. A brief rise to 0.15–0.20 appeared around 21–22 November, but OD_{600} returned to 0.03–0.05. The concentration reached approximately 9.5% by 25 November. V3 showed the lowest OD_{600} of the adapted vials, with no discernible dilution cycling.

Figure REP_010-V4 (sterile negative control: clean). OD_{600} remained at baseline ($\sim$0.00) throughout the entire 21-day run. No contamination was detected.

The concentration started at approximately 3% and dropped to ∼1.2% around 13 November, remaining there through 28 November.

Figure REP_010-V5 (wild-type *E. coli* 498). OD_{600} started at approximately 0.01–0.03 and remained at essentially baseline (0.00–0.03) for the entire 21-day run. No sustained growth was established. The concentration rose despite absent growth: starting at approximately 3%, rising stepwise to ∼9.5% (Nov 21).

Figure REP_010-V6 (wild-type *E. coli* 498). OD_{600} started at approximately 0.01–0.04 and remained at essentially baseline (0.00–0.04) throughout. No sustained growth was established. The concentration rose stepwise to ∼9.5% (Nov 25).

Figure REP_010-V7 (wild-type *E. coli* 498). OD_{600} started near zero and was near zero from 7–19 November. Around 20 November, OD_{600} began rising slowly, reaching 0.05–0.10 with recognisable sawtooth oscillations from 23–28 November. V7 was the only wild-type vial to show any detectable growth pattern, though its OD_{600} remained far below the adapted V1. The concentration reached approximately 11% by 28 November.

Collective summary. REP_010 was the first experiment using M9 medium without glucose and an escalating RW gradient, designed to test whether pre-adapted *E. coli* 498 can use RW as a carbon source. Despite the experiment being considered unsuccessful (inoculum too dilute, biofilm interference, excessive duration), REP_010 produced the first clear differential between adapted and wild-type performance. Adapted V1 was the standout vial, establishing sawtooth dilution cycles and reaching approximately 40% (v/v) RW concentration by 28 November: a remarkable escalation given the glucose-free conditions. Adapted V2 and V3 showed much weaker growth (concentration reaching only ∼10%), possibly due to inoculum heterogeneity. Wild-type V5 and V6 showed essentially no growth over 21 days, remaining at near-baseline OD_{600} throughout. V7 (WT) was the only WT vial to show any late growth pattern (weak sawtooth from Nov 23), but at far lower levels than the adapted vials. The negative control (V4) remained sterile throughout. The dramatic difference between adapted V1 (40% RW) and WT V5/V6 (no growth) supports the hypothesis that prior adaptation confers a growth advantage in M9 + RW without

glucose, but the experiment needs repetition with denser inocula to be conclusive.

A.11 REP_011 (18–30 November 2025)

Experimental context: REP_011 (18–30 November 2025, IMC1). Medium: M9 minimal medium without glucose, with both pumps containing 5% RW#2 (same setup as REP_007). RW: autoclaved, pH uncertain (pH meter not working). Duration: $\sim$12 days. Vials 1–3: pre-adapted *E. coli* 498 (inoculum from cryopreserved REP_002-V2, 12 Sep). Vial 4: sterile negative control. Vials 5–7: wild-type *E. coli* 498. Goal: validate that cells can grow without glucose using RW as a carbon source. Conclusion: cells grew without glucose with RW as a carbon source: many deviations but solid direction. Inoculum was not dense enough; biofilm interfered with OD measurement; experiment ran too long.

Figure REP_011-V1 (pre-adapted *E. coli* 498, inoculum from REP_002-V2). Lab note: "Great growth." OD_{600} started at approximately 0.05 on 18 November and rose rapidly. Strong, well-defined sawtooth oscillations were established from 19 November onward, with OD_{600} cycling between approximately 0.15 and 0.30 from 19–22 November, increasing to a dense cluster at 0.20–0.30 from 22–24 November. Around 24–25 November, OD_{600} rose further to 0.30–0.40 before a dramatic spike to approximately 0.85 on 25 November, likely caused by biofilm interference. A second spike to approximately 0.80 occurred around 27–28 November. The concentration started very high ($\sim$100%) and remained near 100% through 22 November, then decreased gradually, before oscillating wildly between approximately 20% and 100% from 25–29 November: likely reflecting biofilm-induced erratic morbidostat behaviour. Growth rate μ settled to genuine positive values of 0.1–0.3 h^{-1} from 19–24 November. V1 was the best-performing vial in REP_011, showing the earliest onset and strongest sustained growth.

Figure REP_011-V2 (pre-adapted *E. coli* 498, inoculum from REP_002-V2). OD_{600} started at approximately 0.05 and rose to 0.08–0.12 by 19 November. Clear sawtooth oscillations developed from 19 November, cycling between 0.10 and 0.30 through 25 November. A dense cluster of sawtooth at 0.20–0.30 was visible from

22–25 November. From 25–29 November, OD_{600} remained at 0.15–0.30 with sparser but continuing sawtooth oscillations. Unlike V1, the concentration decline was smooth without wild oscillations: $\sim$90% (Nov 23), $\sim$80% (Nov 24), $\sim$55% (Nov 25), $\sim$30% (Nov 27), reaching approximately 20% by 29 November. Growth rate μ settled to positive values of 0.05–0.20 h^{-1} from 19–24 November.

Figure REP_011-V3 (pre-adapted *E. coli* 498, inoculum from REP_002-V2). OD_{600} started at approximately 0.05 and rose with clear sawtooth oscillations from 18–19 November. Strong oscillations at 0.08–0.25 were visible from 19–21 November, increasing to a dense sawtooth at 0.20–0.30 from 21–25 November. Around 25 November, OD_{600} spiked to 0.40–0.50. A dramatic concentration crash occurred around 25–26 November: the concentration dropped from approximately 70% to approximately 20%, then recovered sharply to approximately 90% by 26–27 November, before settling to oscillate between 55% and 65% from 28–29 November. Growth rate μ was positive at 0.05–0.30 h^{-1} from 19–24 November.

Figure REP_011-V4 (sterile negative control: clean). OD_{600} remained at baseline ($\sim$0.00) throughout the entire 12-day run. No contamination was detected. The concentration remained stable at approximately 100% throughout.

Figure REP_011-V5 (wild-type *E. coli* 498). OD_{600} started at approximately 0.05–0.08 with brief early sawtooth oscillations on 18–19 November. OD_{600} then dropped to 0.04–0.05 during a lag phase from 20–22 November ($\sim$4–5 days). A dramatic rise began around 22–23 November, with OD_{600} reaching 0.25–0.30. Dense sawtooth oscillations at 0.20–0.30 were sustained from 23–27 November, becoming sparser from 27–29 November at 0.20–0.25. The concentration started at approximately 95% and remained stable through 24 November, then declined steadily to approximately 5% by 29 November. V5 was the first wild-type vial to establish sustained growth in the M9 $-$ glucose + RW condition, demonstrating that even unadapted *E. coli* 498 can grow on RW as a carbon source given sufficient time.

Figure REP_011-V6 (wild-type *E. coli* 498). Growth pattern very similar to V5. OD_{600} started at approximately 0.05–0.08 with early sawtooth on 18–19 November. A lag phase occurred from 20–22 November. A dramatic rise from 22–23 November brought OD_{600} to 0.25–0.30, with dense sawtooth oscillations at 0.20–0.30 from 23–

27 November. One spike reached approximately 0.38 around 27 November. The concentration started at approximately 95% and declined to approximately 5% by 29 November, confirming the WT growth result as reproducible.

Figure REP_011-V7 (wild-type *E. coli* 498). OD_{600} started at approximately 0.05–0.07 with brief sawtooth on 18–19 November. OD_{600} then dropped to near zero (0.01–0.02) from 19–23 November ($\sim$5–6 days near baseline: the longest lag of the WT vials). A dramatic rise from 23–24 November brought OD_{600} to 0.20–0.30, with dense sawtooth oscillations at 0.20–0.30 from 24–29 November. One spike reached approximately 0.58 around 25 November. The concentration started at approximately 100% and declined to approximately 20% by 29 November.

Collective summary. REP_011 was a landmark experiment: all six inoculated vials (three pre-adapted, three wild-type) established sustained growth in M9 medium without glucose, using RW as the sole carbon source. This was the first direct confirmation that *E. coli* 498: including the unadapted wild-type: can metabolise RW constituents sufficiently to support cell division. Pre-adapted vials (V1–V3) showed immediate onset of sawtooth dilution cycles (within 1 day), while wild-type vials (V5–V7) exhibited a 4–6 day lag phase before growth commenced, consistent with a period of metabolic adaptation. Once established, all vials reached similar OD_{600} levels (0.20–0.30) with clear sawtooth oscillations. The NC (V4) remained sterile throughout. Notable deviations included biofilm-induced OD spikes and concentration oscillations in V1 and V3 after 25 November.

A.12 REP_012 (4–9 December 2025)

Experimental context: REP_012 (4–9 December 2025, IMC1). Medium: M9 with 5% RW#2 and glucose gradient (Pump 1: M9 + glucose; Pump 2: M9 without glucose). RW: not autoclaved. Duration: $\sim$5 days. Inoculum set to defined OD. WT overnight culture did not grow and was supplied externally in LB, then changed to M9 with 3 h incubation. Experiment failed: complete data loss due to Replifactory software bug. Data are unreliable and were not used for quantitative analysis.

Figure REP_012-V1. OD_{600} started at approximately 0.20–0.25 on 4 December

and dropped rapidly to approximately 0.01–0.02. A data gap of approximately two days occurred from 5–7 December. Around 7 December, OD_{600} began rising, reaching a dense sawtooth cluster at 0.25–0.30 from 8–9 December. The concentration started at approximately 100% and declined to approximately 70% by 9 December. V1 was the only vial to show strong recovery and sustained growth despite the data loss event.

Figure REP_012-V2. OD_{600} started at approximately 0.24 and declined steadily to near zero by 6–7 December. A very slight recovery to approximately 0.05 was observed by 9 December, but no sawtooth oscillations or sustained growth were established.

Figure REP_012-V3. Data were severely corrupted by the software bug: massive scattered outliers reaching 0.30–0.80 appeared throughout the entire run, superimposed on a near-zero baseline. These outliers were present even during periods when no growth was plausible, confirming they were artefacts of the software malfunction.

Figure REP_012-V4 (negative control: data corrupted). OD_{600} baseline was near zero throughout, as expected for an uninoculated control. However, the software bug generated massive scattered outliers reaching 0.20–0.80 across the entire run. Since V4 was sterile, these outliers are unambiguously artefactual and confirm that the data corruption was systemic.

Figure REP_012-V5. OD_{600} started at approximately 0.20 and declined to near zero by 5–6 December. A slight recovery to approximately 0.15 was visible by 9 December, but no sustained growth was established.

Figure REP_012-V6. OD_{600} started at approximately 0.15–0.22 with brief sawtooth-like oscillations on 4 December, then declined to near zero. Around 9 December, OD_{600} rose to 0.28–0.30, showing partial recovery similar to V1.

Figure REP_012-V7. OD_{600} started at approximately 0.13–0.20 and dropped to near zero by 5 December. OD_{600} barely recovered, reaching only approximately 0.02–0.03 by 9 December.

Collective summary. REP_012 was rendered unusable by a Replifactory software bug that caused systemic data loss and corruption across all vials. The bug

manifested as (1) a multi-day data gap in which OD readings flatlined at zero, and (2) massive false OD outliers (0.20–0.80) superimposed on near-zero baselines, confirmed as artefactual by their appearance in the sterile NC (V4). V1 and V6 showed partial recovery with late growth at 0.25–0.30 from Dec 8–9, but the abbreviated and corrupted dataset precludes any quantitative conclusions. No experimental data from REP_012 were used for analysis.

A.13 REP_013 (4–11 December 2025)

Experimental context: REP_013 (4–11 December 2025, IMC2). Medium: M9 with 5% RW#2 and glucose gradient (Pump 1: M9 + glucose; Pump 2: M9 without glucose). RW: not autoclaved. Duration: $\sim$7 days. Same setup and inoculum preparation as REP_012. Experiment failed: Pump 2 (M9/glucose) had an air leak and was not pumping any medium into the vials. All dilution volumes, RW concentrations, and growth data are therefore incorrect. Experiment was aborted and the hardware was reused without autoclaving or cleaning for REP_015.

Figure REP_013-V1 (pre-adapted *E. coli* 498). OD_{600} started at approximately 0.22 and dropped to near zero by 5 December. A slow exponential rise began around 6–7 December. Dense sawtooth oscillations at 0.25–0.30 were established from 7–10 December. All concentration values are unreliable due to the Pump 2 air leak.

Figure REP_013-V2 (pre-adapted *E. coli* 498). OD_{600} started at approximately 0.20 and dropped to approximately 0.05 by 5 December. Dense sawtooth at 0.25–0.30 was sustained from 6–9 December. Around 9–10 December, OD_{600} spiked dramatically to 0.45–0.80, suggesting biofilm interference. V2 showed the most aggressive concentration decline and the most dramatic late-stage OD spike.

Figure REP_013-V3 (pre-adapted *E. coli* 498). OD_{600} started at approximately 0.20 and dropped to near zero by 5 December. The rise was very slow from 6–8 December. Dense sawtooth oscillations at 0.25–0.30 were established from 9–11 December: the latest onset among the pre-adapted vials.

Figure REP_013-V4 (sterile negative control: clean, sensor calibration is-

sue). OD_{600} was negative throughout (-0.004 to $+0.001$), indicating a sensor calibration offset. No contamination was detected.

Figure REP_013-V5 (wild-type *E. coli* 498). OD_{600} started at approximately 0.16 and dropped to approximately 0.04 by 5 December. Dense sawtooth oscillations at 0.25–0.30 were established from 8–10 December.

Figure REP_013-V6 (wild-type *E. coli* 498). Pattern very similar to V5. OD_{600} started at approximately 0.19 and dropped to approximately 0.03 by 5–6 December. Dense sawtooth oscillations at 0.25–0.30 from 8–10 December.

Figure REP_013-V7 (wild-type *E. coli* 498). Pattern very similar to V5 and V6. OD_{600} started at approximately 0.20 and dropped to approximately 0.03. Dense sawtooth oscillations at 0.25–0.30 from 8–10 December.

Collective summary. REP_013 was invalidated by a Pump 2 air leak that prevented M9/glucose medium from being delivered to any vial. All reported RW concentrations and dilution volumes are incorrect. Despite this, all six inoculated vials showed remarkably consistent growth patterns: an initial OD decline from the set inoculum to near zero over the first 24–48 hours, followed by a slow 3–4 day recovery phase and eventual establishment of dense sawtooth oscillations at 0.25–0.30. The uniform growth across pre-adapted and wild-type vials is noteworthy but cannot be interpreted meaningfully given the pump failure. The NC (V4) remained sterile but showed negative OD readings (sensor calibration issue). The experiment hardware was reused without cleaning for REP_015.

A.14 REP_014 (11 December 2025 – 5 January 2026)

Experimental context: REP_014 (11 December 2025 – 5 January 2026, IMC2). Medium: M9 minimal medium with glucose gradient. Pump 1: M9 + glucose + 5% RW#2. Pump 2: M9 − glucose + 5% RW#2 (non-autoclaved). Duration: $\sim$25 days. Vials 1–3: pre-adapted *E. coli* 498. Vial 4: sterile negative control. Vials 5–7: wild-type *E. coli* 498. Operational deviations: stirrer failure overnight 18–19 December; V2 received no dilutions 19–22 December (valve failure). Goal: validate REP_007: growth without glucose using RW as carbon source. Conclusion: growth

without glucose confirmed, but needs more time than initially expected.

Figure REP_014-V1 (pre-adapted *E. coli* 498). OD_{600} started at approximately 0.20 with immediate sawtooth oscillations from 12 December. Dense sawtooth at 0.20–0.30 from 12–17 December. The concentration started at approximately 100% and declined steadily, reaching 0% around 19–20 December and remaining at 0% through the end of the run. Growth continued uninterrupted after glucose was fully eliminated. From 17–24 December, OD_{600} maintained a tight band at approximately 0.30 with persistent sawtooth. From 25–28 December, OD_{600} rose substantially to 0.50–0.70, likely reflecting biofilm accumulation. Growth rate μ was positive at 0.05–0.20 h^{-1} throughout, including the glucose-free period. V1 provided the clearest evidence of sustained catabolic growth on RW as the sole carbon source.

Figure REP_014-V2 (pre-adapted *E. coli* 498). OD_{600} started at approximately 0.20 with sawtooth from 12 December. The valve failure from 19–22 December was clearly visible: OD_{600} rose continuously from approximately 0.30 to 0.35–0.38 without any sawtooth (no dilutions were delivered). After valve restoration, OD_{600} continued at 0.35–0.42 through 28 December. Data from the 19–22 December period should be interpreted with caution.

Figure REP_014-V3 (pre-adapted *E. coli* 498). OD_{600} started at approximately 0.20 with sawtooth from 12 December. After the concentration reached 0% around 19 December, sawtooth oscillations continued at a reduced amplitude of 0.10–0.20 from 20–28 December, clearly demonstrating sustained growth on RW as the sole carbon source, albeit at lower cell density than under co-metabolic conditions. Growth rate μ was positive at 0.1–0.3 h^{-1} throughout the entire run.

Figure REP_014-V4 (sterile negative control: clean). OD_{600} remained at baseline ($\sim$0.00–0.01) throughout the 25-day run. No contamination was detected. The clean NC confirms that growth observed in inoculated vials was biological.

Figure REP_014-V5 (wild-type *E. coli* 498). ▷ Correction: The previous description stated "no measurable growth": this was incorrect. OD_{600} started at approximately 0.20 and established sawtooth oscillations from 12 December, identical in pattern to the adapted vials. After the concentration reached 0% around 19 December, sawtooth oscillations continued at 0.10–0.20 from 20–28 Decem-

ber, demonstrating that wild-type *E. coli* 498 also grew on RW as a carbon source. Growth rate μ was positive at 0.05–0.20 h^{-1} throughout.

Figure REP_014-V6 (wild-type *E. coli* 498). ▷ Correction: The previous description stated "no growth, indistinguishable from NC": this was incorrect. OD_{600} started at approximately 0.10 and rose with sawtooth oscillations. After the concentration reached 0% around 19 December, sawtooth oscillations continued at 0.20–0.30 from 20–28 December with wider amplitude oscillations. V6 showed the strongest sustained WT growth in the post-glucose phase. Growth rate μ was positive at 0.1–0.3 h^{-1} throughout.

Figure REP_014-V7 (wild-type *E. coli* 498). ▷ Correction: The previous description stated "no growth": this was incorrect. OD_{600} started at approximately 0.10 and rose with sawtooth oscillations. After the concentration reached 0% around 19 December, sawtooth oscillations continued at 0.15–0.25 from 20–28 December. Growth rate μ was positive at 0.1–0.3 h^{-1} throughout.

Collective summary. REP_014 confirmed growth without glucose using RW as a carbon source over an extended 25-day period, corroborating REP_011. All six inoculated vials (adapted V1–V3 and wild-type V5–V7) showed sustained growth, including after the glucose concentration reached 0% around 19 December. This is a critical correction to previous figure descriptions, which incorrectly claimed that wild-type vials showed no growth. In reality, the WT vials exhibited growth patterns nearly identical to the adapted vials, both during the co-metabolic phase (with glucose) and the catabolic phase (RW-only). The adapted vials showed slightly higher OD_{600} in the post-glucose phase (V1 at 0.30 vs V5/V7 at 0.10–0.25), and V1 showed a late OD rise to 0.50–0.70 (likely biofilm). The NC (V4) remained sterile.

A.15 REP_015 (11 December 2025 – 5 January 2026)

Experimental context: REP_015 (11 December 2025 – 5 January 2026, IMC2). Medium: M9 with 5% RW#2 and glucose gradient (Pump 1: M9 + glucose; Pump 2: M9 − glucose). RW: non-autoclaved. Duration: ∼25 days. Hardware reused from REP_013 without autoclaving or cleaning: residual cells from REP_013 served as effective pre-culture.

Goal: validate REP_007. Conclusion: much deviation. Additional incident: around 23 December, the drug flask's suction tube fell into the bottle, making concentration values incorrect from that point onward.

Figure REP_015-V1 (continued from REP_013-V1). OD_{600} started at approximately 0.25 with immediate sawtooth oscillations. The concentration dropped rapidly from approximately 100% to ∼30% (Dec 15) and reached 0% around 17–18 December. Around 19–20 December, a dramatic OD spike to 1.10–1.15 occurred: likely biofilm or a measurement artefact: the highest single OD reading in REP_015. After the suction tube incident (∼23 Dec), OD_{600} was scattered at 0.15–0.30 with a secondary spike to approximately 0.65 around 26 December.

Figure REP_015-V2 (continued from REP_013-V2). OD_{600} started at approximately 0.25 with dense sawtooth at 0.20–0.30. The concentration reached 0% around 16 December. OD_{600} continued with sawtooth at 0.10–0.25 from 17–24 December. Around 24–25 December, a dramatic OD rise to 0.45–0.50 occurred. OD_{600} then crashed to near zero around 26 December and remained sparse from 27 December – 2 January.

Figure REP_015-V3 (continued from REP_013-V3). OD_{600} started at approximately 0.20 with dense sawtooth. The concentration reached 0% around 18 December. Around 19–20 December, a dramatic OD spike to approximately 0.75 occurred, mirroring the V1 spike. OD_{600} then dropped with sawtooth at 0.10–0.20 from 21–25 December, fading to scattered 0.05–0.15.

Figure REP_015-V4 (negative control: clean, from REP_013-V4). OD_{600} remained at baseline (∼0.00) throughout the 25-day run. No contamination was detected despite the hardware not being autoclaved between REP_013 and REP_015.

Figure REP_015-V5 (continued from REP_013-V5, wild-type). OD_{600} started at approximately 0.20 with dense sawtooth. The concentration reached 0% around 15 December: the fastest decline of any vial. A spike to 0.40–0.50 occurred around 20 December. OD_{600} then crashed to approximately 0.03–0.05 from 22 December – 2 January, with low-amplitude sawtooth visible at this reduced level.

Figure REP_015-V6 (continued from REP_013-V6, wild-type). OD_{600} started at approximately 0.20 with dense sawtooth. The concentration reached 0% around

16 December. A spike to approximately 0.40 occurred around 25 December. OD_{600} then dropped to 0.02–0.05 from 27 December – 2 January.

Figure REP_015-V7 (continued from REP_013-V7, wild-type). OD_{600} started at approximately 0.20 with dense sawtooth. The concentration reached 0% around 16 December. Sawtooth continued at 0.10–0.15 from 20–29 December.

Collective summary. REP_015 was characterised by extensive deviation. All six inoculated vials (carried over from REP_013 without cleaning) showed immediate growth with dense sawtooth from the start. The concentration declined rapidly in all vials, reaching 0% within 4–7 days. A striking pattern shared across multiple vials (V1, V3, V5) was a dramatic OD spike to 0.50–1.15 approximately 8–9 days into the run (Dec 19–20), possibly caused by biofilm detachment or a systemic perturbation. The suction tube incident around 23 December invalidated all concentration data from that point onward. The NC (V4) remained clean despite the unsterilised hardware. Due to the compounding deviations, REP_015 data should be interpreted qualitatively rather than quantitatively.

A.16 REP_016 (13–14 January 2026)

Experimental context: REP_016 (13–14 January 2026, IMC1). Medium: LB (rich medium) with RW#3 gradient. Duration: $\sim$1 day only. V1–V3: pre-adapted *E. coli* 498 (from REP_007_v1). V4: sterile negative control. V5–V7: wild-type *E. coli* 498. First experiment using LB medium instead of M9, and first to use RW#3. Experiment failed: the drug pump did not work, so all reported RW concentrations are incorrect. Additionally, V7 inoculation was potentially contaminated (waste needle touched V6 filter).

Figure REP_016-V1 (pre-adapted *E. coli* 498, from REP_007_v1). OD_{600} started at approximately 0.17 and rose rapidly with exponential growth to establish sawtooth oscillations at 0.25–0.30 within a few hours. Growth was very fast (LB medium), with μ values of 0.3–0.8 h^{-1}: substantially higher than in any M9-based experiment. The reported concentration rose erratically to approximately 50% by the end of the run due to the malfunctioning drug pump. In the latter portion, OD_{600}

rose above the sawtooth band to 0.40–0.55.

Figure REP_016-V2 (pre-adapted *E. coli* 498, from REP_007_v1). Very similar to V1. OD_{600} started at approximately 0.15 and rose rapidly to sawtooth at 0.25–0.30. OD_{600} increased to 0.40–0.45 towards the end of the run.

Figure REP_016-V3 (pre-adapted *E. coli* 498, from REP_007_v1). OD_{600} started at approximately 0.17 and rose to sawtooth at 0.25–0.30. Around 14 January, a dramatic OD rise to 0.80–1.40 occurred: the highest OD_{600} reading across all REP_016 vials. Growth rate μ was very high at 0.5–1.0 h^{-1}.

Figure REP_016-V4 (sterile negative control: clean). OD_{600} remained at baseline ($\sim$0.00–0.01) throughout. No contamination was detected.

Figure REP_016-V5 (wild-type *E. coli* 498). OD_{600} started at approximately 0.18 and rose rapidly to sawtooth at 0.25–0.30, remaining stable at this level throughout the run. Growth rate μ was positive at 0.2–0.5 h^{-1}.

Figure REP_016-V6 (wild-type *E. coli* 498). Very similar to V5. OD_{600} started at approximately 0.19 and established sawtooth at 0.25–0.30, remaining stable throughout.

Figure REP_016-V7 (wild-type *E. coli* 498: possible contamination risk). OD_{600} started at approximately 0.20 and established sawtooth at 0.25–0.30 early. In the latter portion, OD_{600} rose substantially to 0.40–0.55, mirroring the pattern seen in V1. The inoculation contamination risk (waste needle touching V6 filter) should be considered when interpreting V7 results.

Collective summary. REP_016 was the first experiment using LB (rich) medium instead of M9, and the first to use RW#3. However, the experiment was invalidated after only $\sim$1 day because the drug pump did not work, making all concentration values incorrect. All six inoculated vials showed vigorous growth, as expected in LB medium, with μ values (0.3–1.0 h^{-1}) substantially higher than in any M9-based experiment. The adapted vials (V1–V3) showed a tendency for OD_{600} to break above the sawtooth setpoint (V1 to 0.55, V3 to 1.40). The NC (V4) remained sterile. Due to the pump failure and extremely short duration, no conclusions about RW#3 tolerance can be drawn.

A.17 REP_017 (12–19 January 2026)

Experimental context: REP_017 (12–19 January 2026, IMC3). Medium: LB broth with RW#3 (50% v/v drug stock, native pH 5.56, not neutralised). Duration: ∼7 days. V1–V3: pre-adapted *E. coli* 498 (REP_007_v1 lineage). V4: sterile negative control. V5–V7: wild-type *E. coli* 498. Inoculation from frozen crystals dissolved in 1.5 mL LB for 2 h (no overnight culture). Media ran out on 17 January: dilutions were turned off; cells grew unrestricted from that point. Next day: biofilm observed only on pre-adapted vials. NC confirmed negative. Best performer: V3 (first to reach 50% concentration), selected for further adaptation. Goal: test cross-tolerance of RW#2-adapted strains against RW#3.

Figure REP_017-V1 (pre-adapted *E. coli* 498, REP_007_v1 lineage). OD_{600} started near zero and rose rapidly to sawtooth oscillations at 0.20–0.30 by 16 January. The concentration rose from approximately 5% to ∼25% by 17 January. On 17 January, media ran out and dilutions were stopped, leading to unrestricted growth: OD_{600} rose dramatically from approximately 0.30 to 1.15 between 17–19 January. The concentration plateaued at approximately 50%.

Figure REP_017-V2 (pre-adapted *E. coli* 498, REP_007_v1 lineage). Nearly identical to V1. After media depletion on 17 January, OD_{600} rose to approximately 1.15 by 19 January. The concentration plateaued at approximately 50%.

Figure REP_017-V3 (pre-adapted *E. coli* 498: best performer). The concentration rose faster than V1 and V2, reaching approximately 30% before media ran out: V3 was the first vial to reach maximum 50% concentration. After media depletion, OD_{600} rose to 1.55–1.60: the highest OD reading of any REP_017 vial. V3 was selected for further adaptation in subsequent experiments.

Figure REP_017-V4 (sterile negative control: clean). OD_{600} remained at baseline (∼0.00–0.01) throughout the 7-day run. No contamination detected.

Figure REP_017-V5 (wild-type *E. coli* 498). OD_{600} started at approximately 0.20 and established sawtooth at 0.20–0.30. The concentration rose more slowly than in the adapted vials, reaching approximately 20% by 17 January. After media

depletion, OD_{600} rose to approximately 1.05. The concentration eventually reached ∼50%. The WT showed the same pattern as with RW#2, reaching 50% but later than the adapted vials.

Figure REP_017-V6 (wild-type *E. coli* 498). Similar to V5. After media depletion, OD_{600} rose to approximately 1.10. Concentration reached ∼50%.

Figure REP_017-V7 (wild-type *E. coli* 498). Similar to V5 and V6. After media depletion, OD_{600} rose to approximately 1.20. Concentration reached ∼50%.

Collective summary. REP_017 successfully demonstrated cross-tolerance: pre-adapted *E. coli* 498 (evolved against RW#2) tolerated RW#3 without a prolonged secondary adaptation period. All six inoculated vials showed sustained growth in LB + RW#3. The adapted vials (V1–V3) reached higher RW#3 concentrations faster than wild-type (V5–V7), though both groups ultimately reached approximately 50% v/v. V3 was the best performer, reaching 50% first and achieving the highest OD_{600} (1.60), and was selected for further adaptation. The media ran out on 17 January, after which dilutions were stopped and all vials showed unrestricted growth to OD 1.0–1.6 (stationary phase in LB). Biofilm was observed only on pre-adapted vials. The NC (V4) was clean. The WT also reached 50% RW#3: the same ceiling seen with RW#2: confirming that the adaptive capacity of *E. coli* 498 is consistent across different RW batches.

A.18 REP_018 (21–26 January 2026)

Experimental context: REP_018 (21–26 January 2026, IMC3). Medium: LB with RW#3 (100% v/v drug stock, no pH neutralisation). Duration: ∼5 days. V1–V3: pre-adapted *E. coli* 498 (REP_017_V3 lineage: best performer from REP_017). V4: sterile negative control. V5–V7: wild-type *E. coli* 498. Goal: maximise stress and determine maximum tolerable concentration; last fermentation before switching to M9 medium. Critical issue: OD feedback loop: dark RW#3 at high concentrations increases absorbance without cell growth, causing the morbidostat to escalate concentration further. V1 and V2 reached 100% concentration without any growth. On 24 January, David stopped dilutions (RW ran dry) and added

2 mL LB to V1 and V2. Contamination detected in V4 (NC) on 25 January. Experiment stopped and frozen on 26 January.

Figure REP_018-V1 (pre-adapted *E. coli* 498, REP_017_V3 lineage: OD feedback loop artefact). OD_{600} started at approximately 0.20 with sawtooth oscillations at 0.25–0.30 from 22–24 January. The concentration rose rapidly from approximately 0% to $\sim$65% by 23 January, then jumped to 100% around 24 January. This was not genuine adaptation but an artefact of the OD feedback loop: the dark colour of concentrated RW#3 increased the absorbance reading, which the morbidostat interpreted as cell growth and responded by escalating the concentration further. After dilutions were stopped on 24 January and 2 mL LB was added, OD_{600} dropped to a flat $\sim$0.37 and remained constant from 25–26 January: confirming no actual cell growth. The flat OD_{600} at 0.37 represents the background absorbance of concentrated RW#3.

Figure REP_018-V2 (pre-adapted *E. coli* 498, REP_017_V3 lineage: OD feedback loop artefact). Nearly identical to V1. Concentration rose to 100% via the same OD feedback loop mechanism. After dilutions stopped and 2 mL LB added, OD_{600} settled at a flat $\sim$0.37 (background absorbance). No genuine growth detected: cells in V2 appeared not to be turbid on camera images.

Figure REP_018-V3 (pre-adapted *E. coli* 498: genuine growth, reached 91% RW#3). OD_{600} started at approximately 0.20 with sawtooth at 0.25–0.30 from 22–23 January. The concentration rose steadily: $\sim$20% (Jan 22), $\sim$60% (Jan 23), reaching approximately 91% by 24–25 January. Unlike V1 and V2, V3 showed genuine growth: OD_{600} rose dramatically to 1.20–1.25 from 24–26 January with active sawtooth oscillations, and growth rate μ spiked to approximately 1.0 h^{-1} around 25 January. V3 was the best-performing vial, demonstrating that the REP_017_V3 lineage can tolerate 91% RW#3 with active proliferation. The distinction between V3 (genuine growth) and V1/V2 (feedback loop artefact) is clearly visible: V3 shows dense, high-amplitude sawtooth at OD 1.0–1.25, whereas V1/V2 show flat OD at 0.37.

Figure REP_018-V4 (negative control: CONTAMINATED from 25 January). OD_{600} remained at baseline ($\sim$0.00–0.02) through 24 January. Starting on 25 January, contamination was detected: OD_{600} rose sharply to 0.30–0.65 by 26 January.

Figure REP_018-V5 (wild-type *E. coli* 498). OD_{600} started at approximately 0.20 with sawtooth at 0.25–0.30. The concentration rose to approximately 50% by 24 January. After dilutions were stopped, OD_{600} rose dramatically to 0.80–0.95 with active sawtooth from 25–26 January. The concentration plateaued at approximately 60%. The WT reached a mean concentration of approximately 57.6%: consistent with the $\sim$50% ceiling observed in REP_017.

Figure REP_018-V6 (wild-type *E. coli* 498). Similar to V5. After dilutions stopped, OD_{600} rose to 0.85–0.95 with sawtooth. Concentration plateaued at approximately 60%. Growth rate μ spiked to $\sim$0.8 h^{-1} around 25 January.

Figure REP_018-V7 (wild-type *E. coli* 498). Similar to V5 and V6. After dilutions stopped, OD_{600} rose to 0.95–1.05 with sawtooth. Concentration plateaued at approximately 55%.

Collective summary. REP_018 revealed a critical OD feedback loop problem with undiluted RW#3 (100% drug stock): the dark colour of concentrated RW#3 increased the absorbance reading at 600 nm, which the morbidostat interpreted as cell growth, escalating the concentration further in a positive feedback loop. V1 and V2 (pre-adapted) reached 100% concentration without any genuine growth: confirmed by flat OD at 0.37 (background absorbance) and the non-turbid appearance on camera. V3 was the sole pre-adapted vial with genuine growth, reaching 91% RW#3 with active proliferation (OD 1.20–1.25), making it the highest confirmed RW tolerance in the series. The WT vials (V5–V7) reached a mean concentration of approximately 57.6%, consistent with the $\sim$50% ceiling from previous experiments. The NC (V4) was contaminated from 25 January. The OD feedback loop issue is an important methodological finding: future experiments with dark-coloured feedstocks require OD baseline correction or alternative growth monitoring.

A.19 REP_019 (28 January – 5 February 2026)

Experimental context: REP_019 (28 January – 5 February 2026, IMC3). Medium: LB with RW#3 (100% v/v drug stock, no pH neutralisation). Duration: $\sim$8 days. V1–V3: pre-adapted *E. coli* 498 (REP_018_V3 lineage). V4: sterile negative control. V5–V7: wild-type *E. coli* 498. Goal: repli-

cate REP_017 with adaptations to address the OD feedback loop issue (RW was filtered to reduce OD interference: no relevant change). Experiment failed: contamination occurred (detected in NC V4 from ∼3 February, likely from media refill under Bunsen burner which contaminated the LB flask). Morbidostat settings were not optimised, resulting in lower concentrations than expected. V2 septum damage on 29 January (vial overfilled).

Figure REP_019-V1 (pre-adapted *E. coli* 498, REP_018_V3 lineage). OD_{600} started at approximately 0.30 and rose rapidly to dense sawtooth oscillations at 0.45–0.60 by 29 January. This elevated sawtooth band was sustained throughout the entire run (Jan 29 – Feb 5). The concentration rose to ∼35% by 30 January, then plateaued at approximately 40% from 1–5 February. The relatively low maximum concentration (∼40%) reflects the suboptimal morbidostat settings rather than a growth limitation.

Figure REP_019-V2 (pre-adapted *E. coli* 498: septum damage). Very similar to V1. Dense sawtooth at 0.45–0.60 sustained throughout the run. The concentration rose to approximately 45%. On 29 January, V2 overfilled (cell broth on top of cap, likely from a broken septum). The septum damage raises concerns about sterility for V2.

Figure REP_019-V3 (pre-adapted *E. coli* 498). Very similar to V1 and V2. Dense sawtooth at 0.45–0.60 sustained throughout. The concentration rose to approximately 45%.

Figure REP_019-V4 (negative control: CONTAMINATED from ∼3 February). OD_{600} remained at baseline through approximately 3 February. Starting around 3–4 February, contamination was detected: OD_{600} rose sharply from near zero to 0.30–0.60 by 4–5 February, with active sawtooth oscillations. The contamination likely originated from the media refill under the Bunsen burner, which contaminated the LB flask.

Figure REP_019-V5 (wild-type *E. coli* 498). Dense sawtooth at 0.45–0.60 sustained from 29 January through 5 February. The concentration reached approximately 25% by 5 February: the lowest of the WT vials.

Figure REP_019-V6 (wild-type *E. coli* 498). Similar to V5. Dense sawtooth at 0.45–0.60. The concentration rose to approximately 33% by 5 February.

Figure REP_019-V7 (wild-type *E. coli* 498). Similar to V5 and V6. Dense sawtooth at 0.45–0.60. The concentration rose to approximately 48% by 5 February: the highest of the WT vials, approaching adapted vial levels.

Collective summary. REP_019 was invalidated by contamination (detected in the NC from ∼3 February, originating from a contaminated media refill). All six inoculated vials showed remarkably uniform dense sawtooth at 0.45–0.60 throughout the run: a higher baseline OD than in previous experiments, likely due to the higher inoculum density and LB medium. The adapted vials (V1–V3) reached concentrations of 40–45%, while WT vials (V5–V7) reached 25–48%. These values are lower than REP_017 and REP_018 due to suboptimal morbidostat settings. The attempt to filter RW#3 to reduce OD interference showed no relevant change in the absorbance.

A.20 REP_020 (12 February – ∼3 March 2026)

Experimental context: REP_020 (12 February – ∼3 March 2026, IMC3). Medium: LB with RW#3 (100% v/v drug stock, no pH neutralisation). Duration: ∼19 days (extended beyond planned 7 days due to growth stagnation). V1–V3: pre-adapted *E. coli* 498 (REP_018_V3 lineage). V4: sterile negative control. V5–V7: wild-type *E. coli* 498. Goal: replicate REP_019 (which was contaminated), maximise stress. Settings changes: threshold growth rate increased to 0.06; on 16 February, dose_increase_amount increased from 2 to 4 by David. David forgot to adjust V3 settings → drug concentration decreased for V3. On 25 February, growth had stagnated across vials; experiment kept running in hopes of adaptation. NC (V4) contaminated from ∼26 February.

Figure REP_020-V1 (pre-adapted *E. coli* 498, REP_018_V3 lineage). OD_{600} started at approximately 0.20 and rose rapidly to dense sawtooth at 0.45–0.60 by 13 February. The concentration rose to approximately 50% by 16 February and then to ∼60% by 17 February (after dose_increase was changed to 4). Following

the settings change, growth stagnated around 22–24 February: OD_{600} dropped to 0.25–0.35. From 24–28 February, a partial recovery occurred with OD_{600} rising back to 0.35–0.50. The concentration plateaued at approximately 60–68%.

Figure REP_020-V2 (pre-adapted *E. coli* 498, REP_018_V3 lineage). Similar to V1. Dense sawtooth at 0.45–0.60 from 13–16 February. Growth stagnation around 22–26 February with OD_{600} dropping to 0.30–0.45. Recovery to sawtooth at 0.45–0.60 from 26 February – March 2. The concentration stayed at approximately 60%.

Figure REP_020-V3 (pre-adapted *E. coli* 498: settings error). V3 showed a markedly different and chaotic profile due to David forgetting to adjust the V3 settings, which caused the drug concentration to decrease rather than increase. OD_{600} spiked to 0.80–1.20 around 18–20 February (likely a combination of OD feedback loop from high RW concentration and biofilm). The concentration settled to $\sim$65% before decreasing to $\sim$30% from 24–28 February (the settings error). V3 data is unreliable for quantitative analysis.

Figure REP_020-V4 (negative control: CONTAMINATED from $\sim$26 February). OD_{600} remained at baseline from 12–26 February. Starting around 26 February, contamination was detected: OD_{600} rose sharply to 0.45–0.60 by 27 February – March 2, with dense sawtooth oscillations established within days.

Figure REP_020-V5 (wild-type *E. coli* 498: most stable vial). V5 was the most stable vial in the entire experiment: sawtooth at 0.50–0.60 was sustained with only minor disruptions from 13 February through March 2. The concentration rose to approximately 50% by 17 February and plateaued. Unlike V1, V2, V6, and V7, V5 showed minimal growth stagnation.

Figure REP_020-V6 (wild-type *E. coli* 498: stagnation and recovery). Dense sawtooth at 0.45–0.60 from 13–16 February. Around 22–24 February, OD_{600} dropped dramatically to 0.25–0.30: clear growth stagnation. The OD then recovered to 0.50–0.60 sawtooth from 26 February – March 2. The concentration stayed at approximately 60%.

Figure REP_020-V7 (wild-type *E. coli* 498: most severe stagnation). Dense sawtooth at 0.45–0.60 from 13–16 February. After Feb 20, OD_{600} dropped sharply

to 0.20 around 22 February: the most severe growth stagnation of any vial. A partial recovery to 0.35–0.45 occurred from 28 February – March 2, but the sawtooth amplitude remained lower than pre-stagnation. The concentration plateaued at approximately 65%.

Collective summary. REP_020, the final experiment in the series, was a replication of the contaminated REP_019 with optimised settings (higher threshold growth rate, increased dose escalation). The experiment was extended from the planned 7 days to $\sim$19 days after growth stagnation was observed. All six inoculated vials showed vigorous initial growth in LB with dense sawtooth at 0.45–0.60 and rapid concentration escalation to 50–65% RW#3 within 4–5 days. However, after the dose_increase was changed from 2 to 4 on 16 February, growth stagnated across most vials around 22–25 February, with OD_{600} dropping to 0.20–0.35 in V1, V2, V6, and V7. V5 (WT) was notably the most stable vial, maintaining sawtooth throughout. V3 (adapted) was compromised by a settings error. Partial recovery occurred in most vials from $\sim$26 February onward. The NC (V4) was contaminated from $\sim$26 February. The growth stagnation suggests that the increased dose escalation rate (dose_increase 4) may have pushed the RW concentration beyond the tolerance threshold too rapidly for adaptive mutations to accumulate, effectively killing or severely inhibiting the cells before they could adapt.